Immunological Studies of the Anti-inflammatory Protein, Sj16, of *Schistosoma japonicum*

HU, Shaomin

A Thesis Submitted in Partial Fulfilment
of the Requirements for the Degree of
Doctor of Philosophy
in
Biology

February 2009

Thesis committee:

Prof. FUNG, Ming Chiu (Supervisor)
Prof. LAM, Hon Ming (Chairman)
Prof. CHEUNG, Chi Keung Peter (Committee member)
Prof. MAK, Nai Ki (External examiner)

Statement

All the experimental work reported in this thesis was performed by the author, unless otherwise specified.

HU, Shaomin

Acknowledgements

It is a pleasure to thank the many people who made this thesis possible.

I would like to express my deep and sincere gratitude to my supervisor Prof. Ming Chiu Fung. His understanding, encouraging and personal guidance have provided a good basis for the present thesis. His wide knowledge and his logical way of thinking have been of great value to me.

I would also like to express my sincere gratitude to the members of the thesis committee, Prof. H.M. Lam, Prof. N.K. Mak, and Prof. Peter, C.K. Cheung, for their patience of reviewing my thesis and invaluable comments.

I would like to thank Prof. Z.D. Wu at Department of Parasitology, Zhongshan School of Medicine, Sun Yat-sen University for the constructive suggestion on this project. I also thank Prof. K.N. Leung and Ms. Ada, L.P. Kong at Department of Biochemistry, CUHK, for their help in flow cytometry analysis. My special thank also goes to Prof. N.K. Mak at Department of Biology, Hong Kong Baptist University for guiding me in mouse bone marrow cell colony formatting unit assay.

I am grateful to Mr. Wilson, K.W. Lau, Ms. Helen, S.N. Tsai, Mr. Freddie, W.K. Kwok, Mr. Thomas, C.O. Tong, and Ms. Jessie, P.K. Lee for their expert and enthusiastic technical assistance and helpful advice.

My appreciation also goes to Ms. Marilyn, M.L. Yau and Dr. Ken, W.K. Lau for their excellent laboratory management and valuable advice. I would also like to express my thankfulness to my labmates, Ms. Josephine S.M. Liu, Dr. Terisa, P.C. Leung, Ms. Sylvia, C.L. Lok, Ms. Pecky, P.K. Law, Mr. Kelvin, K.M. Chan, Ms. Winnie, W.W. Choi, Mr. Kan Liu, Mr. S.W. Zhang, Mr. Hogan, H.L. Tang, Mr. Jack, K.C. Wu, Mr. K.L. Yuen, Mr. X.W. Chen, for providing valuable feedback and advice, and for sharing experiences and knowledge during the time of study.

Abstract

Schistosome is the causative agent of schistosomiasis which is one of the world's most prevalent tropical diseases. In the skin of infected host, significant inflammatory response to the parasite is not observed. Previous studies from *Schistosoma mansoni* showed that this subdued inflammatory response was due to a 16-KDa protein, Sm16, which is present abundantly in the secretions of schistosomulae. Provided that *Schistosoma japonicum* shares the same infective pathway as *S. mansoni* by penetrating the skin, it seems logical that *S. japonicum* has a protein with a similar role to Sm16 to down-regulate host immune responses. According to the cDNA sequence of Sm16, a corresponding gene (designated Sj16) of Sm16 has previously been amplified and cloned from the cercarial cDNA of *S. japonicum*. Sequence analysis showed that Sj16 shares 99% identity with Sm16 in its nucleotide sequence, and 100% identity in its protein sequence. While previous studiers reported their failure in obtaining the soluble recombinant protein of Sm16, we expressed and purified the recombinant Sj16 (rSj16) from *E. coli* in the present study. Western blot and ELISA analysis showed that *S. japonicum*-infected rabbit sera could not recognize rSj16, indicating that native Sj16 might fail to induce circulating antibodies during *S. japonicum* infection. In the *in vivo* study, rSj16 dramatically suppressed not only the recruitment of leukocytes to the peritoneal cavity of BALB/c mice injected with thioglycollate, but also the maturation of thioglycollate-induced peritoneal macrophages. The suppression effect was accompanied by a marked up-regulation of IL-10 and IL-1RA transcripts, and down-regulation of IL-12p35, IL-1β and MIP-2 transcripts in peritoneal cells. Further analysis revealed that rSj16 also inhibited both humoral and cellular immune responses to heterologous antigens. In addition, rSj16 was found to induce macrophage differentiation of the murine myeloid leukemia WEHI-3B (JCS) cells, and regulate the differentiation of mouse hematopoietic cells towards the macrophage lineage. Although previous studies indicated the involvement of endogenous IL-1α, IL-1β and TNF-α in the macrophage differentiation of JCS cells, the results from this study suggested that rSj16-induced JCS cell differentiation do not rely on the endogenous production of these three cytokines. This is the first study to successfully express and purify sufficient soluble rSj16, and demonstrate the anti-inflammatory and immunomodulatory effects of the rSj16.

摘要

血吸蟲病是世界衛生組織認定和推薦的 8 種最重要、最常見的熱帶病之一。血吸蟲是血吸蟲病的病原體。在血吸蟲感染過程中，宿主不會對其產生嚴重的炎症反應。先前的研究表明曼氏血吸蟲童蟲在皮膚移行過程中會大量分泌一種分子量為 16 道爾頓的蛋白 Sm16，該蛋白可以抑制宿主對蟲體的炎症反應。由於日本血吸蟲和曼氏血吸蟲一樣是通過鑽入宿主的皮膚而感染宿主，我們設想日本血吸蟲童蟲在皮膚移行過程中也會分泌一種類似 Sm16 的蛋白以調節宿主的免疫反應。基於 Sm16 的 DNA 序列，本研究組之前已成功從日本血吸蟲尾蚴 cDNA 克隆了 Sm16 的同源基因並命名為 Sj16。序列分析表明 Sj16 和 Sm16 的氨基酸序列完全相同。儘管先前的研究者都未能純化到可溶性的重組 Sm16 蛋白，本研究首次成功從大腸杆菌株 *E.coli* 中表達並純化了可溶性重組 Sj16 蛋白，並通過動物實驗證明重組 Sj16 可以抑制硫乙醇酸鹽誘導的白細胞趨化及腹腔巨噬細胞成熟，同時上調 IL-10 和 IL-1RA 以及下調 IL-12p35，IL-1β 和 MIP-2 在腹腔細胞中的表達。此外，本研究也發現重組 Sj16 可抑制宿主對異種抗原的細胞及體液免疫應答。通過體外實驗，本研究表明重組 Sj16 能抑制小鼠髓系白血病細胞 WEHI-3B(JCS)增生，誘導其巨噬細胞分化，而且證實該巨噬細胞分化與重組 Sj16 誘導的內源性 IL-1α，IL-1β 和 TNF-α 表達無關。最後，本研究也證明重組 Sj16 能調節小鼠骨髓造血幹細胞分化。

Table of content

1 Introduction

1.1 Schistosomiasis

In 1852, Theodor Bilharz described for the first time a tropical parasitic disease (bilharzia, later termed schistosomiasis) caused by blood-dwelling trematode fluke worms of the genus *Schistosoma*(1).

1.2 Causative agents of schistosomiasis-schistosomes

The main forms of human schistosomiasis are caused by five different species of the fluke worms, known as schistosomes(1): *Schistosoma mansoni* (*S. mansoni*), which is transmitted by *Biomphalaria* snails and causes intestinal and hepatic schistosomiasis in Africa, the Arabian peninsula, and South America; *S. haematobium*, transmitted by *Bulinus* snails and causing urinary schistosomiasis in Africa and the Arabian peninsula; and *S. japonicum*, transmitted by the amphibian snail *Oncomelania* and causing intestinal and hepatosplenic schistosomiasis in China, the Philippines, and Indonesia. *S. intercalatum* and *S. mekongi* are only of local importance, but have also well-described associations with chronic hepatic and intestinal fibrosis and their attendant consequences. *S. japonicum* is a zoonotic parasite, which infects a wide range of animals including cattle, dogs, pigs, and rodents. *S. mansoni* is also found in rodents and primates, but human beings are the main host. Besides, a dozen other schistosome species (e.g., *S. bovis* or *S. margrebowiei*) are animal parasites, some of which occasionally infect human.

The distribution of the different species depends mainly on the ecology of the snail hosts(1). Natural streams, ponds, and lakes are typical sources of infection, but over the past few decades man-made reservoirs and irrigation systems have contributed to the spread of schistosomiasis. The disease is largely a rural problem, but urban foci can be found in many endemic areas(2).

1.3 Biology of schistosomes

Schistosomes differ in a number of ways from other trematodes(3). They are diecious (having male and female reproductive organs in separate individuals), and adult worms of the two sexes are dissimilar in appearance. Female worms are long (1.2 to 2.6 cm) and slender, with a body almost circular in cross section and 0.3 mm or less in diameter. Male worms are 0.6 to 2.2 cm long, and although the body is flattened behind the ventral sucker, it looks cylindrical, as it is characteristically incurved ventrally to form a gynecophoral canal in which the female reposes.

The schistosomes have a complex life cycle which alternates between two hosts and with short-lived water-born form (Fig.1.3). Eggs are eliminated with feces or urine from the infected hosts. Under optimal conditions the eggs hatch and release miracidia, which seek out and penetrate specific snail intermediate hosts. The growth stage of schistosome in the snail includes 2 generations of sporocysts and the production of cercariae. Upon release from the snail, the free-swimming infective cercariae penetrate the skin of the human host, and shed their forked tail, becoming schistosomulae. The actual penetration of the parasite through the host skin is a combined mechanical and secretory process. The penetration process is companied by secreting proteolytic enzymes (e.g. cercarial elastase secretion from the penetration glands) and immune regulatory materials which facilitate the penetration(4-8). The schistosomulae migrate through several tissues and stages to their residence in the veins. Adult worms in humans reside in the mesenteric venules in various locations, which at times seem to be specific for each species: *S. japonicum* is more frequently found in the superior mesenteric veins draining the small intestine, and *S. mansoni* resides more often in the superior mesenteric veins draining the large intestine. The females deposit eggs in the small venules of the portal and perivesical systems. The eggs are moved progressively toward the

lumen of the intestine (*S. mansoni* and *S. japonicum*) and of the bladder and ureters (*S. haematobium*), and are eliminated with feces or urine, respectively.

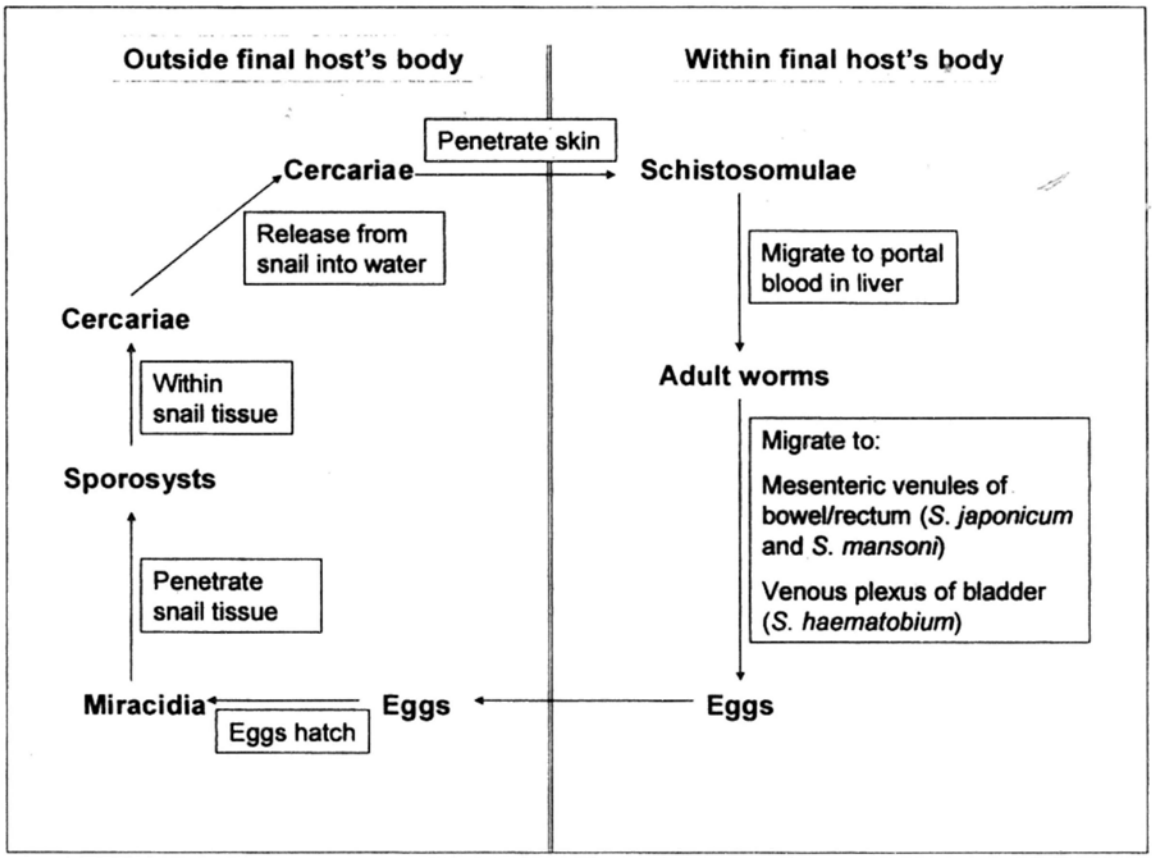

Fig.1.3 Life cycle of schistosome. Modified from http://www.dpd.cdc.gov/dpdx/html/schistosomiasis.htm.

1.4 Disease burden

Schistosomiasis is the second most prevalent tropical disease in the world. It is estimated that 200 million people in 74 countries are infected with the snail-transmitted, water-borne parasitic helminth, and that 120 million of them have symptoms, and 20 million have severe illness(9, 10). Annually an estimated 20,000 deaths are associated with the severe consequences of the infection, including bladder cancer or renal failure (*S. haematobium*) and liver fibrosis and portal hypertension (*S. mansoni*). In sub-Saharan Africa where schistosomiasis constitutes

an important public health problem, a survey in year 2000 of disease-specific mortality reported that 70 million individuals out of 682 million had experienced haematuria and 32 million dysuria associated with *S. haematobium* infection. It was estimated that 18 million individuals suffered bladder wall pathology and 10 million hydronephrosis. Infection with *S. mansoni* was estimated to cause diarrhoea in 0.78 million individuals, blood in stool in 4.4 million and hepatomegaly in 8.5 million. With the limited data available, mortality rates due to non-functioning kidney (from *S. haematobium*) and haematemesis (from *S. mansoni*) have been estimated at 150,000 and 130,000 per year, respectively. Although these are global estimates of the schistosomiasis disease burden, the public health impact of schistosomiasis in the field has been poorly evaluated and is still subject to controversy. Apart from a few situations where schistosomiasis is or was recognized as an obvious public health problem, as in Brazil, China, Egypt, the Philippines, northern Senegal and Uganda, the disease is often not a priority for health authorities. Moreover, the lack of a simple clinical case definition does not enable rapid identification of the disease by health personnel.

Schistosomiasis is the most important human helminth infection in terms of morbidity and mortality(11); a recent meta-analysis assigned 2 to 15% disability weight to the disease(12). There is also emerging evidence that schistosome infections may impact the etiology and transmission of human immunodeficiency virus/AIDS (HIV/AIDS)(13-18), hepatitis C virus(18), tuberculosis(14, 19-22), and malaria(23-28), and vice versa. In particular, the possible interaction between schistosomiasis and HIV/AIDS is receiving increasing attention, given the role of immune responses in both diseases and the geographic overlap in distribution; low $CD4^+$ T-cell counts resulting from HIV infection may increase susceptibility to schistosome infection and influence egg excretion (1, 29, 30). Thus, schistosomiasis

imposes a high socioeconomic burden on many affected developing countries(11).

1.5 Schistosomiasis in China

In China, schistosomiasis is caused by the infection of *S. japonicum*. It is mainly endemic in the 12 provinces along the Yangtze River and in the southern part of the river (31). According to geographical patterns of the endemic areas and ecological characteristics of the vector snail, schistosomiasis endemic regions in China have been stratified into three types, namely, plain regions with water-way networks, swamp and lake regions, and hilly and mountainous regions(32). *S. japonicum* in China has the widest variety of mammalian hosts as shown by a series of epidemiological surveys and laboratory experiments. It has been shown that most mammals can be infected with the parasite, although the effects of the infection on the animals vary considerably. The final hosts of *S. japonicum* including 40 species of domestic and wild mammals belonging to 28 genera have been identified in China. Their importance in the maintenance of schistosomiasis varies with the animal host and, in the same host, from one endemic area to the other(32, 33).

According to the recent nation-wide sampling survey on schistosomiasis conducted in 1995, there was a total 3.6 billion m^2 of snail habitats, 90% of the total lake region, practically no reduction during the recent years. Infected subjects amounted to 865,084, and among them, 55,961 were advanced cases. Furthermore, an estimation of infected cattle and buffaloes was 100,251 in 1995 which serve as important reservoirs in the transmission of *S. japonicum* infection(32, 34). The population at risk with the infection is as high as 40 million, and there are about 810,000 people are infected throughout the country.

1.6 Pathology of schistosomiasis

Many patients with brief exposure to schistosomiasis may have either no symptoms or symptoms that do not differ materially from those of noninfected

control travelers(3). Following penetration of the skin by cercariae, a transient reaction may be seen. Petechial hemorrhages occur at the site of penetration, with some localized edema and pruritus, which disappear in 4 days or less. During the succeeding 3 weeks there may be generalized malaise, fever, giant urticaria, vague intestinal complaints, and so forth, partly depend on the intensity of the infection. Migration of the worm throughout the lungs may cause cough or hemoptysis. Soon after the developing schistosomes reach the liver, acute hepatitis may develop.

When the flukes reach the mesenteric or vesical venules and egg laying commences, the acute stage of the disease (acute schistosomiasis, or Katayama fever) is seen(3). The onset of the Katayama fever may occur a few weeks to months after a primary infection(35). The clinical disease at this stage is usually seen only in relatively heavy infection or in persons recently arrived in an endemic area(36, 37). And the degree of the disease is not necessarily proportional to the number of parasites involved. The disease usually starts suddenly with fever, fatigue, myalgia, malaise, non-productive cough, eosinophilia, and patchy infiltrates on chest radiography. Abdominal symptoms can develop later, caused by the migration and positioning of the mature worms. Most patients recover spontaneously after 2–10 weeks, but some develop persistent and more serious disease with weight loss, dyspnoea, diarrhoea, diffuse abdominal pain, toxaemia, hepatosplenomegaly and widespread rash(1). The Katayama fever due to *S. japonicum* can also occur in people living in endemic areas and with a history of previous infections.

The chronic stage of the disease (chronic schistosomiasis) comes on gradually, and the main lesions in chronic infection are due not to the adult worms but to eggs that are trapped in the tissues during the perivesical or peri-intestinal migration or after embolisation in the liver, spleen, lungs, or cerebrospinal system(3). Eggs deposition takes place in the smaller vessels, close to the lumen of the intestine or

bladder. Secretions of the contained miracidia evoke typical eosinophilic inflammatory and granulomatous reactions, which are progressively replaced by fibrotic deposits(38). The severity of the symptoms is thus related both to the intensity of infection and to individual immune responses (http://www.who.int/tdr/diseases/schisto/diseaseinfo.htm).

Hepatosplenic schistosomiasis is the most common of chronic infection in patients with *S. mansoni* or *S. japonicum*, also regularly in *S. haematobium* infections. Hepatic parenchymal damage may be found in approximately 50% of the patients with *S. japonicum* infection. Eggs lodge in the liver, where granulomas form around them. Over a period of time, the liver becomes grossly enlarged and the left lobe disproportionately so. The spleen may be barely palpable or massively enlarged. Portal hypertension, resulting from the fibrotic hepatic disease, leads to esophageal varices, which may bleed, and finally to massive ascites(3) (http://www.who.int/tdr/diseases/schisto/ diseaseinfo.htm).

In urinary schistosomiasis (due to *S. haematobium*) damage to the urinary tract is revealed by blood in the urine. Urination becomes painful and is accompanied by progressive damage to the bladder, ureters and then the kidneys. Bladder cancer is common in advanced cases (http://www.who.int/tdr/diseases/schisto/diseaseinfo.htm).

In intestinal schistosomiasis (infection with *S. mansoni, S. japonicum*, *S. mekongi*), the disease is slower to develop. There is a progressive enlargement of the liver and spleen, intestinal damage due to fibrotic lesions around eggs lodged in these tissues, and hypertension of the abdominal blood vessels. Bleeding from these vessels leads to the presence of blood in stools, and can be fatal. Sufferers become seriously weakened by the disease and, in some cases, the functioning of organs such as spleen and kidney becomes impaired.

Death is mostly due to bladder cancer associated with urinary schistosomiasis and the bleeding from varicose veins in the oesopahagus associated with intestinal schistosomiasis. Children are especially vulnerable to infection, which develops into chronic disease if not treated.

1.7 Control of schistosomiasis

Control of schistosomiasis is based on drug treatment, snail control, improved sanitation and health education.

At present, the main steps towards the control of schistosomiasis are transmission control of intermediate host snail and praziquantel-based morbidity control. However, due to the vast transmission areas, ecological transformations (e.g. retuning farmland to the buffer lakes, flooding), along with global warming, it is difficult to eliminate snail (39-41). Praziquantel is a safe, orally active, broad-spectrum and highly efficacious antischistosomal drug (42-44). Schistosomiasis control using praziquantel chemotherapy is highly effective in reducing morbidity, but does not prevent reinfection, and it requires a substantial infrastructure to deliver the drugs to all the endemic area in a regular basis (45, 46). In addition, for those individuals with a high worm burden, transition to severe and irreversible pathology is usually diagnosed at too late a stage for chemotherapy to affect the outcome(47). Moreover, although there is no clear evidence of the existence of praziquantel-resistant strains, a decreased susceptibility to the drug has been observed in several countries (48-50).

Health education on schistosomiasis has greater importance than ever before. The introduction into schools of diagnosis and treatment has made children and parents much more aware of the problem connected with disease. Schoolteachers and local health workers are effective in explaining the role played by people in the transmission of schistosomiasis. Campaigns in the Egyptian mass media have proved

particularly successful in increasing awareness of the need for diagnosis and treatment (http://www.who.int/tdr/).

The supply of safe drinking water and sanitation is fundamental to schistosomiasis control. The beneficial results of chemotherapy - normally quite spectacular - are even more marked in communities with adequate water and sanitation supplies. The high prevalence of schistosomiasis is clearly a reliable criterion to select communities for installing a clean water and sanitation supply (http://www.who.int/tdr/).

1.8 Vaccine for schistosomiasis

It has taken more than 80 years to develop the vaccine against Schistosome. But, unfortunately, we fail to obtain any genuinely effective vaccines at present. Previous studies showed that animals vaccinated with attenuated cercariae (the young stage of the parasite) could get 70-90% protection against cercariae challenge infection(11, 51). However, due to the limit of cercariae supply and transportation, it is not feasible to use irradiated cercariae as vaccine. Then, with the development of molecular biology, researchers transferred their attention on antigen molecules of the worm. In 1998, WHO/TDR selected six biologically active molecules, including glutathione-S-transferase (GST), triose phosphate isomerase (TPI), IrV-5, Sm23, Sm14 and paramyosin, to undertake independent mouse studies in parallel(45, 52-56). However, none of them could give a consistent induction of 40% protection. Among many causes for the failure, the limited understanding of Schistosome in gene level and the less knowledge about the mechanisms of immune evasion may be the major reasons.

1.9 Host-parasite molecular interaction

Successful completion of the mammalian part of the life cycle of schistosome appears to require immunological components. This is demonstrated clearly by the

observations that schistosome fecundity and /or the excretion of eggs is reduced in mice with severe combined immunodeficiency (SCID), and in nude mice and T-cell depleted mice(57-59). Further studies indicated that the reproductive processes in schistosomes are in some way triggered by T cells. In addition, interleukin-7 (IL-7) has been found to not only influence the development of schistosomes, but also may function as a signal used by the parasites to migrate properly (60). Tumour necrosis factor-alpha (TNF-α) has also been demonstrated to influence the egg production in female parasites (61). These studies suggest that schistosomes receive crucial developmental signals from host cytokines.

The evidence that schistosome biology is modulated by host-derived immune factors has fuelled interest in the actual parasites receptor that can interact with such molecules. Pearce and Beall (2001) have discovered two transmembrane receptor serine threonine kinases, SmRK1 and SmRK2, which are capable signaling in response to host transforming growth factor-beta (TGF-β) superfamily cytokines(62-64). Besides, other components of the TGF-β signal pathway, e.g. Smad 1, 2, 4, have been identified in the schistosomes (65, 66). These reports therefore demonstrate that schistosomes possess the components required for a receptor-based signaling system to sense immunological components in the environments.

1.10 Evade the host immune attack by schistosome(59)

Once schistosome cercariae penetrate the skin of their host, they can remain in this environment as schistosomulae for up to 5 days before entering the vasculature and beginning their migration to the lungs and, subsequently, the hepatic portal vein(67). During this journey, which may take 3 weeks, and thereafter, schistosome parasites must contend with an assortment of host immune factors(67). Yet, as is well known, these parasites are able to complete the journey to their final destination and live for years. Research has shown that schistosomes have adapted a variety of

mechanisms that enable them to evade a strong and potentially lethal host immune response.

Skin stage parasites. Upon penetrating the host, cercariae transform into schistosomulae by shedding their glycocalyx. Since the glycocalyx is a potent activator of the host complement system, this transformation is the first step towards allowing the parasites to survive within mammalian hosts (68, 69). In addition, it has been shown experimentally that schistosomulae can produce prostaglandin D2 (PGD2) which interferes with the migration of Langerhans cell (LC) to the draining LN (70); schistosome glutathione-S- transferase (Sm28GST) has been implicated in the production of PGD2 (71). In addition to PGD2, schistosomulae produce PGE2 and induce the production of PGE2 and IL-10 in both human and mouse keratinocytes (72). Furthermore, skin stage schistosomulae also secrete molecules that interfere with T cell responses. Chen *et al.* (2002) found evidence that schistosomulae secrete a 23-kDa protein that is proapoptotic for skin T lymphocytes(73).

Lung stage parasites. In the lung capillaries, parasites are in close association with endothelial cells. PGE2 secretion by schistosomulae has been reported to induce IL-6 production by endothelial cells (70). It is thought that IL-6 diminishes inflammation in the lungs and favours successful migration of the parasites through this tissue. In addition to inducing IL-6 production, lung stage schistosomulae minimize local cellular infiltration by secreting molecules that can downregulate the expression of endothelial adhesion molecules such as E-selectin and VCAM-1, which have been shown to play a role in the binding and transmigration of leukocytes to sites of inflammation (74).

Adult parasites. The immune evasion mechanisms used by adult schistosomes are perhaps the most intriguing. Adult parasites live for many years in the portal

vasculature where they are in constant contact with immune cells, antibodies and complement proteins. Several mechanisms of adult-stage immune evasion have been postulated. Early hypotheses, particularly those by Damian (1967)(75), and Smithers *et al.* (1969)(76), suggested that the parasites protect themselves from immune recognition by coating their surfaces with host antigens, as a form of concealment. In addition, during *in vivo* development, the parasites can reduce their surface antigenicity by antigen-shedding or molecular mimicry (77, 78). Besides, adult stage of schistosomes and eggs could also produce components which regulate host's immune responses(78-80). For examples, the developing egg-antigens induce TH2 response which downregulates the production and effector functions of pro-inflammatory mediators(79, 81).

1.11 Sm16

As mentioned before, human infection of the schistosome occurs when cercariae penetrate intact skin and enter into the body. During this process the parasite remains in the skin for up to five days before migrating to the lung. This stay in the skin potentially provides ample opportunity for the host immune system to mount an effective immune response against the migrating parasite. Yet the host fails to elicit any marked tissue response against the skin-residing schistosomulae(82). Interestingly, previous studies from *S. mansoni* indicated that a reduced tissue response is evident only around live parasites in the skin of naïve hosts, whereas, dead parasites in the skin or intradermal injection of extracts of *S. mansoni* elicit a marked inflammatory response (83). Also, cutaneous penetration of the schistosomulae of *Trichobilharzia ocellata* (*T. ocellata*), a bird schistosome, often results in severe dermatitis in humans (as non-naïve host) (84). This suggested that the live parasites may be producing and secreting substances that potentially down-regulate inflammatory responses in the naïve host. Subsequent studies showed that

excretory/secretory (ES) products of the schistosomulae of *S. mansoni* contain activities that down-regulate production of the pro-inflammatory cytokines IL-1α and IL-1β and increase production of the anti-inflammatory cytokines interleukin 1 receptor antagonist (IL-1ra) in human keratinocytes (85). Then, by comparing the ES products of the schistosomulae of *S. mansoni* and *T. ocellata*, Ramaswamy *et al.* found this subdued inflammatory response was due to a 16-KDa protein (designated **Sm16**) present abundantly in the secretions of schistosomulae of *S. mansoni* (86).

Subsequent *in vitro* studies demonstrated that Sm16 stimulates IL-1ra production in human keratinocytes and suppresses transcription of the pro-inflammatory cytokines IL-1α. Further studies showed that Sm16 inhibit antigen-induced lymphoproliferation and suppress IL-2 production from spleen and skin-draining lymph node cells (86). When injected intradermaly, Sm16 inhibited intercellular adhesion molecule-1(ICAM-1) expression on endothelial cells and prevented lipopolysaccharide (LPS) induced neutrophil infiltration into the dermis (87). Then, the gene encoding for Sm16 was cloned and partially characterized (85). A single intradermal injection of a full-length cDNA of Sm16 resulted in a significant suppression of cutaneous inflammation by reducing cutaneous edema, decreasing neutrophil infiltration, suppressing pro-inflammatory cytokines, and down-regulating the ICAM-1 expression in the skin inflammatory site(88). Besides, cells collected from the skin-draining lymph nodes around the injection site showed reduced proliferation to mitogen(88). Thus, Sm16 showed potential properties of an anti-inflammatory agent. However, the mechanism of Sm16-induced anti-inflammatory activity is still poorly understood.

Beside of Sm16, two other independent groups have also reported the cloning of two stage-specific genes, named SmSPO-1(89) and SmSLP(90) respectively, from *S. mansoni*. Since all of the three genes Sm16, SmSPO-1 and SmSLP share 100%

identity in DNA sequence, they should be the same gene. However, as Ramaswamy group demonstrated the anti-inflammatory and immunomodulatory function of Sm16 (85, 86, 88), Valle group's studies suggested that SmSLP inhibits tubulin assembly and causes the depolymerization of preassembled microtubes, thus probably fulfilling regulatory roles in critical steps of schistosome development (90). It should be mentioned that the microtube regulatory-function of SmSLP was recently refuted by Holmfeldt *et al.* who demonstrated that the SmSLP lacked the microtube regulatory-function(91). Instead, Holmfeldt *et al.* found that the expression of Sm16 in human cell line resulted in a caspase-dependent apoptotic response(91). Both Ramaswamy group and Valle group have also attempted to express recombinant Sm16/SmSLP using bacterial, yeast and insect expression systems, but invariably very low yields of the recombinant protein were obtained, accompanied by signs of death of the host cells(85, 90). Taken together, Sm16/SmSLP/SmSPO-1 is very difficult to be expressed in the recombinant protein expression system, which may partly due to its interference of host cells growth.

1.12 Sj16

Previously, the complete coding sequence of the corresponding gene (designated **Sj16**) of Sm16 has been amplified and cloned from the cercarial cDNA cercariae of *S. japonicum* in our lab. The sequence analysis showed that Sj16 has 99% identity with Sm16 in DNA sequence, while 100% identity in protein sequence. The Sj16 was cloned into vector pBluescript II SK(-).

It is well known that *S. japonicum* shares similar infective pathway with *S. mansoni* by penetrating the skin and the vast majority of the parasites can travel to the lung successfully(5). Together with that the protein sequences of Sj16 and Sm16 are identical, it seems logical that Sj16 may play the same role as Sm16 to modulate

the host immune responses, so as to facilitate the penetration and migration of the *S. japonicum*.

1.13 Objectives of project

The specific objectives of this project are:

1). to express and purify functional recombinant Sj16 (rSj16) protein.

2). to study the anti-inflammatory and immunomodulatory effects of rSj16 on host immune responses.

3). to investigated the effect of rSj16 on hematopoiesis of mouse bone marrow cells.

2 Materials

2.1 Mouse Strain

Female BALB/c mice, 6~12-week-old, were provided by the Laboratory Animal Services Centre, the Chinese University of Hong Kong.

2.2 Cell lines

The murine myeloid leukemia cell line WEHI 3B (JCS)(92, 93) were cultured in complete RPMI 1640 medium (See Materials 2.8). The cultures were incubated under a humidified atmosphere of 95% air, 5% CO_2 at 37°C.

2.3 Bacteria and yeast Strains

Bacteria: *Escherichia coli* DH5α and *Escherichia coli* BL21 (DE3)

Yeast: *Saccharomyces cerevisiae*

2.4 Plasmids

pBluescript II SK(-)/Sj16	Lab stock
pET28a(+)	Novagen 69864-3
pET30a(+)	Novagen 69909-3
pET32a(+)	Novagen 69015-3
pGEX-4T-1	Amersham Pharmacia biotech 27-4580-01
pCold-TF	Takara 3365
pTYB4	New England Biolabs N6704S

2.5 Chemicals

Acetic acid, 99.8%	RDH 33209
Acetonitrile (ACN)	LAB-SCAN C2502
Acrylamide	Amersham Pharmacia biotech 17-1304-01
Agar (Bacteriological grade)	Ajax 863

Agar (cell culture grade)	Sigma A1296
Agarose, Seakem LE	FMC50004
Alum	Sigma A8222
Amido black	Bio-Rad 161-0402
Ammonium persulphate (APS)	Amersham Pharmacia biotech 17-1311-01
Ampicillin	Sigma A9518
Bis-acrylamide	Pharmacia 17-1304-01
Bovine serum albumin (BSA)	Sigma B7030
5-bromo-4-chloro-3-indolyl phosphate -4-toluidine salt (BCIP)	Boehringer Mannheim 1585002
Bromophenol blue	Bio-Rad 161-0404
Canada balsam (for slide mounting)	Sigma C-1795
Chloroform	Ajax 152
Commassie brilliant blue R-250	Bio-Rad 161-0400
Concanavalin A (ConA)	Sigma C0412
alpha-cyano-4-hydroxycinnamic acid	Sigma C8982
Diethyl pyrocarbonate (DEPC)	Sigma D5758
N,N-dimethyl formamide (DMF)	Sigma D4551
Dimethyl sulfoxide (DMSO)	Sigma D2650
Ethanol, absolute	Ajax 214
Ethidium bromide	Invitrogen 15585-011
Ethylenediamine-tetraacetic acid (EDTA)	Sigma E5134
Glutathione, reduced	Sigma G4251
Glycerol	Sigma G7893
Glycine	Sigma G8898

Guanidine hydrochloride	Sigma G4630
Human serum albumin (HSA)	Fluka 05430
Hydrocloric acid, 32%	Ajax 265
Isopropyl-β-D-thiogalactopyranoside (IPTG)	Sigma I5502
Kanamycin	Sigma K1377
Lauryl sulfate, sodium salt (SDS)	Sigma L5750
Lipopolysacchride (LPS)	Sigma L2630
Magnesium chloride	Sigma M9272
Magnesium sulfate	Sigma M2773
Methanol	Tedia MS1922
N, N'-methylenebisacrylamide	Amersham Pharmacia biotech 17-1304-02
β-mercapto-ethanol	Sigma M7154
Nitro blue tetrazolium chloride (NBT)	Roche 1-087-479
Paraformaldehye	Sigma P6148
Peptone	DIFCO 0118-01-8
Pig serum albumin (PSA)	Sigma A4414
Propidium iodine	Molecular probes P21493
Sodium acetate	Sigma S8750
Sodium azide	Sigma S2002
Sodium bicarbonate	Sigma S5761
Sodium chloride	Sigma S9625
Sodium deoxycholate	Sigma D6750
Sodium hydroxide	Sigma S5881
Sodium phosphate	Sigma S0876

N-N-N'-N'-Tetramethylethylenediamine (TEMED)	Sigma T9281
Thiazolyl Blue Tetrazolium Bromide (MTT)	Sigma M5655
Trifluoroacetic acid (TFA)	Sigma T6508
Thioglycollate medium brewer modified (BTG)	BD 211716
Tris-acetate EDTA (TAE) buffer	Ameresco 796
Tris base	Amersham Pharmacia biotech 17-1321-01
Triton X-100	Sigma T6878
Trizol reagent	Invitrogen 15596-026
Trypan blue solution (0.4%)	Sigma T8154
Tryptone	Oxoid L42
Tween 20	Sigma P1379
Yeast extract	Difco 0127-17-9

2.6 Kits, Reagents

Annexin V-FITC Apoptosis Detection Kit	BD Pharmingen 556547
Antibiotic-antimycotic (PSF)	GibcoBRL 15240-062
1 kb plus DNA ladder™	GibcoBRL 10787-026
BigDye® Terminator v3.1 Cycle Sequencing Kit	Applied Biosystem 4337455
Cell proliferation ELISA, BrdU (colorimetric) kit	Roche 11-647-229-001
Control Standard Endotoxin	Associates of Cape Cod, Inc E0005
Cytotoxicity Detection Kit	Roche 1 644 793
Detoxi-Gel™ Endotoxin Removing Gel	Pierce 20344
Dulbecco's phosphate-buffered saline (DPBS)	GibcoBRL 21600-010
Fetal calf serum (FCS)	HyClone CH330160-02
FlowCytomix Mouse Th1/Th2 10plex	Bender MedSystems BMS820FF
Freund's adjuvant, complete	Sigma F5881
Freund's adjuvant, incomplete	Sigma F5506
GSTrap™ HP column	GE Healthcare 17-5281-01
Hemacolor rapid staining set	Merck 1.11661

HiDi formamide	Perkin Elmer 4311320
HiTrap Benzamidine FF (high sub)	GE Healthcare 17-5143-01
LAL Reagent Water	Associates of Cape Cod, Inc W0504
Mouse IL-1 alpha/IL-1F1 DuoSet	R&D DY400
Mouse IL-1 beta/IL-1F2 DuoSet	R&D DY401
Mouse TNF-alpha/TNFSF1A DuoSet	R&D DY410
Mouse IFN-gamma DuoSet	R&D DY485
Mouse IL-10 DuoSet	R&D DY417
Mouse IgE ELISA Set	BD Biosciences 555248
Mouse macrophage-colony stimulating factor (M-CSF)	Sigma M9170
Mouse interleukin-3 (IL-3)	Sigma I4144
Mouse granulocyte-colony stimulating factor (G-CSF)	Sigma G8160
$Pd(T)_{12-18}$	Amersham Pharmacia biotech 27-7858-01
Protein Assay Dye Reagent Concentrate	Bio-Rad 500-0006
Pyrotell® Gel-Clot Formulation	Associates of Cape Cod, Inc GS250
QIAEX II gel extraction kit	Qiagen 20021
RNaseOUT (Recombinant ribonuclease inhibitor)	Invitrogen 10777-019
RPMI 1640 (Powder)	GibcoBRL 23400-021
SDS-PAGE molecular weight standard, broad range	Bio-Rad 161-0317
Slide-A-Lyzer dialysis kit	Pierce 66372
iTaq™ SYBR Green Supermix	Bio-Rad 172-5851
Ultrapure dNTPs sets (2'-deoxynucleoside 5'-triphosphate)	Amersham Pharmacia biotech 27-2035-03
Wizard® Plus SV minipreps DNA purification system	Promega A1460
Wizard® SV Gel and PCR Clean-Up System	Promega A9281

2.7 Antibodies and Immunoglobins

AP conjugated horse anti-mouse IgG (H+L)	Vector AP-2000
AP conjugated goat anti-rabbit IgG	Boeringer Mannheim 1 214 632
Peroxidase- rat anti-mouse IgG	Zymed 04-6020
Peroxidase- goat anti-rabbit IgG (H+L)	Zymed 65-6120

HRP Rat anti-mouse IgG	Zymed 04-0620
HRP Goat anti-mouse IgM	Zymed 62-6820
HRP Goat anti-mouse IgA	Zymed 62-6720
Mouse IgG	Sigma I538
Rat IgG	Sigma I4131
Monoclonal anti-mouse TNF-alpha/TNFSF1A antibody (Clone MP6-XT22)	R&D MAB4101
Monoclonal anti-mouse IL-1 alpha/IL-1F1 antibody (Clone 40508)	R&D MAB400
Monoclonal anti-mouse IL-1 beta/IL-1F2 antibody (Clone 30311)	R&D MAB401
Biotin Rat Anti-Mouse IgG2a	BD Pharmingen 553388
Biotin Rat Anti-Mouse IgG1	BD Pharmingen 553441
Streptavidin HRP	BD Pharmingen 554066
Affinity Purified antimouse CD11b (Mac-1a)	eBiosciences 14-0112
Affinity Purified antimouse Ly6G (Gr1)	eBiosciences 14-5931
Affinity Purified antimouse F4/80 Antigen – Pan Macrophage Marker, M8	eBiosciences 14-4801
FITC goat anti-Rat Ig Specific Polyclonal Antibody	BD Pharmingen 554016
Normal rabbit sera *	
S. japonicum infected rabbit sera *	

* Provided by Dr. Zhongdao Wu at Department of Parasitology, Zhongshan School of Medicine, Sun Yat-sen University, Guangzhou, P.R.China.

2.8 Solutions

1. Acrylamide (SDS-PAGE)	29.2g acrylamide, 0.8g N,N'-methylenebisacrylamide was dissolved in 100ml distilled water, warmed to 37℃ to dissolve and degassed.
2. Agarose gel, 1%	1% (w/v) agarose in 1 × TAE buffer and autoclaved.
3. Alkaline phosphatase (AP)	100mM NaCl, 5mM $MgCl_2$, 100mM Tris-Cl (pH9.5)

Buffer (Western Blotting)	
4. Alkaline phosphatase (AP) color-development solution	0.3μg/ml nitro blue tetrazolium and 0.15μg/ml 5-bromo-4-chloro-3-indolyl phosphate in alkaline phosphatase buffer
5. Amido black staining solution	0.1% (w/v) amido black, 10% methanol, 2% acetic acid
6. Amido black destaining solution	50% methanol, 7% acetic acid
7. 5% non-fat milk solution (Western Blotting)	0.5g non-fat dried milk was dissolved in 10ml 1X PBS (with 0.02% Tween 20)
8. Coomassie blue stain solution (SDS-PAGE)	2.5 g coomassie blue was dissolved in 100 ml glacial acetic acid, 450 ml methanol and made up to 1 litre by distilled water.
9. DEPC-treated water	0.1% DEPC was added to Milli-Q water and shaken vigorously. After treating overnight, the solution was autoclaved to degrade the remaining DEPC.
10. Destain solution (SDS-PAGE)	100ml methanol, 100ml glacial acetic acid and made up to 1litre by distilled water.
11. 0.5 M EDTA (M. W. = 372.24)	18.61 g EDTA was dissolved in 100 ml distilled water and adjusted to pH8.0 using NaOH.
12. FACS fixative buffer	1% paraformaldehyde in 1 × PBS.
13. FACS medium	2% FCS and 0.05% sodium azide in 1 × PBS
14. hematoxylin solution	Sigma GHS232
15. LB agar / broth	10g NaCl, 10g Tryptone and 5g Yeast Extract (for LB agar add 15g bacterograde agar). Add with 1 liter of distilled water and autoclaved.
16. LB+Amp^{100} agar /	LB agar / broth added with filter sterilized ampicillin to

broth	final concentration of 100μg/ml.
17. LB+Kan^{50} agar / broth	LB agar / broth added with filter sterilized kanamycin to final concentration of 50μg/ml.
18. Matrix solution (for mass spectrometry)	Dissolve the contents of a 10 mg tube of alpha-cyano-4-hydroxycinnamic acid in 1 ml of the 50% acetonitrile (ACN) in 0.05% trifluoroacetic acid (TFA) solution.
19. Phosphate buffer saline (PBS)	140mM NaCl, 2.7mM KCl, 8mM Na_2HPO_4, 1.4mM KH_2PO_4
20. Red blood cell lysis buffer	Dissolve the following in 800ml distilled H_2O: 8.3g NH_4Cl, 1.0g $KHCO_3$, 1.8ml of 5% EDTA. Filter sterilize through 0.2um filter. Then add distilled H_2O to 1000ml.
21. RF 1 solution	10mM RbCl, 50mM $MnCl_2$, 30mM potassium acetate (pH 7.5), 10mM $CaCl_2$, 15% (w/v) glycerol were mixed and adjusted to pH5.8 with 0.2M acetic acid. Filter sterilize by passing through a 0.22μm membrane.
22. RF 2 solution	10mM MOPS, 10mM RbCl, 75mM $CaCl_2$, 15% (w/v) glycerol were mixed and adjusted to pH 6.8 with NaOH. Filter sterilize by passing through a 0.22μm membrane.
23. Complete RPMI 1640 medium	The RPMI powder was dissolved in Milli-Q water, added with sodium bicarbonate to 2 g per litre, adjusted to pH 7.2 and filter sterilized by passing through a 0.22μm membrane. The complete medium was prepared by supplementing plain RPMI medium with 1 % antibiotics (PSF) and 10% FCS.
24. 2 × RPMI 1640	A bag of RPMI powder (for one litre) was dissolved in Milli-Q water in a final volume of 500 ml, containing 4 g/L of sodium bicarbonate, adjusted to pH 7.2 and filter sterilized by passing through a 0.22μm membrane.
25. 2× RPMI 1640 mix	2 × RPMI 1640 supplemented with 40% FCS and 2%

	PSF. This medium was freshly prepared and used for 2-3 weeks.
26. 0.66% agar	0.33 g of agar (cell culture grade) was dissolved in 50 ml of Milli-Q H_2O by microwaving. Avoid evaporation during microwave. Freshly prepared.
27. 10 × SDS running buffer	30g Tris-base, 188g glycine, 10g SDS were dissolved in 1 litre of distilled water.
28. 5 × SDS PAGE sample buffer	0.6 ml 1M Tris-HCl (pH6.8), 5 ml 50% glycerol, 2 ml 10% SDS, 0.5 ml β-mercaptoethanol, 1 ml 1% bromophenol blue, 0.9 ml distilled water. Store at -20°C.
29. 3M sodium acetate (M.W. = 82.03)	123.04g NaOAc was dissolved in 500 ml DEPC treated distilled water and adjusted to pH5.2 using glacial acetic acid. Treated with DEPC and autoclaved.
30. 3% Thioglycollate medium brewer modified (3% TG)	3g thioglycollate medium brewer modified was resuspended in 100ml distilled water. Boiled to dissolve completely.
31. Transfer Buffer (Western Blotting)	39mM glycine, 48mM Tris-base, 0.037% SDS, 20% methanol
32. SOB medium	Tryptone 10 g, yeast extract 2.5 g, NaCl 0.2922 g, KCl 0.093 g, add milli-Q H_2O to 495 ml, sterilize by autoclave. Aseptically add 5 ml 2 M Mg^{2+} solution, and mix well.
33. SOB agar	Tryptone 10 g, yeast extract 2.5 g, NaCl 0.2922 g, KCl 0.093 g, agar 7.5 g, add milli-Q H_2O to 495 ml, mix well. Sterilize by autoclave. Aseptically add 5 ml 2 M Mg^{2+} solution, mix well, and pour into petri plates.
34. TBS buffer	50mM Tris, 0.14 M NaCl, pH8.0
35. TBST buffer	50mM Tris, 0.14 M NaCl, 0.05% Tween 20, pH8.0

2.9 Enzymes

1. EcoR I (12 U/μl)	Promega R6011
2. Sal I (10 U/μl)	Promega R6051

3. Xho I (10U/μl)	Promega R6161
4. Thermoprime^{Plus} DNA polymerase kit	Thermo Scientific AB-0301
5. T4 DNA ligase (3U/μl) kit	Promega M180A
6. Lysozyme	Sigma L6876
8. RNase A	Roche diagnostic GmBH 109 134
9. Thrombin	GE Healthcare 27-0846-01
10. M-MLV reverse transcriptase kit	Invitrogen 28025-013
11. Trypsin, porcine	Promega V511A
12. Trypsin-EDTA	GibcoBRL 25200-056

2.10 Major equipments and materials

1. ABI Prism^{TM} 3100 Genetic Analyzer	Applied Biosystems
2. ABI 4700 Proteomics Analyzer	Applied Biosystems
3. Bench-top microcentrifuge	Eppendorf 5415D
4. Centrifuge	Eppendorf 5402
5. Centrifuge	Beckman Coulter CS-15R
6. Cytospin centrifuge	Shandow cytospin 3
7. Cuvette for Biophotometer (Uvette)	Eppendorf-0030106.300
8. DNA sequencer	Applied Biosystems ABI Prism 3100 genetic analyzer
9. Flow cytometer	Becton Dickinson BD FACScan™
10. Gel documentation system	Bio-Rad GS-670
11. High speed centrifuge	Beckman Coulter Avanti J-E
12. Horizon^{TM} 20.25 gel electrophoresis apparatus and power supply	Gibco 1069BD
13. Hybridization oven	Hybaid, MIDI DUAL 14
14. Microplate reader	Molecular Devices Spectra

	max 250
15. Micro-cooler (for ligation reaction)	VWR 13278-801
16. PCR machine	MJ research, PTC-200
17. PVDF membrane	Bio-Rad 162-0184
18. Sonicator, bath	Branson 3210
19. Spectrophotometer	Eppendorf 6131 000.012
20. SpeedVac concentrator	Savant SC110
21. Thermal cycler	MJ research PTC-200
22. Trans-Blot SD semi-dry electrophoretic transfer cell	Bio-Rad 170-3940
23. Transilluminators, white light	UVP 95-0214-01
24. Ultracentrifuge polyallomer tubes	Beckman 270-233833
25. Ultracentrifuge (SW60Ti)	Beckman Coulter, Optimal L-100 XP
26. Ultrasonic processor	GENEQ inc. SOVC505-00

2.11. Primers

Primer	Code		Primer sequence 5' – 3'
pET30a(+)/ pET32a(+)/ pET28a(+)	MF596	Sequencing primer	CTA GTT ATT GCT CAG CGG
Sj16	Sj16S1	Upper	CGG AAT TCT TGA TCA CAG CTA CAA CGT TAG
	Sj16P2	Lower	CGC GTC GAC CTA AGA CGA TTC ATA T
	Sj16S2	Lower	CCG CTC GAG CAA AGA CGA TTC ATA T
GAPDH	MF214	Upper	ACC ACA GTC CAT GCC ATC AC
	MF215	Lower	TCC ACC ACC CTG TTG CTG TA
IL-1α	MF142	Upper	ACA GTA TCA GCA ACG TCA AGC AA
	MF143	Lower	CCG ACT TTG TTC TTT GGT GGC A
IL-1β	MF144	Upper	GAG CTT CAG GCA GGC AGT ATC
	MF145	Lower	GTA TAG ATT CTT TCC TTT CAG
TNF-α	MF79	Upper	TCC CCA AAG GGA TGA GAA GTT C
	MF80	Lower	TCA TAC CAG GGT TTG AGC TCA G
MCP-5	MF414	Upper	CCT CAA CAT GAA GAT TTC CAC AC
	MF415	Lower	GTT TTT GGA ACT CTC AGC CTA GA
RANTES	MF889	Upper	GAA GAT CTC TGC AGC TGC CCT
	MF890	Lower	GCT CAT CTC CAA ATA GTT GA
IL-1ra	MF1071	Upper	GCT TTA CCT TCA TCC GCT CTG
	MF1072	Lower	AGG GGT AGG GTG GGT GGT AG
IL-12p35	MF208	Upper	TGC CAG GTG TCT TAG CCA GTC
	MF209	Lower	ATT TTC ACT CTG TAA GGG TCT GC
IL-12p40	MF211	Upper	CAG CTT CTT CAT CAG GGA CAT C
	MF212	Lower	TTT CCT TTC CAA CGT TGC ATC CT

IL-10	MF736 MF737	Upper Lower	AGC CGG GAA GAC AAT AAC TGC A AAT TCA TTC ATG GCC TTG TAG ACA
KC	MF1339 MF1340	Upper Lower	GGA TTC ACC TCA AGA ACA TCC AGA G CAC CCT TCT ACT AGC ACA GTG GTT G
MIP-2	MF1341 MF1342	Upper Lower	TGT CAA TGC CTG AAG ACC CTG CC AAC TTT TTG ACC GCC CTT GAG AGT GG
MIP-1α	MF1343 MF1344	Upper Lower	CCT CTG TCA CCT GCT CAA CAT C TCC TCG CTG CCT CCA AGA CTC T

3 Methodology

3.1 Expression and purification of recombinant Sj16 (rSj16) and recombinant GST (rGST)

3.1.1 Preparation of DH5α and BL21 (DE3) competent cells

The competent cells were prepared as described before(94). Briefly, frozen DH5α or BL21 (DE3) bacteria-glycerol was scrapped by sterile inoculating loop and streaked on SOB agar plate. The plate was incubated at 37°C overnight to allow the growth of bacterial colonies. Single colony was picked and inoculated into 10 ml SOB medium in a 150 ml flask. The bacterial culture was shaken overnight at 225 rpm, 37°C as a starter culture. One ml of overnight starter culture was added to 100 ml pre-warmed SOB medium (with 1:100 dilution) in a one-litre-flask and shaken at 225 rpm, 37°C until the optical density (O.D.) of the culture at 550 nm reached 0.2 - 0.4 (with cell density around 4-7 × 10^7 cells/ml) for BL21 (DE3), or 0.35-0.60 (with cell density around 4-7 × 10^7 cells/ml) for DH5α. The culture was collected and chilled on ice for 15 minutes. The bacterial cells were harvested by centrifugation at 1,000 × g, 4°C for 15 minutes. The cell pellet was resuspended in 30 ml of ice cold RF 1 solution. The cell suspension was incubated on ice for 15 minutes and harvested by centrifugation at 1,000 × g, 4°C for 15 minutes. The cell pellet was resuspended in 8 ml ice cold RF 2 solution and incubated for 15 minutes on ice. 150 µl of cell suspension was aliquoted into chilled 1.5 ml microcentrifuge tubes. The aliquoted competent cells were frozen by liquid nitrogen and stored at -70°C.

3.1.2 Purification of plasmid DNA

The plasmid DNAs from the bacterial cells were purified using the Wizard® *Plus* SV Minipreps DNA Purification System (Promega) according to the manufacturer's instruction.

Fresh bacterial colonies were obtained from the frozen bacteria-glycerol stock.

Bacteria-glycerol stock was scrapped by sterile inoculating loop and streaked onto LB plates supplemented with 50 μg/ml kanamycin (for the selection of pET28a(+) and pET30a(+) plasmid vectors) or 100 μg/ml ampicillin (for the selection of pET32a(+), pGEX-4T-1, pTYB4, and pCold TF plasmid vectors). The plates were incubated overnight at 37°C for the bacterial colonies to grow. Single, well-isolated colony was picked and inoculated into 15 ml of LB medium supplemented with 50 μg/ml kanamycin or 100 μg/ml ampicillin in a 150 ml flask. The bacterial culture was shaken at 225 rpm, 37°C overnight.

Five ml of overnight bacterial culture was harvested by centrifugation at 5000 × g for 15 minutes. The supernatant was discarded and the tube was inverted to blot excess media on paper towel. The cell pellet was completely resuspended in 250 μl of cell resuspension solution by vortexing. The resuspeneded cells were transferred to a sterile 1.5 ml microcentrifuge tube. 250 μl of cell lysis solutions were added and mixed by inverting the tube 4 times gently. 10 μl of alkaline protease solutions were added and mixed by inverting the tube 4 times gently and incubated at room temperature for approximately 5 minutes until the cell suspension was clear. 350 μl of neutralization solutions were added and mixed immediately by inverting the tube 4 times gently to neutralize the cell lysate. The neutralized cell lysate was centrifuged at 16,000 × g, room temperature for 15 minutes. Cleared lysate was transferred carefully to the spin column in a 2 ml collection tube and centrifuged at 16,000 × g, room temperature for 1 minute. The flow-through was discarded. 750 μl of column wash solution was added into the spin column and centrifuged at 16,000 × g for 1 minute and the flow-through was discarded. Repeated with 250 μl column wash solution and centrifuged at 16,000 × g for 2 minutes. The spin column was transferred to a new sterile microcentrifuge tube, and the plasmid DNA was eluted by adding 100 μl of autoclaved Milli-Q water to the spin column and centrifuged at

16,000 × g for 1 minute. The eluted plasmid DNA was stored at -20°C.

The quality and quantity of the extracted plasmid DNA was determined by measuring the O.D.260 and O.D.280. The estimation on the purity of nucleic acids is based on the ratio of O.D.260 and O.D.280(95). The ratio is around 1.80 for DNA free of contaminants.

3.1.3 Polymerase chain reaction (PCR) amplification of Sj16 fragment (without signal peptide)

The coding region (without the 54 bp at the 5' terminal coding for signal peptide) of the Sj16 was amplified by PCR with pBluescript II SK(-)/Sj16 as template(96). Three primers were designed with franked restriction sites: Sj16S1, *Eco*R I; Sj16P2, *Sal* I; Sj16S2, *Xho* I. 50 µl of PCR reaction mix contained 1.25 units of thermoprime^{PLUS} DNA polymerase, 1.5 mM $MgCl_2$, 1 × reaction buffer IV (ABgene), 0.2 mM of each dNTP (Amersham Pharmacia biotech), 25 pmole each of specific primers (Sj16S1 and Sj16P2, or Sj16S1 and Sj16S2), and 10 ng of pBluescript II SK(-)/Sj16 plasmid DNA. PCR parameters were 94 °C of initial denaturation for 3 minutes; 94 °C of denaturation for 30 s, 57°C of primer annealing for 30 s, 72 °C of primer extension for 30 s, and cycled for 30 cycles; a final extension of 10 minutes was performed at 72 °C. 10 µl of amplified PCR products were electrophoresed at 100V on 2% agarose gel with 0.25 µg/ml ethidium bromide (Invitrogen) to visualize the amplified band under UV illumination. The theoretically predicted size of DNA fragments amplified with Sj16S1/Sj16P2 or Sj16S1/Sj16S2 is 317 bp.

3.1.4 Purification of PCR product

The amplified DNA fragments by PCR were purified using Wizard® SV Gel and PCR Clean-Up System (Promega) according to the kit's manual. 100 µl of PCR product were added into a 1.5 ml microcentrifuge tube containing 100 µl of Direct Purification Buffer, and mixed gently. The mixture was then transferred to SV

Minicolumn placed in a Collection Tube, and incubated for 1 minute at room temperature. The SV Minicolumn assembly was centrifuged at 16,000 × g room temperature for 1 minute. The flow-through was discarded. 700 µl of Membrane Wash Solution was added into the SV Minicolumn and centrifuged at 16,000 × g for 1 minute and the flow-through was discarded. Repeated with 500 µl Membrane Wash Solution and centrifuged at 16,000 × g for 5 minutes. The SV Minicolumn was transferred to a new sterile microcentrifuge tube, and the DNA fragment was eluted by adding 100 µl of Nuclease-Free Water to the center of the SV Minicolumn, incubated at room temperature for 1 minute, and centrifuged at 16,000 × g for 1 minute. The eluted DNA was determined by measuring the O.D.260 and O.D.280(95), and stored at -20°C until use.

3.1.5 Restriction enzyme digestion of DNA

The plasmid vectors or the target DNA fragments were digested with restriction enzymes to generate sticky ends that are compatible and can be ligated to form recombinant plasmids. The plasmid DNA pET28a(+), pET30a(+), pCold TF, pET32a(+), pGEX-4T-1 and purified PCR production of Sj16S1/Sj16P2 were digested with enzymes *Eco*R I and *Sal* I (Promega). The digestion reaction was set up according to the manual recommended by the enzyme's manufacturer: RE 10 × D Buffer 4 µl, acetylated BSA (10 µg/µl) 0.4 µl, plasmid DNA 3 µg or PCR fragment 0.75 µg, *Eco*R I (12 U/µl) 1 µl and *Sal* I (10 U/µ) 1 µl, and sterilized Milli-Q H_2O to 40 µl. The plasmid DNA pTYB4 and PCR production Sj16S1/Sj16S2 were digested with *Eco*R I and *Xho* I. The digestion reaction was set up as following: RE 10 × D Buffer 4 µl, acetylated BSA (10 µg/µl) 0.4 µl, plasmid DNA 3 µg or PCR fragment 0.75 µg, *Eco*R I (12 U/µ) 1 µl and *Xho* I (10 U/µ) 1 µl, and sterilized Milli-Q H_2O to 40 µ. The reaction was mixed gently, and incubated at 37°C for 7 hours.

3.1.6 Purification of DNA fragments from agarose gel

After restriction enzyme digestion, plasmid DNA and PCR DNA fragments were purified from agarose gel using the QIAEX II Gel Extraction Kit (Qiagen) according the kit's manual.

Restriction enzymes digested DNA was resolved in 1.5% agarose gel by agarose gel electrophoresis in autoclaved 1 × TAE buffer. After gel electrophoresis, the DNA bands of corresponding size were excised from the gel by sterile blades under long wave UV illumination. The excised gel was put into a 1.5 ml microcentrifuge tube and weighted. For each 100 mg gel slice, 300 µl of QX1 Buffer was added to solubilize the agarose gel matrix. Then 10 µl of resuspended QIAEX II resin was added and the mixture was incubated at 50°C for 10 minutes. The mixture was mixed gently every 2 minutes to keep QIAEX resin in suspension and thus enhancing DNA binding capacity. The suspension was centrifuged at 16,000 × g for 30 seconds and the supernatant was discarded. The resin pellet was washed with 500 µl QX1 Buffer and centrifuged at 16,000 × g for 30 seconds and repeated twice with 500 µl PE Buffer. Finally, the resin pellet was air-dried for 15 minutes to remove any volatile PE Buffer, and DNA was eluted by resuspending the pellet in 20 µl Milli-Q water and incubating for 10 minutes at room temperature. The suspension was centrifuged at 16,000 × g for 1 minute to pellet the resin. The eluted DNA supernatant was transferred carefully into a microcentrifuge tube and stored at -20°C. The quality and quantity of the extracted plasmid DNA was determined by measuring the O.D.260 and O.D.280 (95).

3.1.7 Ligation of purified DNA fragments

After the plasmids and DNA fragments were digested with restriction enzymes as described in methodology 3.1.5 and purified as described in methodology 3.1.6, plasmids were ligated to the corresponding target DNA fragments at the compatible ends with T4 DNA ligase (Promega) according to the manufacturer's protocol:

pET28a(+), pET30a(+), pET32a(+), pGEX-4T-1, and pCold TF were ligated with the PCR fragment of Sj16S1/Sj16P2; pTYB4 was ligated with the PCR fragment of Sj16S1/Sj16S2. 25 ng of PCR DNA fragments and 75 ng of vector DNA fragments were mixed with 1 μl of 10 × T4 DNA Ligase Buffer and 1 unit of T4 DNA ligase (Promega) in a final reaction volume of 10 μl. The reaction mixture was incubated overnight at 15°C for 16 hours.

3.1.8 Transformation of recombinant plasmids

The ligated recombinant plasmids prepared as described in methodology 3.1.7 were transformed into competent DH5α. Frozen DH5α bacteria-glycerol competent cell (150 μl, prepared as described in methodology 3.1.1) was thawed on ice. 10 μl of ligated recombinant constructs was added to the competent cells (97). The mixture was chilled on ice for 30 minutes. Heat-shock was performed by putting the tube in 42°C water bath for 90 seconds, and then chilled on ice immediately for 5 minutes. 800 μl of pre-warmed LB medium was added to the tube, and shaken at 37°C, 150 rpm for 1 hour. 200 μl of the mixture were then spread on LB agar plate containing appropriate antibiotics (see methodology 3.1.2), and incubated at 37°C overnight.

3.1.9 Screening of transformed clones by PCR

The transformants were screened by PCR using Sj16 gene specific primers (Sj16S1 and Sj16P2 for pET28a(+)/Sj16, pET30a(+)/Sj16, pET32a(+)/Sj16, pGEX-4T-1/Sj16 and pCold TF/Sj16; Sj16S1 and Sj16S2 for pTYB4/Sj16). Well isolated, single colonies were picked randomly from plates. Each colony picked was subcultured on a master plate and incubated overnight at 37°C. The master plates were stored at 4°C. Each isolated colonies was resuspended in 100μl of distilled water and boiled for 10 minutes. The resuspension was chilled on ice immediately after boiling, and spun down the cell debris at 16,000 × g for 5 minutes. 10 μl of supernatant which contained the DNA was used as template for PCR. The PCR

reaction was performed as described in methodology 3.1.3. 5 µl of amplified PCR products were electrophoresed at 100V on 2% agarose gel with 0.25 µg/ml ethidium bromide to confirm the clone was transformed with recombinant plasmids. The bacteria-glycerol stock of successfully transformed colony was prepared and stored at -70°C.

3.1.10 Cycle sequencing

The successfully transformed colony with recombinant plasmid as screened by PCR was picked from the master plate, and inoculated into 10 ml of LB medium, and shaken at 37°C, 225 rpm overnight. The recombinant plasmid DNA was then purified as described in methodology 3.1.2. The sequence of the recombinant plasmid was confirmed by DNA sequencing using ABI 3100 DNA sequencer (Applied Biosystem). BigDye® Terminator v3.1 Cycle Sequencing Kit (Applied Biosystem) was used for cycle sequencing. 250 ng of plasmid DNA was mixed with 4 µl of terminator ready reaction mix and 1.6 pmole suitable sequencing primer. The sequencing primers for: pET28a(+)/Sj16, pET30a(+)/Sj16 and pET32a(+)/Sj16: MF596; pGEX-4T-1/Sj16 and pCold TF/Sj16: upper Sj16S1, lower Sj16P2; pTYB4/Sj16: upper Sj16S1, lower Sj16S2. The mixture was made up to a final volume of 10 µl with sterile distilled water in PCR tube. The template DNA was denatured at 96°C for 2 minutes and amplified for 25 cycles with the thermal cycle profile: 96°C for 30 seconds, 50°C for 15 seconds and 60°C for 4 minutes. After the cycle sequencing reaction, the PCR products were purified by ethanol precipitation. The PCR products were transferred into a 1.5 ml centrifuge tube. 1 µl of 3 M sodium acetate (pH5.2) and 25 µl (2.5 volumes) of absolute ethanol were added and mixed gently. The mixture was chilled on ice for at least 15 minutes to precipitate the extension product. The product was centrifuged at 16,000 × g, 4°C for 30 minutes. The supernatant was discarded, and the pellet was rinsed with 250 µl of 75% ethanol

and centrifuged again at 16,000 × g, 4°C for 30 minutes. The supernatant was removed carefully as much as possible, and the pellet was dried under vacuum by SpeedVac (Savant). The dried pellet was resuspended in 10 µl of HiDi formamide (Perkin Elmer), vortexed and heated at 95°C for 5 minutes. The samples were chilled on ice immediately and transferred to MicroAmp® Optical 96-well Reaction Plate (Applied Biosystem), covered by MicroAmp® Strip Caps (Applied Biosystem). The samples were loaded on ABI Prism™ 3100 Genetic Analyzer (Applied Biosystem) for reading the nucleotide sequence. The samples were injected at 2.4 kV for 30 seconds, and electrophoresis was run at 12.2 kV, 42°C for 140 minutes. Raw data of the sequencing reaction were collected by ABI Prism™ 3100 Genetic Analyzer Sequencing Analysis program.

3.1.11 Transformation of plasmids into BL21 (DE3)

After confirmed by cycle sequencing, each recombinant plasmid was transformed into BL21 (DE3) competent cell as described in methodology 3.1.8. Successfully transformed colonies were screened by PCR, and then confirmed by cycle sequencing as described in methodology 3.1.9 and 3.1.10. For expression of recombinant glutathione-S-transferase (GST) of *S. japonicum*, plasmid pGEX-4T-1 (which containing a copy of *S. japonicum* GST cDNA) was transformed into BL21 (DE3) competent cell. The bacteria-glycerol stock of successfully transformed colonies were prepared and stored at -70°C.

3.1.12 Expression of recombinant proteins in bacterial system

3.1.12.1 For BL21 (DE3) transformed with plasmids other than pCold TF/Sj16

After successful transformation of plasmids into the bacterial expression host BL21 (DE3) as described in methodology 3.1.11, single colony was picked and inoculated into 15 ml LB medium supplemented with appropriate antibiotics (50

μg/ml kanamycin for pET28a(+)/Sj16 and pET30a(+)/Sj16, 100 μg/ml ampicillin for pET32a(+)/Sj16, pTYB4/Sj16, pGEX-4T-1/Sj16, and pGEX-4T-1) in a 150 ml flask. The bacterial culture was shaken at 225 rpm, 37°C overnight as a starter culture. 50 μl of overnight starter culture was added to 5 ml pre-warmed LB medium supplemented with appropriate antibiotics (with 1:100 dilution) and shaken at 225 rpm, 37°C until the O.D.600 reached 0.6-0.8. Then the culture was induced by IPTG with a final concentration of 1mM and shaken at 225 rpm, 37°C (98). 1 ml samples were collected at different time points: 3.5 hours for pGEX-4T-1/Sj16 and pGEX-4T-1; and 0.5, 1, 1.5, 2, 2.5, 3, 4 or 24 hours for pET28a(+)/Sj16, pET30a(+)/Sj16, pET32a(+)/Sj16, and pTYB4/Sj16. The collected samples were centrifuged at 16,000 × g for 1 minute. The pellets were resuspended in 100 μl 1 × SDS loading buffer and boiled for 10 minutes. After boiling, the samples were chilled on ice immediately and spun at 16,000 × g for 5 minutes. 15 μl of samples were loaded into 12.5% SDS-PAGE gel and run at a constant voltage of 80 V in stacking gel, and then 120 V in separating gel to analyze the differential expression of the recombinant protein at different time points. The gel was stained with Coomassie blue stain solution overnight and then destained with destain solution for 3 hours.

3.1.12.2 For BL21 (DE3) transformed with pCold TF/Sj16

After successful transformation of the plasmid into the bacterial expression host BL21 (DE3) as described in methodology 3.1.11, single colony was picked and inoculated into 5 ml LB medium supplemented with 100 μg/ml ampicillin in a 50 ml flask. The bacterial culture was shaken at 225 rpm, 37°C until the O.D.600 reached 0.4 – 0.5. Then the culture was refrigerated at 15°C for 30 minutes. The culture was then induced with 0.5 mM IPTG and shaken at 225 rpm, 15°C for 24 hours. 1 ml samples were collected after 24 hours and the protein expression was analyzed by SDS-PAGE gel electrophoresis as described in methodology 3.1.12.1. Sample

collected before IPTG induction was used as control.

3.1.13 Expression and purification of recombinant Sj16 (rSj16) and recombinant GST (rGST)

BL21 (DE3) transformed with pGEX-4T-1/Sj16 or pGEX-4T-1 alone was inoculated into LB medium supplemented with 100 μg/ml ampicillin, and shaken at 225 rpm, 37°C overnight as a starter culture. The overnight starter culture was added to pre-warmed fresh LB medium containing 100 μg/ml ampicillin at a ratio of 1:100 and shaken at 225 rpm, 37°C until the O.D.600 of the culture reached 0.6-0.8. Then the culture was induced by IPTG with a final concentration of 1 mM and shaken at 225 rpm, 37°C for 3.5 hours. The cells were harvested by centrifugation at 12,000 × g for 20 minutes. The pellet from per 100 ml culture was resuspended with 3 ml Binding buffer. Lysozyme was added into the cell suspension at a final concentration of 1 mg/ml and incubated on ice for 30 minutes with occasional vortex. The cell suspension was then sonicated using an ultrasonic processor (GENEQ inc., Canada) for 6 minutes (including the resting time) on ice bath, in short 5 seconds bursts alternated with 10 seconds of resting on ice (98). The disrupted cell suspension was centrifuged at 30,000 × g for 30 minutes, and the supernatant were collected.

The sample was filtered through a 0.45 μm filter immediately before it was applied to the GSTrap HP column (GE Healthcare). The GSTrap HP column was equilibrated with 5 column volumes of Binding buffer, and the sample was applied using a syringe with a flow rate of 0.2 ml/minute. The column was then washed with approximate 20 ml of binding buffer, at a flow rate of 2 ml/minute.

(1) For purification of rGST or rGST-Sj16 fusion protein, the column was eluted with 5 ml of elution buffer with a flow rate of 1 ml/minute, and the eluate containing rGST or rGST-Sj16 fusion protein was collected. The sample was then dialysised against Binding buffer to remove reduced glutathione.

(2) For purification of rSj16, 80 U of thrombin (GE Healthcare) in 1 ml Binding buffer were loaded onto the column using a syringe, and incubated at 24°C for 16 hours. At the end of incubation, a HiTrap Benzamidine FF (high sub) 1 ml column (GE Healthcare) was washed with dH_2O and equilibrated with 20 mM sodium phosphate, 0.15 M NaCl, pH 7.5. The column was then placed in series directly after the GSTrap HP column. The columns were washed with 5 ml Binding buffer, the cleaved rSj16 and the thrombin were washed out from the GSTrap HP column directly onto the HiTrap Benzamidine FF (high sub) 1 ml column. The thrombin was bound to the HiTrap Benzamidine FF, while the rSj16 was passed through and was collected in the eluate.

3.1.14 Removal of endotoxin

The endotoxin in the purified recombinant proteins and solutions were removed using Detoxi-Gel™ Endotoxin Removing Gel (Pierce) according to the manufacturer's protocol. The Endotoxin Removing Gel column was regenerated by washed with 5 ml of 1% sodium deoxycholate (Sigma), followed by 5 ml of pyrogen-free PBS to remove the detergent, and then equilibrated with 5 ml of pyrogen-free PBS again. The sample was applied to the column, followed by loading pyrogen-free PBS if necessary, and the flow-through was collected. Above processes were repeated once more again to remove any bound endotoxin.

3.1.15 Detection of endotoxin

The presence of endotoxin in the purified recombinant proteins and solutions was further detected by Limulus amebocyte lysate (LAL) test using Pyrotell® Gel-Clot Formulation single test vial (Associates of Cape Cod) according to the manufacturer's protocol. 0.2 ml of each teat specimen, 0.2 ml of endotoxin-free LAL reagent water (Associates of Cape Cod), 0.2 ml of control standard endotoxin (Associates of Cape Cod) at concentration of 0.5 EU/ml, 0.25 EU/ml, 0.125 EU/ml

or 0.0625 EU/ml, were added into the single test vials, shaken vigorously for 20-30 seconds, and then placed in 37°C water bath for 60 minutes. The test vials were then removed one at a time, and inverted in one smooth motion. A positive test in indicated by the formation of a gel which does not collapse when the tube is inverted.

3.1.16 Determination of concentration of purified recombinant proteins

The concentration of purified recombinant proteins was determined by method of Bradford using Protein Assay Dye Reagent Concentrate (Bio-Rad). The dye reagent was prepared by diluting 1 part Dye Reagent Concentrate with 4 parts Milli-Q H_2O, and then filtered through a Whatman #1 filter to remove particles. Linear range of BSA standards at 0, 0.1, 0.2, 0.3 0.4 or 0.5 mg/ml were prepared. 10 µl of each sample and standard solution were added into separate 96-well microtiter plate wells (Nunc) in duplicate. 200 µl of diluted dye regent were added to each well, mixed thoroughly, and incubated at room temperature for 5 minutes. The absorbance was measured using a microplate reader (Dynatech Laboratories) at 595 nm, and the concentration of the each sample was calculated according the standard curve using software (Dynatech Laboratories, USA).

3.1.17 Identification of purified recombinant proteins by mass spectrometry

Purified rSj16 or rGST was analyzed by SDS-PAGE gel electrophoresis as described in methodology 3.1.12.1. After destaining, corresponding band representing rSj16 or rGST was excised and cut into small pieces in 1.5 microcentrifuge tube. The gel was destained with 200 µl 50% methanol containing 25 mM NH_4HCO_3 for 10 minutes with vortex, and repeated twice until the gel was colorless. The gel was then dehydrated with 200 µl of acetonitrile (CAN, LAB-SCAN) for 5 minutes, and repeated twice. After the gel was vacuum dried by SpeedVac (Savant) for 5 minutes, approximate 10-15 µl of trypsin (Promega) at concentration of 40 ng/ml in 25 mM NH_4HCO_3 solution were added into the gel and

incubated in ice bath for 30 minutes. Approximate 10 μl of 25 mM NH_4HCO_3 solution were then added onto the gel and incubated at 30°C overnight. After incubation, the tube was sonicated for 10 minutes using a bath sonicator (Branson ultrasonics), and the supernatant were transferred to a new microcentrifuge tube. After 10 μl of 50% ACN containing 2.5% trifluoroacetic acid (TFA) was added onto the gel, the tube was sonicated again for 10 minutes, and the supernatant were transferred and combined with previous part. 0.5 μl of the supernatant was spotted onto the mass spectrometry plate, and waited until air dry. The spotting step was repeated twice. 0.4 μl of matrix solution was then spotted onto each sample and air dried. The plate was subjected to tandem mass spectrometry analysis using ABI 4700 Proteomics Analyzer (Applied Biosystems) and blasted against NCBI eukaryotic database.

3.1.18 Testing the effect of rSj16 expression on bacterial growth

BL21 (DE3) transformed with pGEX-4T-1/Sj16 or pGEX-4T-1 alone was inoculated into LB medium supplemented with 100 μg/ml ampicillin, and shaken at 225 rpm, 37°C overnight as a starter culture. The overnight starter culture was added to pre-warmed fresh LB medium containing 100 μg/ml ampicillin at a ratio of 1:100 and shaken at 225 rpm, 37°C until the O.D.600 of the culture reached 0.6-0.8. 50 μl of each culture was taken out, 1:5 diluted with fresh LB medium, and the O.D.600 was measured. Then each of the culture was aliquoted into 6 flasks: 3 of them were induced by 1 mM IPTG with shake at 225 rpm, 37°C for 3.5 hours; the other 3 of them were shaken at 225 rpm, 37°C for 3.5 hours without IPTG induction. After 3.5 hours, 50 μl of cultures were taken out from each culture flask, 1:5 diluted with fresh LB medium, and the O.D.600 was then measured.

3.2 Evaluation of immunogenicity of rSj16 and detection of Sj16-specific antibody in *Schistosoma japonicum*-infected rabbit sera

3.2.1 Immunogenicity of rSj16

Immunogenicity is the ability of any agent to induce an immune response. To evaluate the immunogenicity of rSj16, rSj16 was applied to immunize BALB/c mice, and rSj16 specific antibodies were then detected by Western-blot and enzyme-linked immunosorbent assay (ELISA)(99). If the rSj16 could provoke the mice to produce rSj16-specific antibodies, it is immunogenicity.

3.2.1.1 Immunization of BALB/c with rSj16

For immunization of one mouse, 25 μg of rSj16 was used for each injection. Each mouse was injected for three times. Appropriate amounts of purified rSj16 for 10 mice were subjected to SDS-PAGE gel electrophoresis as described in methodology 3.1.12.1. The gel was stained in Coomassie blue stain solution (Bio-Rad) for 3 hour and destined in destain solution for 3 hours to visualize the band. The gel was rinsed with distilled water thoroughly. The rSj16 band was cut out using a clean blade and stored in microcentrifuge tubes at -70°C until immunization. For immunization, the cut gel was grinded into a paste using pestle and mortar, then transferred to microcentrifuge tubes and spun down briefly. Equal volume of Freund's adjuvant was added, vortexed to mix. For the first immunization, complete Freund's adjuvant (Sigma) was used; for the second and third immunizations, incomplete Freund's adjuvant (Sigma) was used. The mixture was run through a 23G syringe to sheer the large pieces. Each mouse was injected intradermally with about 0.1 ml of this mixture which containing 25 μg rSj16. After the first immunization, the second and third immunizations were injected at 2 weeks intervals. Immunized mouse serum was obtained 14 days after the last immunization. A sharp blade was used to cut a small wound at the tail and about 500 μl of blood was collected from one mouse. The blood was settled at 4°C for 3 hours and centrifuged at 5000 × g, 4°C for 30 minutes. The clear supernatant was transferred to a clean microcentrifuge

tube and further centrifuged at 16,000 × g, 4°C for 10 minutes. The supernatant was collected, aliquoted and stored at -70°C. Before first injection, about 100 µl of serum, named pre-immunized mouse serum (PIMS) or control mouse serum, was also collected from each mouse. These sera were served as control in the later Western-blot and ELISA analysis.

3.2.1.2 Western-blot analysis of anti-rSj16 antibodies production

1 ml of uninduced or IPTG induced pGEX-4T-1/Sj16/BL21 (DE3) culture (as described in Mothodology 3.1.13) was collected, and centrifuged at 16,000 × g for 1 minute to harvest the cells. The pellet was resuspended with 100 µl 1 × SDS loading buffer. 48 µl (approximate 6 µg) rGST-Sj16 fusion protein or 48 µl (approximate 3 µg) rSj16 was mixed with 12 µl 5 × SDS loading buffer, and boiled for 10 minutes. After boiling, the samples were chilled on ice immediately and spun at 16,000 × g for 5 minutes. 15 µl of each sample was loaded onto each 12.5% SDS-PAGE gel (total 3 gels) and run as described in Methodology 3.1.12.1. For Western-blot, for each gel, 6 pieces of 3mm filter paper were cut into appropriate size and pre-soaked in transfer buffer. PVDF membrane was cut into appropriate size, wetted in 100% methanol for several seconds and rinsed with transfer buffer. The assembly was set up (from bottom to top) by stacking 3 pieces of filter papers, the PVDF membrane, the SDS-PAGE gel and another 3 pieces of filter paper at the semi-dry transblotter (Bio-Rad) (100). After transferred at 15V constant voltage for 45 minutes, the membranes was removed. One of the membranes was stained with amido black staining solution for approximate 10 minutes and than destained with amido black destaining solution. The other two membranes were blocked with 5% non-fat milk solution overnight (100). Preimmunized or rSj16 immunized mouse serum was used as primary antibody and added with the dilution of 1:3000 in 5% non-fat milk containing 0.05% Tween 20. The membranes were incubated at room temperature for 2 hours with

shaking. The membranes were washed 10 minutes × 3 times with shaking using PBS containing 0.05% Tween 20. Alkaline phosphatase (AP) conjugated horse anti-mouse IgG (H+L) (Vector) was added with the dilution of 1:1000 in 5% non-fat milk containing 0.05% Tween 20 as secondary antibody, and incubated at room temperature for 1 hour with shaking. The membranes were washed 3 times as above and then further washed 10 minutes with AP buffer. Color development was done by adding each membrane into 10 ml AP color-development solution (100). The membranes were incubated at room temperature until color developed, then washed with PBS containing 2 mM EDTA and air-dried at room temperature.

3.2.1.3 ELISA detection of anti-rSj16 antibodies production

ELISA assays were performed as previously described with some modification (101). 96-well MaxiSorp plates (Nunc) were coated overnight at 4°C with 100 µl/well of 5 µg/ml rSj16 in carbonate-bicarbonate buffer (pH 9.6). The plates were then washed three times with TBST buffer, and were blocked at RT for 2 hours with 200 µl of TBS buffer containing 1% BSA. The plates were washed three times, and individual preimmunized or rSj16 immunized mouse serum 2-fold serially diluted in TBST containing 1% BSA beginning at 1/500 was applied to the wells in duplicate. The plates were incubated for 2 hours at room temperature, and then washed for 5 times with TBST. 1/2000 diluted peroxidase- rat anti-mouse IgG (Zymed) were added in the plates and incubated at room temperature for 2 hours. The plates were again washed five times, developed with 100 µl/well substrate solution (Sigma) and then stopped with 50 µl/well 1 M H_2SO_4. The optical densities were read at 450 nm using a microplate reader (Dynatech Laboratories). Serum titers are defined as the dilutions which give optical density readings at least two-fold higher than the mean background of unimmunized mouse serum.

3.2.2 Detection of anti-Sj16 antibody in *S. japonicum*-infected rabbits

Normal rabbit sera (NRS) from uninfected New Zealand white rabbits and *S. japonicum*-infected rabbit sera (IRS) from New Zealand white rabbits subcutaneously infected with 2000 *S. japonicum* cercariae for 45 days were generous gifts from Dr. Zhongdao Wu, Department of Parasitology, Zhongshan School of Medicine, Sun Yat-sen University, P.R.China.

3.2.2.1 Preparation of *S. japonicum* soluble worm antigen preparation (SWAP)

300 *S. japonicum* worms obtained by liver perfusion of infected rabbits were washed and suspended in 1.0 ml of PBS (pH 7.4). The worms were homogenized with homogenizers, followed by sonication with an ultrasonic processor (GENEQ inc.) for 6 minutes (including the resting time) on ice bath, in short 5 seconds bursts alternated with 10 seconds of resting on ice (102-104). The antigen was then centrifuged at 16,000 × g for 60 min at 4°C. The supernatant was filtered through a 0.45μm membrane filter and stored at -70°C. Protein content was 10 mg/ml as measured by Bradford method as described in Methodology 3.1.16.

3.2.2.2 Western-blot analysis of anti-Sj16 antibody in infected rabbits

48 μl (approximate 3 μg) rSj16 was mixed with 12 μl 5 × SDS loading buffer, and boiled for 10 minutes. 20 μl SWAP (10 mg/ml) was mixed with 40 μl 1.5 × SDS loading buffer, and boiled for 10 minutes. After boiling, the samples were chilled on ice immediately and spun at 16,000 × g for 5 minutes. 15 μl of each sample was loaded onto each 12.5% SDS-PAGE gel (total 3 gels) and run as described in Methodology 3.1.12.1. For Western-blot, for each gel, 6 pieces of 3mm filter paper were cut into appropriate size and pre-soaked in transfer buffer. PVDF membrane was cut into appropriate size, wetted in 100% methanol for several seconds and rinsed with transfer buffer. The assembly was set up (from bottom to top) by stacking 3 pieces of filter papers, the PVDF membrane, the SDS-PAGE gel and another 3 pieces of filter paper at the semi-dry transblotter (Bio-Rad). After transferred at 15V

constant voltage for 45 minutes, the membranes was removed. One of the membranes was stained with amido black staining solution for approximate 10 minutes and than destained with amido black destaining solution. The other two membranes were blocked with 5% non-fat milk solution overnight. Normal rabbit sera (NRS) or *S. japonicum*-infected rabbit sera (IRS) was used as primary antibody and added with the dilution of 1:1,000 in 5% non-fat milk containing 0.05% Tween 20. The membranes were incubated at room temperature (RT) for 2 hours with shaking. The membranes were washed 10 minutes × 3 times with shaking using PBS containing 0.05% Tween 20. AP conjugated anti-rabbit IgG (Boeringer Mannheim) was added with the dilution of 1:1000 in 5% non-fat milk containing 0.05% Tween 20 as secondary antibody, and incubated at room temperature for 1 hour with shaking. The membranes were washed 3 times as above and then further washed 10 minutes with AP buffer. Color development was done by adding each membrane into 10 ml AP color-development solution. The membranes were incubated at room temperature until color developed, then washed with PBS containing 2 mM EDTA and air-dried at room temperature. If the anti-serum could probe against a protein, purple-grey band would appear.

3.2.2.3 Detection of anti-Sj16 antibody in infected rabbits by ELISA

ELISA assays were performed as previously described with some modification (101). 96-well MaxiSorp plates (Nunc) were coated overnight at 4°C with 100 µl/well of 5 µg/ml rSj16 in carbonate-bicarbonate buffer (pH 9.6). The plates were then washed three times with TBST buffer, and were blocked at RT for 2 hours with 200 µl of TBS buffer containing 1% BSA. The plates were washed three times, and individual NRS or IRS 2-fold serially diluted in TBST containing 1% BSA beginning at 1/50 was applied to the wells in duplicate. The plates were incubated for 2 hours at room temperature, and then washed for 5 times with TBST. 1/3000 diluted

peroxidase- goat anti-rabbit IgG (H+L) (Zymed) were added in the plates and incubated at room temperature for 2 hours. The plates were again washed five times, developed with 100 µl/well substrate solution (Sigma) and then stopped with 50 µl/well 1 M H_2SO_4. The optical densities were read at 450 nm using a microplate reader (Dynatech Laboratories). Serum titers are defined as the dilutions which give optical density readings at least two-fold higher than the mean background of NRS.

3.3 Evaluation of the anti-inflammatory activity of rSj16

Thioglycollate has been widely used as an agitator of acute peritoneal inflammation model in mouse (105). In this study, thioglycollate-induced peritoneal inflammation model was used to assess the anti-inflammatory function of rSj16.

3.3.1 Experimental peritonitis

Different concentrations of rSj16 (5 µg, 0.5 µg, 0.05 µg, 17ng, 1.7ng, or 0.17ng) in 1 ml PBS, rGST (5 µg or 0.5 µg) in 1 ml PBS, or 1 ml PBS alone were injected into peritoneal cavity of groups of 6 BALB/c mice. 1 hour later, each mouse was further injected with 1 ml of aged 3% Brewer thioglycollate medium (TG; Difco) or PBS and incubated for the time indicated for leukocytes recruitment(105, 106). The mice were then cervical dislocated, and the total peritoneal exudate cells (PECs) were isolated by lavage of the peritoneal cavity with sterile PBS as described before(107). The total PECs from each mouse were counted using a hemacytometer (Hausser Scientific). In some experiments, the peritoneal lavage fluids were centrifuged at 4°C, 300 × g for 10 min, and the cell pellets were then subjected to RNA isolation and real-time RT-PCR analysis as described below. The peritoneal membranes were also collected for RNA isolation and real-time RT-PCR analysis.

3.3.2 Cytospin and staining of PECs

A cytospin smear of the total PECs was prepared and stained with modified Wright-Giemsa stain (Sigma), and differential cell counts were performed using a

light microscope (Nikon). For cytospin, microscopic slides were cleaned with 70% ethanol. The slides were assembled on the clipper by assembling the filter card between the sample chamber and microscopic slide. The whole setup was stood vertically and samples were applied to the sample chamber. The number of cells loaded was 5×10^4 in 100 µl cell suspension. The setup was put into the cytocentrifuge (Shandon, USA), spun at 500 rpm for 5 minutes. The samples were air-dried after cytospin. The cytospin smear was stained with modified Wright-Giemsa stain according to the manufacturer's manual. For staining, the smear was fixed in methanol for 1 minute and dried. Then the smear was immersed into Wright-Giemsa stain for approximate 30 seconds. The smear was then removed from the stain and placed into Milli-Q H_2O for 10 minutes. The smear was then rinsed briefly with running water Milli-Q H_2O, and air-dried thoroughly. The stained smear was last embedded with mounting medium and covered with coverslip. The morphology of the cells was observed under microscope, and the differential cell counts were performed.

3.3.3 Cell cytotoxicity of rSj16 on PECs

The cell cytotoxicity was assessed by measuring the lactate dehydrogenase (LDH) released into culture supernatants using Cytotoxicity Detection Kit (Roche Molecular Biochemicals) according to the manufacturer's instruction. Briefly, PECs were isolated from normal BALB/c mice (resident PECs), 3 hours post 3% TG-treated mice (3 hours PECs) or 3 d post 3% TG-treated mice (3 d PECs) as mentioned in Methodology 3.3.1. The cells were suspended in RPMI 1640 medium (GibcoBRL) supplemented with 1% fetal bovine serum (GibcoBRL), 10 mM L-glutamine, 100 U/ml penicillin, 100 µg/ml streptomycin, and 0.25 µg/ml amphotericin B (assay medium). Cells at optimal density were then incubated with assay medium containing 0.5 µg/ml rSj16 in a volume of 200 µl/well in 96-well microplate (Nunc)

for 24 h. The controls were set as following: background control, assay medium; low control, PECs in assay medium; high control, PECs in assay medium containing 1% Triton X-100; substance control, assay medium containing 0.5 μg/ml rSj16. The plate was then centrifuged, 100 μl supernatant from each well was removed and incubated for 20 min with reaction mixture. The absorbance was measured using a microplate reader (Dynatech Laboratories) at a wavelength of 492 nm with a reference wavelength of 620 nm. Each assay was performed in triplicate. According to the optical density values, the cytotoxicity was calculated: cytotoxicity (%) = (experimental value-low control)/(high control-low control)×100.

3.3.4 Peripheral white blood cell (WBC) count

Groups of 4 BALB/c mice were i.p. injected with 0.5 μg rSj16 in 1 ml PBS, or 1 ml PBS alone, and incubated for 48 h. 20 μl blood samples were then collected from each mouse by tail bleeds and dropped into 0.38 ml 3% acetic acid solution, mixed gently. The total number of WBCs was then counted using a hemacytometer (Hausser Scientific).

3.3.5 Isolation of total RNA from PECs and peritoneal membrane

Total RNA was extracted using TRIZOL reagent (Invitrogen) according to the manufacturer's protocol. Once cut out, the peritoneal membranes were immediately frozen in waiting liquid nitrogen in the mortar, and ground into powder with a cold pestle. The powders were then transferred to a manual homogenizer containing 1 ml TRIZOL and homogenized thoroughly. The PECs were harvested by centrifuging the total peritoneal fluids at 4°C, 300 × g for 10 min. The cell pellet were resuspended with 1 ml of TRIZOL, and pipetted up and down for several times to facilitate the lysis of the cells. Both kinds of samples in TRIZOL were incubated at room temperature for 5 minutes to permit the complete dissociation of nucleoprotein complexes. 0.2 ml of chloroform was added into each tube, shaken vigorously by

hand for 15 seconds, and incubated at room temperature for 3 minutes. The samples were centrifuged at 12,000 × g for 15 minutes at 4°C. Following centrifugation, the aqueous phase was transferred into a fresh tube and mixed with 0.5 ml of isopropyl alcohol. The samples were incubated at room temperature for 10 minutes and then centrifuged at 12,000 × g for 10 minutes at 4°C. The supernatant were removed and the RNA pellet was washed twice with 1 ml 75% ethanol, and then centrifuged at 7,500 × g for 5 minutes at 4°C. The RNA pellet was vacuum dried for about 10 minutes and dissolved in RNase-free water. The quality and quantity of the extracted RNA was determined by measuring the O.D.260 and O.D.280.

3.3.6 Reverse transcription

Reverse transcription was performed using M-MLV reverse transcriptase (Invitrogen) according to the manufacturer's manual. 1 μg of total RNA in 10 μl distilled water was incubated with 0.5 μg (1 μl) oligo $(dT)_{12-18}$ (Amersham Pharmacia biotech), 1 μl of 10 mM each dNTP (Amersham Pharmacia biotech) at 65°C for 5 minutes and chilled on ice immediately. Then 4 μl of 5 × First-Strand Buffer, 2 μl of 0.1 M DTT, 1 μl of RNaseOUT (Invitrogen) were added into the tube, and incubated at 37°C for 2 minutes. 1 μl of M-MLV reverse transcriptase was added into the mixture and mixed by pipetting gently up and down. The total reaction mixture with final volume of 20 μl was incubated at 37°C for 60 minutes, and then inactivated at 70°C for 15 minutes. The reaction mixture was then diluted 5 fold with distilled water after the RT reaction. The diluted sample was boiled for 5 minutes to denature the first strand DNA from the RNA template and then chilled on ice immediately for 2 minutes. The diluted sample was stored at -70°C.

3.3.7 Detection of cytokines and chemokines mRNA by real-time RT-PCR analysis

The mRNA expression of cytokine and chemokines was measured by real-time

RT-PCR using the iQ5 Real-Time PCR Detection System (Bio-Rad) according to the manufacturer's instructions. Briefly, The real time PCR were set as 25 μl reaction containing 12.5 μl of 2 × iTaq™ SYBR Green Supermix (Bio-Rad), 5 μl of diluted cDNA sample (see Methodology 3.3.6), 1 μl of forward primer (25 μM) and 1 μl reverse primer (25 μM). The real-time PCR was performed for 40 cycles of denaturation at 95°C (30 sec), annealing at optimal temperature (30 sec), and extension at 72°C (40 sec). The threshold cycle of each PCR was converted to a DNA equivalent by reading against standard curves generated by amplifying dilutions of cDNA containing the relevant target sequences. The mRNA expression was determined as the ratio of the each gene to glyceraldehyde 3-phosphate dehydrogenase (GAPDH)(108-110).

3.4 Assessing the effect of rSj16 on the adaptive immune responses to heterologous antigen HSA

3.4.1 Method of immunization

Female BALB/c mice, 10-week-old, were used in this experiment (Fig. 3.4.1). Groups of four mice were immunized i.p. with PBS followed 1 hour later by HSA (50 μg); PBS followed 1 hour later by alum (1.3 mg) along with HSA (10 μg) (alum-HSA), 0.5 μg rSj16 followed 1 hour later by alum-HSA, PBS followed 1 hour later by alum-HSA along with 0.5 μg rSj16, 0.5 μg rGST followed 1 hour later by alum-HSA; PBS followed 1 hour later by LPS (25 μg) along with HSA (50 μg) (LPS-HSA), 0.5 μg rSj16 followed 1 hour later by LPS-HSA, PBS followed 1 hour later by LPS-HSA together with 0.5 μg rSj16, 0.5 μg rGST followed 1 hour later by LPS-HSA in a total volume of 250 μl. Two weeks later, mice were boosted by i.p. with the same antigens used for sensitizing(111). All mice were challenged i.p. daily using 5 μg HSA from day 22 to 24. 4 mice i.p. injected with 250 μl Dulbecco's PBS at the same time point were used as control(111). Serum samples were obtained for

antibody determination after sensitization, boost and last challenge at day 13, 21 and 25 respectively. Mice were sacrificed 24 hour after last challenge and the spleens were isolated for analysis.

In addition, groups of four mice were immunized i.p. with PBS followed 1 hour later by PSA (50 μg), PBS followed 1 hour later by LPS (25 μg)-PSA (50 μg), 0.5 μg rSj16 followed 1 hour later by LPS-PSA, 0.5 μg rGST followed 1 hour later by LPS-PSA in a total volume of 250 μl. The mice were then boosted with the same antigens 2 week later, and challenged i.p. daily using 5 μg PSA from day 22 to 24. One day following the last challenge, serum samples were collected for antibody determination.

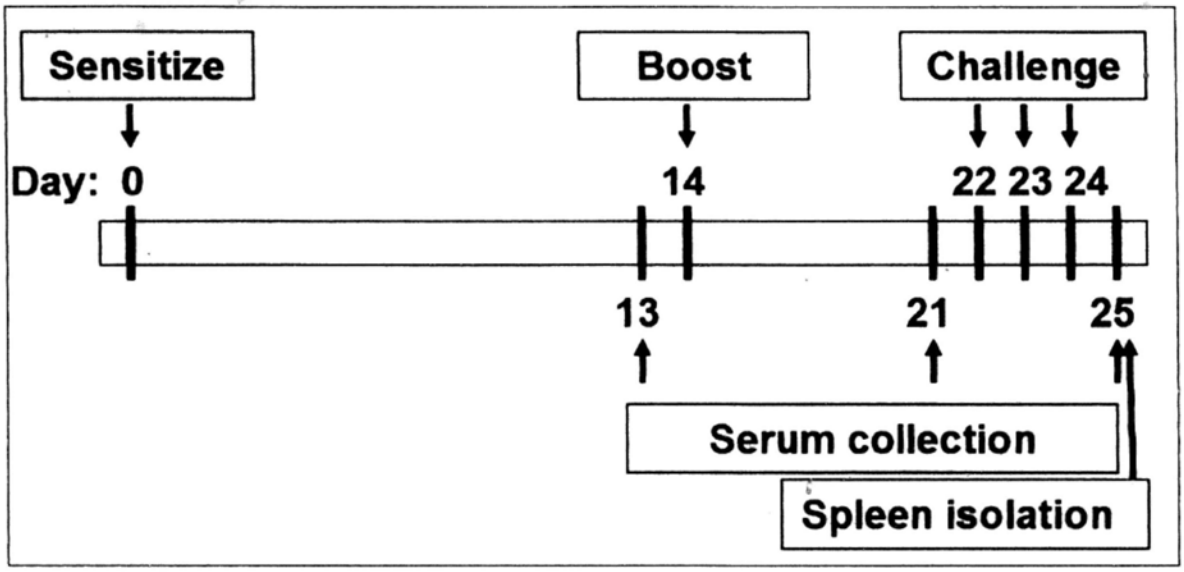

Fig.3.4.1 Methods of immunization. Groups of four BALB/c mice were immunized i.p. with HSA, alum along with HSA (alum-HSA), rSj16 followed 1 hour later by alum-HSA, alum-HSA along with rSj16, rGST followed 1 hour later by alum-HSA, LPS along with HSA (LPS-HSA), rSj16 followed 1 hour later by LPS-HSA, LPS-HSA together with rSj16, or rGST followed 1 hour later by LPS-HSA; PSA, LPS along with PSA (LPS-PSA), rSj16 followed 1 hour later by LPS-PSA, rGST followed 1 hour later by LPS-PSA. Two weeks later, mice were boosted by i.p. with the same antigens used for sensitizing. All mice were challenged i.p. daily using 5 μg HSA or PSA from day 22 to 24. 4 mice i.p. injected with 250 μl Dulbecco's PBS at the same time point were used as control. Serum samples were obtained for antibody determination after sensitization, boost and last challenge at day 13, 21 and 25 respectively. Mice were sacrificed 24 hour after last challenge and the spleens were isolated for analysis.

3.4.2 Determination of ag-specific IgG, IgM, IgA, IgE, IgG1 and IgG2a

Serum levels of Ag-specific Abs were determined by ELISA(111). Briefly, 96-well MaxiSorp plates (Nunc, Denmark) were coated overnight at 4°C with 100 μl/well of 5 μg/ml HSA or PSA in carbonate-bicarbonate buffer (pH 9.6). The plates

were then washed three times with TBS (50mM Tris, 0.14 M NaCl, pH8.0) containing 0.05% Tween 20, and were blocked at RT for 2 hour with 200 ul of TBS containing 1% BSA. For IgG, IgM, IgA, IgG1 and IgG2a, plates were washed three times, and individual serum 2-fold serially diluted in sample diluent (TBS containing 0.05% Tween 20 and 1% BSA) beginning at 1/100 was applied to the wells in duplicate. For IgE, serum in 1/6 dilution in sample diluent was plated in duplicate after three times wash. The plates were incubated for 2 housr at RT, and then washed for 5 times. For the detection of antigen-specific IgG, IgM and IgA, optimally diluted peroxidase- rat anti-mouse IgG (1/2000 dilution, Zymed, USA), peroxidase-goat anti-mouse IgM (1/4000 dilution, Zymed, USA) and IgA (1/2000 dilution, Zymed, USA) were incubated in the plates at RT for 2 h. For the detection of antigen-specific IgG1, IgG2a and IgE, the plates were incubated with biotin-rat anti-mouse IgG2a (1/2000 dilution, BD Pharmingen, USA), IgG1 (1/4000 dilution, BD Pharmingen, USA) and IgE (1/2000 dilution, BD Pharmingen, USA) at RT for 1 h, washed for 5 times, and then incubated with Streptavidin-Horseradish Peroxidase (1/1000 dilution, BD Pharmingen, USA) for 1 hours at RT. The plates were again washed five times, developed with substrate solution (Sigma, USA) and then stopped with 1 M H_2SO_4. The optical densities (O.D.) were read at 450 nm using a microplate reader (Dynatech Laboratories, USA). Except IgE, serum titers are defined as the dilutions which give optical density readings at least two-fold higher than the mean background of unimmunized mouse serum. Levels of HSA-specific IgE were presented as the absorbance at 450 nm from duplicate wells of 1/6 serum dilution.

3.4.3 Preparation of spleen cell suspensions

100 μm cell strainers were placed in 60 mm petri dishes (one for each spleen) containing 8-10 ml of complete RPMI-1640 medium (111). Freshly removed spleens were placed in the cell strainers, and cut in several places with scissors. The spleens

were then mashed through the cell strainers into the petri dishes using the end of a 5 ml syringe plunger. The cell strainers were rinsed with 5 ml of complete RPMI-1640 medium. The suspended cells were transferred into 15 ml centrifuge tubes, and centrifuged at 300 × g for 5 minutes. The supernatants were discarded, and the pellets were resuspended in 3 ml of red blood cell lysis buffer and incubated at room temperature for 5 minutes. The cells were centrifuged as before. The supernatants were discarded and the pellets were resuspended in 5 ml of complete RPMI-1640 medium. 10 µl of cell suspensions were diluted in trypan blue solution and the cell number were counted with hemacytometer (Hausser Scientific).

3.4.4 *In vitro* culture of spleen cell

Spleen cell suspensions from naïve or antigen-immunized mice were prepared as described in Methodology 3.1.3. Cell suspensions containing 1×10^6 spleen cells/ml were cultured with or without HSA (5 µg/ml) in complete RPMI-1640 medium containing 5×10^{-5} M 2-mercaptoethanol (Sigma, USA) in flat-bottom 24-well plates (Nunc) or in flat-bottom 96-well plates (Nunc) at 37°C(111). After 48 hours incubation, cell supernatants in 24-well plates were collected and stored at -80°C until cytokines determination. Spleen cell proliferation in 96-well plates was assessed as described below (see Methodology 3.4.5) after 72 hours incubation.

Spleen cell suspensions from naïve or LPS-HSA immunized (as described in Methodology 3.1.1) mice were also prepared and pre-treated with 0.5 µg/ml of rSj16, 0.5 µg/ml of rGST or PBS for 1 hours, and then incubated at 37°C for 72 hours in the presence of 5 µg/ml of ConA (for spleen cell from naïve mice) or 5 µg/ml of HSA (for spleen cell from LPS-HSA immunized mice). The spleen cell proliferation was then assessed.

3.4.5 Spleen cell proliferation assay

Spleen cell proliferation was determined with BrdU cell proliferation ELISA

(Roche Applied Science) according to the manufacturer's manual. Briefly, after treatment, the cells were added with 10 μM BrdU and incubated at 37°C for 3 hours. The plates were then centrifuged at 300 × g for 10 minutes, and the media were removed by suction. After dried at 60°C for 1 hour, the cells were incubated with 200 μl/well of FixDenat for 30 minutes at room temperature. After removal of FixDenat, the cells were incubated with 100 μl/well of anti-BrdU-POD working solution for 90 minutes at room temperature, followed by three washes with washing solution. 100 μl of substrate solutions were added to each well, incubated for 20 minutes at room temperature, and then stopped with 2 N H_2SO_4. The absorbances were measured in a microplate reader (Dynatech Laboratories, USA) at 450 nm with a reference wavelength of 690 nm. The results were expressed as proliferation indexes which equal to the ratio of mean O.D. 450 of triplicate wells with HSA or ConA stimulation /mean O.D.450 of corresponding triplicate wells without HSA or ConA stimulation.

3.4.6 Cytokine determination by Sandwich ELISA

Levels of IL-10 and IFN-γ in the culture supernatants were measured using DuoSet ELISA Development kit (R&D Systems, USA) according to the manufacturer's protocol. Briefly, 96-well Maxisorp multititer plates (Nunc) were coated overnight at 4°C with appropriate capture Abs (4 μg/ml) in PBS at pH 7.4, and then washed three times with PBS containing 0.05% Tween 20. The plates were blocked for 2 hours at room temperature with 1% BSA in PBS, followed with three washes as described above. Murine recombinant cytokine standards IL-10 (0–2,000 pg/ml), or IFN-γ (0 –2,000 pg/ml) and the culture supernatants were then added in duplicate and incubated for 2 hours at room temperature. After three washes, the plates were incubated for 2 hours at room temperature with appropriate biotinylated detection Abs, and then washed again. To detect biotinylated Abs, streptavidin-linked horseradish peroxidase (1/1,000 dilution) was added and incubated for 20 minutes in

the dark at room temperature. After a final washing of five times, 3,3',5,5'-tetramethylbenzidine liquid substrate (TMB, Sigma) was added to each well. The absorbance was read at 450 nm with the wavelength correction at 570 nm using a microplate reader (Dynatech Laboratories, USA), and the concentration of the samples was calculated using the standard curve.

3.4.7 Cytokine determination by FlowCytomix

Levels of GM-CSF, IL-1α, IL-2, IL-4, IL-5, IL-6, IL-17 and TNF-α in the culture supernatants were measured using FlowCytomix kit (Bender MedSystems, Austria) according to the manufacturer's manual. Briefly, 25 μl of each standard mixture dilution, 25 μl of each sample, or 25 μl of assay buffer (PBS with 1% BSA, served as blank) were mixed with 25 μl of bead mixture respectively. 50 μl of biotin-conjugate mixture were then added to each tube, and incubated in dark at RT for 2 hours. The tubes were washed twice with 1 ml of assay buffer, and then added with 50 μl of streptavidin-PE solution, and incubated in dark at RT for 1 hour. After two washes, the contents in each tube were resuspended with 500 μl assay buffer and subjected to flow cytometry analysis with a FC500 instrument (Beckman Coulter, USA). The concentration of each cytokine in the supernatants was calculated using FlowCytomix Pro 2.2 software (Bender MedSystems).

3.5 Effects of rSj16 on the differentiation of JCS and hematopoiesis of mouse bone marrow cells

3.5.1 Anti-proliferative effect of rSj16 on JCS

The colorimetric MTT (*3-(4, 5-dimethylthiazolyl-2)-2, 5-diphenyltetrazolium bromide*) assay was employed to quantify the cell proliferation(112, 113). Briefly, JCS cells were incubated with complete RPMI 1640 medium containing serially diluted rSj16 or rGST in 96-well microplates (Nunc) for 24 hours, 48 hours, 72 hours, or 96 hours. 20 μl MTT (5mg/ml stock solution, Sigma, USA) were then added into

each well and incubated for 4 h, and the plates were centrifuged at 500 × g for 10 min. The MTT solution was removed and replaced by 150 µl of DMSO, and the plates were shaken until the formazans were thoroughly dissolved. The optical density was determined using a microplate reader (Dynatech Laboratories) at a wavelength of 570 nm. Each assay was performed in triplicate.

3.5.2 Effect of rSj16 on JCS Cell viability

Cell viability was determined using trypan blue exclusion assay(114). JCS cells were incubated with complete RPMI 1640 medium in the presence or absence of 0.5 µg/ml rSj16 or 0.5 µg/ml rGST for 24 hours, 48 hours and 72 hours. The cells were then collected and mixed 1:1 with 0.4% trypan blue (Sigma, USA). The percentage of viable cells was recorded within 10 minutes with an inverted microscope. Greater than 300 cells per sample were examined and the data were expressed as percentage (%) viability.

3.5.3 Cell cycle analysis

Cell cycle analysis was performed on JCS cells incubated for 1-4 days with either rSj16 (0.5 µg/ml) or rGST (0.5 µg/ml) (115). After treatment, the cells were collected, and washed three times with PBS. The cells were then fixed in chilled ethanol overnight. The cells were again washed with PBS for three times, and then stained by incubated with propidium iodide staining solution (3.8 mM sodium citrate, 50 µg/ml propidium iodide in PBS) containing 50 µg/ml RNase A at room temperature for 30 minutes. Analysis was performed immediately after staining using a FACScan (Becton Dickinson, USA) and CELLFit program (Becton Dickinson, USA).

3.5.4 Analysis of JCS cell differentiation

JCS cells were cultured with either rGST (0.5 µg/ml), or rSj16 (0.5 µg/ml) in the presence/absence of serially diluted neutralizing anti-IL-1α, anti-IL-1β, anti-TNF-α, or these three antibodies together (R&D Systems) for up to 72 hours. The adherent

and suspension cells were collected respectively and counted with a hemacytometer (Hausser Scientific) 24, 48, and 72 hours after treatment. The percentage of adherent cells was calculated. The culture supernatants after 24, 48, and 72 hours treatment were collected, stored at -80°C until cytokine analysis.

The morphology of the JCS cells after treated with rGST (0.5 μg/ml), PBS control, or rSj16 (0.5 μg/ml) was studied up to 72 hours of treatment using a phase-contrast microscope (Nikon, Japan). Monocytic differentiation of the treated cells was also examined using modified Wright-Giemsa stain (Sigma). For monocytic differentiation examination, JCS cells were treated with 0.5 μg/ml rSj16, 0.5 μg/ml rGST or PBS control for 3 days. The cells were then collected and subjected to cytospin and Wright-Giemsa staining. For cytospin, microscopic slides were cleaned with 70% ethanol. The slides were assembled on the clipper by assembling the filter card between the sample chamber and microscopic slide. The whole setup was stood vertically and samples were applied to the sample chamber. The number of cells loaded was 5×10^4 in 100 μl cell suspension. The setup was put into the cytocentrifuge (Shandon), spun at 500 rpm for 5 minutes. The samples were air-dried after cytospin. The cytospin smear was stained with modified Wright-Giemsa stain. For staining, the smear was fixed in methanol for 1 minute and dried. Then the smear was immersed into Wright-Giemsa stain for approximate 30 seconds. The smear was then removed from the stain and placed into Milli-Q H_2O for 10 minutes. The smear was then rinsed briefly with running water Milli-Q H_2O, and air-dried thoroughly. The stained smear was last embedded with mounting medium and covered with coverslip. The morphology of the cells was observed under microscope. All experiments were independently done at least 3 times.

Expression of cell surface antigens was determined by flow cytometry 72 hours after treatment(93, 116). After twice washing with FACS medium (phosphate-

buffered saline (PBS), supplemented with 2% heat-inactivated FCS and 0.05% sodium azide). JCS cells were incubated for 30 minutes with anti-mouse FcγR Ab (CD16/CD32, eBioscience, USA). The cells were then washed twice with FACS medium, and incubated 30 minutes with affinity purified anti-mouse F4/80 or anti-mouse Gr-1 antibodies (both from eBioscience, USA). Isotype-matched control antibodies (eBioscience, USA) were used as negative control. Unbound antibodies were removed by washing the cells twice with FACS medium. The cells were then stained with FITC-conjugated sheep anti-rat IgG (BD Pharmingen, USA) for 30 minutes, washed 3 times with FACS medium, and fixed with 1% (w/v) paraformaldehyde in PBS. Cells were analyzed by a FACScan (Becton Dickinson).

Phagocytic activity of JCS was determined by the modified yeast phagocytosis assay as described previously(117, 118). Briefly, opsonized yeasts were prepared by incubating heat-inactivated yeast cells (*Saccharomyces cerevisiae*) with fresh mouse serum at 37°C for 30 minutes. 2×10^7 opsonized yeasts were added to untreated, 72 hours post rSj16 or rGST treated JCS cell cultures in a 6-well microplate (Nunc). The mixtures were incubated at 37°C for 16 hours, and the percentages of phagocytic cells were counted. Cells with a minimum of three ingested yeasts were considered positive. A total of 500 cells were counted in each sample.

3.5.5 Apoptosis analysis

To study the induction of apoptosis by rSj16, annexin V assay (Annexin V-FITC Apoptosis Detection Kit; BD Pharmingen, USA) was performed according to the manufacturer's instructions. Briefly, JCS cells were harvested 1, 2, or 3 days after exposure to either rSj16 (0.5 μg/ml) or rGST (0.5 μg/ml), washed twice with PBS, incubated with FITC conjugated annexin V and PI for 15 minutes, and measured by FACScan (Becton Dickinson, USA).

3.5.6 Cytokine determination

Levels of IL-1α, IL-1β, and TNF-α in the culture supernatants were measured using DuoSet ELISA Development kit (R&D Systems, USA) according to the manufacturer's protocol. Briefly, 96-well Maxisorp multititer plates (Nunc, Denmark) were coated overnight at 4°C with appropriate capture Abs (2 μg/ml for anti-IL-1α, 4 μg/ml for anti-IL-1β, and 0.8 μg/ml for anti-TNF-α) in PBS at pH 7.4, and then washed three times with PBS containing 0.05% Tween 20. The plates were blocked for 2 hours at room temperature with 1% BSA in PBS, followed with three washes as described above. Murine recombinant cytokine standards IL-1α (0–1,000 pg/ml), IL-1β (0 –1,000 pg/ml), or TNF-α (0 –1,000 pg/ml) and the culture supernatants were then added in duplicate and incubated for 2 hours at room temperature. After three washes, the plates were incubated for 2 hours at room temperature with appropriate biotinylated detection Abs, and then washed again. To detect biotinylated Abs, streptavidin-linked horseradish peroxidase (1/1,000 dilution) was added and incubated for 20 minutes in the dark at room temperature. After a final washing of five times, 3,3′,5,5′-tetramethylbenzidine liquid substrate (TMB, Sigma, USA) was added to each well. The absorbance was read at 450 nm with the wavelength correction at 570 nm using a microplate reader (Dynatech Laboratories, USA), and the concentration of the samples was calculated using the standard curve.

3.5.7 IL-1α, IL-1β, and TNF-α neutralization assay (by MTT assay)

For neutralization assay, JCS cells were incubated in 96-well microplates (Nunc) with complete RPMI 1640 medium containing 0.5 μg/ml rSj16 in the presence or absence of serially diluted neutralizing anti-IL-1α, anti-IL-1β, anti-TNF-α, or these three antibodies together (R&D Systems) for 72 hours. To test whether anti-IL-1α, anti-IL-1β or anti-TNF-α antibody itself affects the JCS proliferation, JCS cells were also incubated in 96-well microplates (Nunc) with RPMI 1640 medium containing serially diluted anti-IL-1α, anti-IL-1β or anti-TNF-α antibody (R&D Systems). 20 μl

MTT (5mg/ml stock solution, Sigma, USA) were then added into each well and incubated for 4 h, and the plates were centrifuged at 500 × g for 10 min. The MTT solution was removed and replaced by 150 μl DMSO, and the plates were shaken until the formazans were thoroughly dissolved. The optical density was determined using a microplate reader (Dynatech Laboratories) at a wavelength of 570 nm. Each assay was performed in triplicate. For testing the effect of anti-IL-1α, anti-IL-1β or anti-TNF-α antibody itself on JCS proliferation, the results were expressed as inhibition index which was calculated as following: **inhibition index** = mean O.D.570 of triplicate wells with RPMI 1640 medium containing anti-IL-1α, anti-IL-1β or anti-TNF-α antibodies/mean O.D.570 of triplicate wells with RPMI 1640 medium alone. For neutralization assay, the results were expressed as proliferation index which was calculated as following: **proliferation index** = mean O.D.570 of triplicate wells containing 0.5 μg/ml rSj16 in the presence of neutralizing anti-IL-1α, anti-IL-1β or anti-TNF-α antibodies/ mean O.D.570 of triplicate wells containing 0.5 μg/ml rSj16 in the absence of neutralizing anti-IL-1α, anti-IL-1β or anti-TNF-α antibodies.

3.5.8 Mouse bone marrow cell colony-forming unit assay

Female BALB/c mice of 6-8-week old were sacrificed and wet thoroughly with 70% ethanol. The femurs were isolated and the ends of the bones were trimmed to expose the interior marrow shaft. The bone marrows were flushed out with 1-3 ml of cold complete RPMI-1640 medium using a 5 ml syringe with a 21 gauge needle. The single cell suspension was then prepared by drawing the medium and bone marrows up and down for 3-4 times with a 5 ml syringe and 21 gauge needle. To measure the number of nucleated cells, 10 μl of the single cell suspension was first diluted in 490 μl of 3% acetic acid and then counted using a hemacytometer (Hausser Scientific).

The cell suspension was adjusted to 5×10^6 nucleated cells per ml with cold complete RPMI-1640 medium.

The 37°C pre-warmed 2 × RPMI mix and the 42°C pre-warmed 0.66% agar were 1: 1 (v/v) mixed, followed quickly by adding the bone marrow cell suspension (60 μl of cell suspension per 6 ml of mixture) and mixing well. The mixture was transferred into 24-well plates (Nunc), 0.4 ml per well, before solidification. The plates were kept at room temperature for 15 minutes to allow the agar solidification. After solidification, 25 μl of PBS alone, 25 μl of PBS containing 0.5 μg/ml of rSj16 or 0.5 μg/ml rGST was added into corresponding wells, and incubated in a humidified 37°C incubator for one hour, followed by adding 25 μl of PBS, 25 μl of PBS containing 0.5 ng/ml of IL-3, 25 μl of PBS containing 36 ng/ml of macrophage-colony stimulating factor (M-CSF), or 25 μl of PBS containing 12 ng/ml of granulocyte-colony stimulating factor (G-CSF) into corresponding wells and incubated for further seven days. Each semi-solid agar gel was then transferred onto a cleaning glass slide, covered with 3 layers of Whatman filter papers, and dried overnight at 37°C oven. The slides were fixed with absolute methanol for 10 minutes, followed by twice fixation with 50% methanol for 30 seconds. After fixation, the slides were stained with hematoxylin solution for 2 minutes, and then rinsed with running water. After covered with coverslips, the slides were observed under light microscope, and the cell colonies of greater than 40 cells were counted. All samples were run in triplicate.

3.6 Statistics

Data within experiments were compared and significance was determined using the student's *t*-test except indicated in the figure legends. All data were shown as arithmetic mean ± S.E.M.

4 Results

4.1 Expression and purification of recombinant Sj16 (rSj16) and recombinant GST (rGST)

4.1.1 Amplification of Sj16 for cloning to pET28a(+), pET30a(+), pET32a(+), pGEX-4T-1, and pCold TF

The coding sequence of Sj16 cDNA amplified from *S. japonicum* cercarial cDNA was previously cloned into plasmid pBluescript II SK(-) in our lab. Sequence analysis showed that Sj16 has one nucleotide different from Sm16 in its DNA sequence (Fig.4.1.1.1), while it shares 100% identity in its protein sequence with Sm16. Rao and Ramaswamy (2000) have reported that Sm16 is a secretory protein with a signal peptide of 18 amino acids (aa) (85). Signal peptide analysis performed using SignalP 3.0 server at Technical University of Denmark at http://www.cbs.dtu.dk/services/SignalP/ also suggested that Sj16 has a putative signal peptide with potential cleavage site between aa 16 and aa 17, or between aa 18 and aa 19 (Fig.4.1.1.2). Therefore, in this project, just the coding sequence corresponding to the mature protein of Sj16 (without signal peptide) was cloned into prokaryotic expression vectors and expressed. Previous studies indicated that Sm16 was extremely hard to be expressed and purified from *E. coli*, yeast and baculovirus system. In other hand, it is also non-reasonable to obtain sufficient native Sj16 protein from *S. japonicum*. Thus, in this study, Sj16 was cloned and tried to express in several different plasmid vectors, so as to obtain an optimal expression of the protein. For cloning into pET28a(+), pET30a(+), pET32a(+), pGEX-4T-1, and pCold TF, primer pair Sj16S1 with franked restriction site *EcoR* I and Sj16P2 with franked restriction site *Sal* I were used to amplify Sj16 fragment from template pBluescript II SK(-)/Sj16. After amplification, the PCR products were applied to agarose gel electrophoresis as described in Methodology 3.1.3. A DNA fragment of approximate

317 bp was amplified (Fig.4.1.2, lane 1).

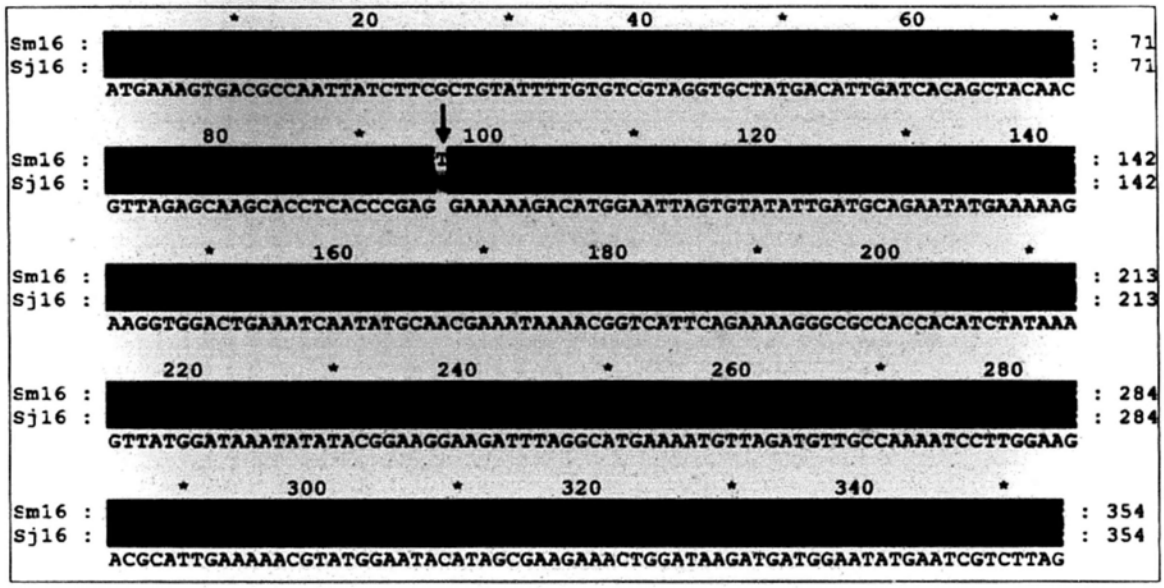

Fig.4.1.1.1 Alignment of DNA sequence of Sj16 with Sm16. There is just one base pair difference between these two sequences (arrow).

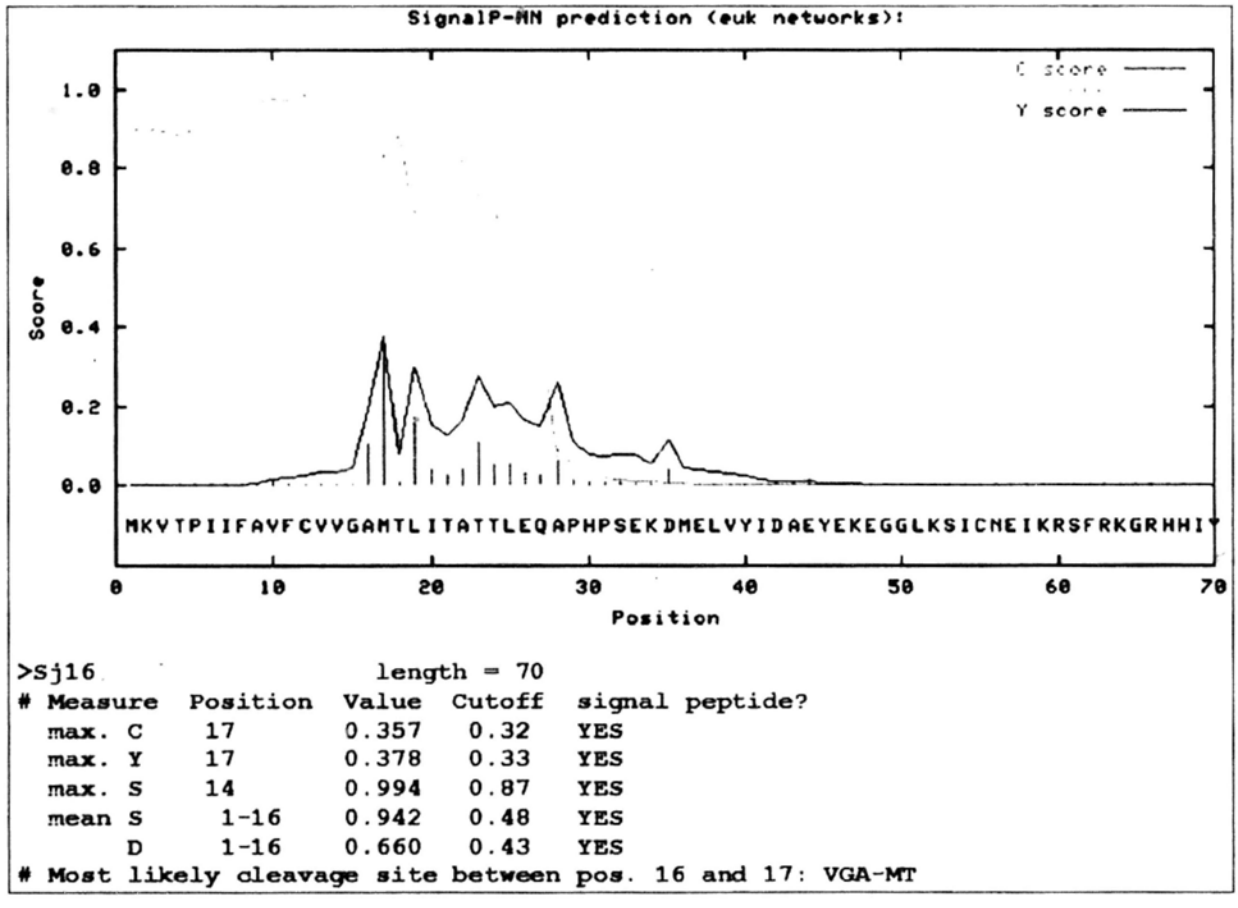

Fig.4.1.1.2 Predicted signal peptide cleavage sites of Sj16 by SignalP 3.0 using neural networks (NN) trained on eukaryotes. It indicated that Sj16 most likely has a signal peptide between the amino acid 16 and 17.

4.1.2 Amplification of Sj16 for cloning to pTYB4

For cloning into pTYB4, primer pair Sj16S1 with franking restriction site *EcoR* I and Sj16S2 with franking restriction site *Xho* I were used to amplify Sj16 fragment from template pBluescript II SK(-)/Sj16. After amplification, the PCR products were applied to 1.5% agarose gel electrophoresis as described in Methodology 3.1.3. A DNA fragment of approximate 317 bp was amplified (Fig.4.1.2, lane 2).

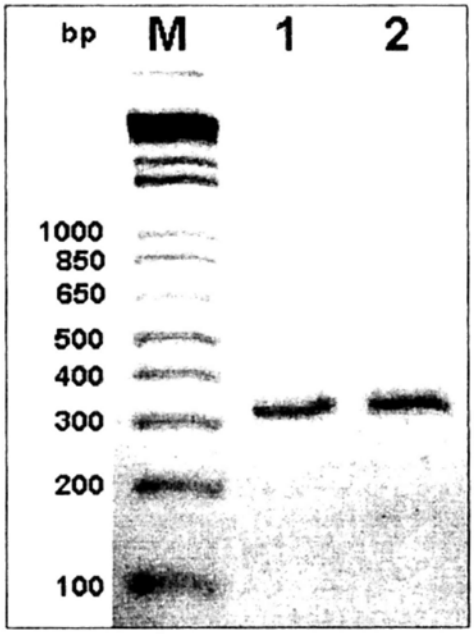

Fig.4.1.2 PCR amplification of Sj16. Lane 1, DNA fragment amplified with primer Sj16S1 and Sj16P2; lane 2, DNA fragment amplified with primer Sj16S1 and Sj16S2; lane M, 1 kb plus DNA ladder.

4.1.3 Cloning of Sj16 into pET28a(+), pET30a(+), pET32a(+), pGEX-4T-1, and pCold TF

The amplified fragment using primer pair Sj16S1/Sj16P2 was directly purified Wizard® SV Gel and PCR Clean-Up System (Promega) as described in Methodology 3.1.4. The purified plasmid DNA of pET28a(+), pET30a(+), pET32a(+), pGEX-4T-1, pCold TF, and purified PCR fragment were respectively

double digested with restriction enzyme *EcoR* I and *Sal* I. After purification of each digested product from agarose gel, the Sj16S1/Sj16P2 fragment was ligated with pET28a(+), pET30a(+), pET32a(+), pGEX-4T-1 or pCold TF respectively (Methodology 3.1.5-3.1.7). The ligation products were transformed into *E. coli* DH5α respectively and selected on LB agar plates containing appropriate antibiotics (Methodology 3.1.8.). After transformation, the positive colonies screened by PCR were picked up and inoculated to LB medium and shaken at 37 °C overnight. The recombinant plasmids were extracted from the overnight cultures respectively, and the insertion and linker region were sequenced by cycle sequencing (Methodology 3.1.9-3.1.10). The sequencing results indicated that the Sj16 was correctly inserted into each plasmid in the right position without any mutation.

4.1.4 Cloning of Sj16 into pTYB4

The amplified fragment using primer pair Sj16S1/Sj16S2 was directly purified Wizard® SV Gel and PCR Clean-Up System (Promega) as described in Methodology 3.1.4. The purified pTYB4 plasmid DNA, and purified PCR fragment Sj16S1/Sj16S2 were respectively double digested with restriction enzyme *EcoR* I and *Xho* I. After purification of each digested product from agarose gel, the Sj16S1/Sj16S2 fragment was ligated with pTYB4 (Methodology 3.1.5-3.1.7). The ligation products were transformed into *E. coli* DH5α and selected on LB agar plate containing ampicillin (Methodology 3.1.8.). After transformation, the positive colonies screened by PCR were picked up and inoculated to LB medium and shaken at 37°C overnight. The recombinant plasmids were extracted from the overnight culture, and the insertion and linker region were sequenced by cycle sequencing (Methodology 3.1.9-3.1.10). The sequencing results indicated that the Sj16 was correctly inserted into the plasmid in the right position without any mutation.

4.1.5 Testing the rSj16 expression using recombinant pET28a(+)/Sj16,

pET30a(+)/Sj16, pET32a(+)/Sj16, pTYB4/Sj16, pCold TF/Sj16, or pGEX-4T-1/Sj16

After confirmed by cycle sequencing, the successfully cloned recombinant plasmids were transformed into BL21 (DE3) and induced with IPTG (see Methodology 3.1.11-3.1.12). The expression of rSj16 was then analyzed by SDS-PAGE electrophoresis. The results showed that there was no apparent recombinant protein band been induced in pET28a(+)/Sj16, pET30a(+)/Sj16, pET32a(+)/Sj16 or pTYB4/Sj16 transformed bacteria culture after induction with IPTG for indicated time (see Methodology 3.1.11-3.1.12) (data not shown). In contrast, obvious expression of recombinant protein was induced in pCold TF/Sj16 transformed bacteria culture (Fig.4.1.5), or pGEX-4T-1/Sj16 transformed bacteria culture (Fig.4.1.6, lane 2), although still in a very low level. According to the protein molecular mass standards applied in SDS-PAGE electrophoresis analysis, the estimated molecular sizes of the recombinant fusion proteins expressed from pCold TF/Sj16 or pGEX-4T-1/Sj16 transformed bacteria were around 70 KDa (Fig.4.1.5) and 30 KDa (Fig.4.1.6, lane 2) respectively, which corresponded with their theoretically predicted sizes.

The pCold TF Vector is a fusion cold shock expression vector that expresses Trigger Factor (TF) chaperone as a soluble tag. A His-Tag sequence is included at the 5' of the Multiple Cloning Site to facilitate the purification of recombinant protein (Cold Shock Expression System pCold^{TM} TF DNA, TAKARA BIO INC.). So after induction, the recombinant protein needs to be purified by His-affinity chromatography. However, in His-affinity chromatography, the recombinant protein is usually eluted with a high concentration of imidazole which can be removed before the protein was subjected to additional treatment or functional assay. In addition, in order to remove the TF tag, the recombinant protein should be digested

with appreciate enzyme and then gone through the His-affinity chromatography again. These processes are time-consuming, and have more chance to lose the target protein. Unlike pCold TF Vector, the pGEX-4T-1 vector is a fusion expression vector that expresses *S. japonicum* GST as a soluble tag which could be purified by affinity chromatography using immobilizing glutathione column (GST Gene Fusion System Manual, GE Healthcare). Since the column wash buffer is compatible with the thrombin working buffer (both are PBS), the GST tag can be easily removed by on-column thrombin digestion, followed by a PBS elution (GSTrap HP Instructions, GE Healthcare). Through this process, GST still binds on the column, while free rSj16 is eluted in PBS. Therefore, the rSj16 was expressed and purified using pGEX-4T-1 vector system in this study.

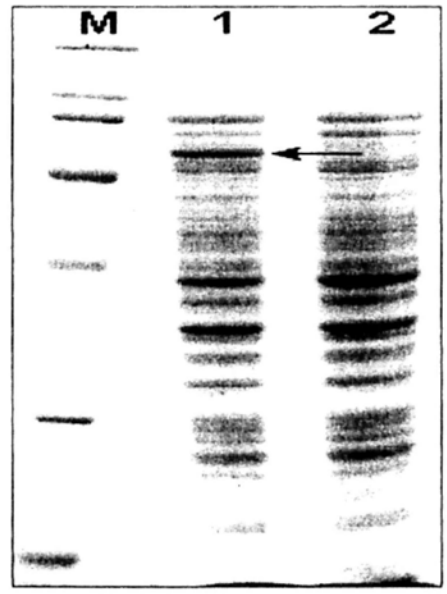

Fig.4.1.5 SDS-PAGE (12.5%) analysis of rSj16 expression in pCold TF/Sj16 transformed BL21 (DE3). Lane 1, total cell lysate of *E. coli* BL21(DE3) cells after isopropylthiogalactoside (IPTG) induction; lane 2, total cell lysate of *E. coli* BL21(DE3) cells before IPTG induction; lane M, molecular mass standards (Myosin, ß-galactosidase, Phosphorylase b, Serum albumin, Ovalbumin, Carbonic anhydrase , Trypsin inhibitor). Arrow indicated the induced rSj16 fusion protein band.

4.1.6 Expression and purification of rSj16

The recombinant fusion protein GST-Sj16 was purified by affinity chromatography, and the GST tag was removed by thrombin enzyme digestion to release the free rSj16 (see Methodology 3.1.13). Two additional affinity chromatography processes were then performed to remove the thrombin and endotoxin mixed in rSj16 (see Methodology 3.1.14). Both purified fusion protein GST-Sj16 (Fig.4.1.6, lane 3) and free rSj16 (Fig.4.1.6, lane 4) were analyzed with SDS-PAGE electrophoresis. The theoretically calculated molecular weight of Sj16 (without signal peptide) is 11.734 kDa. However, previous studies from three independent groups have reported the molecular size of Sm16/SmSPO-1/SmSLP (Sm16, SmSPO-1 and SmSLP were cloned from *S. mansoni* by three independent groups, and have the same amino acid sequence as Sj16) as 16, 16 and 19 kDa, respectively, and interpreted this discrepancy as a result of post-transcriptional modification and anomalous electrophoretic behavior(85, 89, 90). In current study, we found the size of rSj16 was approximately 19 kDa (Fig.4.1.6, lane 4) as estimated from SDS-PAGE analysis, which corresponded to Valle's report about SmSLP(90). The presence of endotoxin in rSj16 was less than 0.25 EU/ml as measured by a *Limulus* amebocyte lysate test (see Methodology 3.1.15). The concentration of purified rSj16 was about 75μg/ml as measured by Bradford method using BSA as standard (see Methodology 3.1.16). The protein was adequately prepared and deep frozen until use.

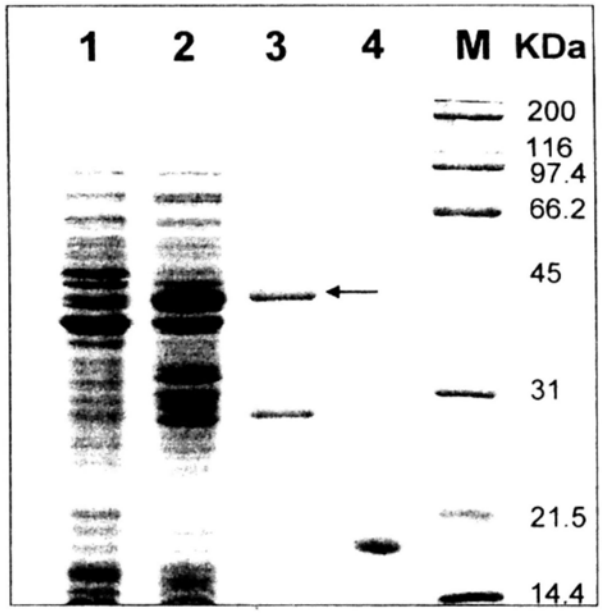

Fig.4.1.6 SDS-PAGE (12.5%) analysis of recombinant anti-inflammatory protein rSj16. Lane 1, total cell lysate of *Escherichia coli* BL21(DE3) cells before isopropylthiogalactoside (IPTG) induction; lane 2, total cell lysate of *E. coli* BL21(DE3) cells after IPTG induction; lane 3, recombinant fusion protein (arrow indicated) purified by affinity purification; lane 4, rSj16 released from the fusion protein by thrombin digestion; lane M, molecular mass standards.

4.1.7 Expression and purification of rGST

During purification of rSj16, traces of rGST may not be absolutely excluded from the rSj16 solution. In other hand, the GST tag in pGEX-4T-1 vector is also *S. japonicum* originated. These made rGST as an ideal control protein during the rSj16 functionary assays. Thus, the rGST was purified (as described Methodology 3.1.13) and used as a control protein throughout the study. The purified rGST was analyzed with SDS-PAGE electrophoresis (Fig.4.1.7). The size of rGST was approximately 26 kDa as estimated from SDS-PAGE analysis, which corresponded to the theoretically predicted size of GST. The presence of endotoxin in the rGST was less than 0.25 EU/ml as measured by a *Limulus* amebocyte lysate test (see Methodology 3.1.15).

The concentration of purified rGST was about 100μg/ml as measured by Bradford method using BSA as standard (see Methodology 3.1.16). The protein was adequately prepared and deep frozen until use.

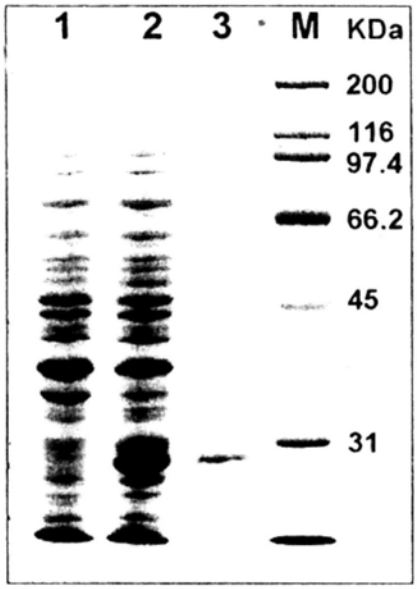

Fig.4.1.7 SDS-PAGE (12.5%) analysis of expressed and purified rGST. Lane 1, total cell lysate of *Escherichia coli* BL21(DE3) cells before isopropylthiogalactoside (IPTG) induction; lane 2, total cell lysate of *E. coli* BL21(DE3) cells after IPTG induction; lane 3, recombinant protein purified by affinity purification; lane M, molecular mass standards.

4.1.8 Confirmation of purified rGST and rSj16 by mass spectrometry

To confirm the authenticity of the purified proteins, both rSj16 and rGST were subjected to mass spectrometry analysis, and the results showed that rSj16 matched with the anti-inflammatory protein 16 [*Schistosoma mansoni*] (NCBI Accession No. gi|8468613) and the SPO-1 protein [*Schistosoma mansoni*] (NCBI Accession No. gi|4588483) (Fig.4.1.8.1), while rGST matched with the similar to GenBank Accession Number U13854 glutathione S-transferase [*Schistosoma japonicum*] (NCBI Accession No. gi|29841216) (Fig.4.1.8.2).

Gel Id/Pos	59/C17	Instr/Gel Origin	Ab347000116/MSMS 070606	Process Status	Analysis Succeeded
Plate [#] Name	[1] 003303	Instrument Sample Name		Spectra	7

Rank	Protein Name	Accession No.	Protein MW	Protein PI	Pep. Count	Protein Score	Protein Score C. I. %	MS Ion Intensity	Intensity Matched	Best Ion Score	Best Ion Species C. I. %
1	anti-inflammatory protein 16 [Schistosoma mansoni]	gi|3468613	10458.4	9.16	7	114	100	1263386.25	19.575	25	78.773

Peptide Information

Calc. Mass	Obsrv. Mass	± da	± ppm	Start Seq.	End Seq.	Sequence	Ion Score	C. I. %	Modification	Rank	Result Type
754.3803	754.3756	-0.0047	-6	71	76	MEYAK	25	78.773			Mascot
892.3083	892.3211	0.0149	17	51	57	MMEYESS			Oxidation (M)[1]		Mascot
908.4702	908.4675	-0.0027	-3	71	77	MEYAKK			Oxidation (M)[1]		Mascot
910.4814	910.4839	0.0025	3	70	76	RMEYIAK					Mascot
910.5005	910.4839	-0.0166	-18	35	41	GRHIYK					Mascot
924.4971	924.4984	0.0013	1	42	48	VMDKYR					Mascot
924.4971	924.4984	0.0013	1	42	48	VMDKYR	0	[illegible]			Mascot
926.4764	926.4921	0.0157	17	70	76	RMEYIAK			Oxidation (M)[2]		Mascot
982.5087	982.51	0.0013	1	23	30	SICNEIKR					Mascot

Fig.4.1.8.1 Mass spectrometry analysis of expressed and purified rSj16. Purified rSj16 was subjected to tandem mass spectrometry analysis as described in Methodology 3.1.17. Figure shows the matched protein and related peptide information.

Gel Idx/Pos	73/C22	Instr./Gel Origin	Ab347000116/MSMS 070606	Process Status	Analysis Succeeded
Plate [#] Name	[1] 003303	Instrument Sample Name		Spectra	7

Rank	Protein Name	Accession No.	Protein MW	Protein PI	Pep. Count	Protein Score	Protein Score C. I. %	MS Ion Intensity	Intensity Matched	Best Ion Score	Best Ion C. I. %	Species
1	similar to GenBank Accession Number U13854 glutathione S-transferase [Schistosoma japonicum]	gil29841216	25482	6.09	14	414	100	2433249.25	46.617	71	100	

Peptide Information

Calc. Mass	Obsrv. Mass	± da	± ppm	Start Seq.	End Seq.	Sequence	Ion Score	C. I. %	Modification	Rank	Result Type
770.4516	770.4529	0.001	1	12	18	GLVQPTR	29	90.456			Mascot
905.4111	905.415	0.0049	5	36	42	DEGDKWR	34	97.636			Mascot
905.4111	905.415	0.0049	5	36	42	DEGDKWR					Mascot
963.5298	963.5314	0.0016	2	2	9	SPILGYWK	52	99.996			Mascot
963.5298	963.5314	0.0016	2	2	9	SPILGYWK					Mascot
1026.583	1026.5809	-0.0021	-2	183	191	IEAIPQIDK					Mascot
1032.597	1032.5932	0.0063	6	65	73	LTQSMAIR					Mascot
1032.597	1032.5933	0.0063	6	65	73	LTQSMAIR	26	84.973			Mascot
1048.5619	1048.5645	0.0026	2	65	73	LTQSMAIR					Mascot
1094.5703	1094.5746	0.0043	4	1	9	MSPILGYWK	71	100			Mascot
1094.5703	1094.5746	0.0043	4	1	9	MSPILGYWK					Mascot
1110.5652	1110.5677	0.0025	2	1	9	MSPILGYWK					Mascot
1138.5184	1138.5234	0.007	6	28	35	YEEHLYER					Mascot
1182.6641	1182.6909	0.0267	6	183	191	REAIPQIDK					Mascot
1214.694	1214.6979	0.0039	3	109	119	IAYSKDFETLK					Mascot
1430.8253	1430.8319	0.0066	5	183	194	IEAIPQIDKYLK					Mascot
1516.804	1516.8127	0.0087	6	90	103	AEISMLEGAVLDIR					Mascot
1532.7989	1532.8038	0.005	3	90	103	AEISMLEGAVLDIR			Oxidation (M)(5)		Mascot
2269.1387	2269.1304	-0.0083	-4	19	35	LLLEYLEEKYEEHLYER					Mascot
2326.1404	2326.1479	0.0075	3	198	218	YIAWPLQGWQATFGGGDHPPK	40	99.446			Mascot
2326.1404	2326.1479	0.0075	3	198	218	YIAWPLQGWQATFGGGDHPPK					Mascot
2357.2063	2357.2041	-0.0022	-1	45	64	KFELGLEFPNLPYYIDGDVK					Mascot

Fig.4.1.8.2 Mass spectrometry analysis of expressed and purified rGST. Purified rGST was subjected to tandem mass spectrometry analysis as described in Methodology 3.1.17. Figure shows the matched protein and related peptide information.

4.1.9 Inhibition of bacterial growth by rSj16 expression

To evaluate if the rSj16 suppresses the host bacterial cells growth, BL21 (DE3) transformed with pGEX-4T-1/Sj16 was inoculated and cultured overnight as describe in Methodology 3.1.18. The O.D.600 of the culture was measured before or after 3.5 hours' induction in the presence or absence of 1 mM IPTG. Since after 3.5-hours induction some of the cultures were too dense, all of the cultures were diluted 5-fold before being applied to O.D.600 measurement. Before adding IPTG, the O.D.600 of 1:5 diluted pGEX-4T-1/Sj16 culture at 600 nm was 0.141 (Fig.4.1.9a). After 3.5 hours culture without IPTG induction, the O.D.600 of 1:5 diluted pGEX-4T-1/Sj16 increased to 0.801 ± 0.001 (Fig.4.1.9a). However, if the culture was induced with 1 mM IPTG for 3.5 hours at the same conditions, the O.D.600 dramatically decreased to 0.190 ± 0.004 (Fig.4.1.9a). This result indicated that the induced rSj16 could dramatically inhibit the host bacterial growth.

To test whether the suppressed bacterial growth was caused by the IPTG or some vector proteins that induced by IPTG, the pGEX-4T-1 alone transformed BL21 (DE3) was cultured, inducted in the presence or absence of 1 mM IPTG, and the O.D.600 was also measured the same as the pGEX-4T-1/Sj16 culture. The results showed that 3.5-hours's induction with 1 mM IPTG did not result in significant difference in the densities of the pGEX-4T-1 cultures (Fig.4.1.9b).

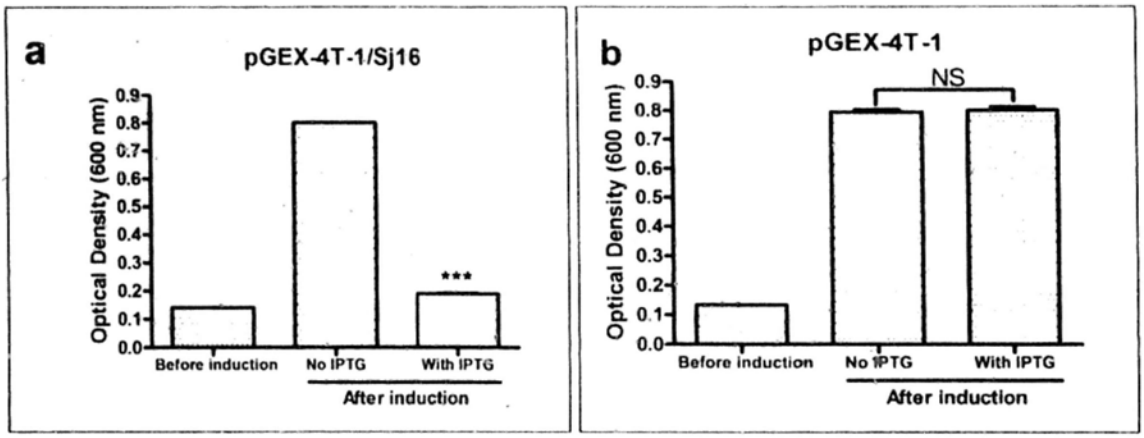

Fig.4.1.9 rSj16 expression suppressed host bacterial cells growth. BL21 (DE3) transformed with pGEX-4T-1/Sj16 (a) or pGEX-4T-1 (b) was induced in the presence or absence of 1 mM IPTG for 3.5 hours. The O.D.600 of the cultures was measured before or after induction. All of the cultures were diluted for 5 fold before O.D.600 measurement. The data in the figure are the mean ± S.E.M of the O.D.600 of 1:5 diluted cultures, n=3. ***, $P < 0.001$; NS, not significant as compared with those of No IPTG induction group. Data are representative of three individual experiments.

4.2 Immunogenicity of rSj16

After immunization, specific anti-rSj16 antibodies in mice sera were detected by ELISA and immunoblot. The results showed that mice immunized with the protein developed specific IgG antibodies to titers >1: 16,000 as determined by ELISA (Fig.4.2a). These antibodies were able to recognize the recombinant protein Sj16 (Fig.4.2b) by immunoblot. Sera collected before immunization did not recognize the recombinant protein either by ELISA or immunoblot (Fig.4.2).

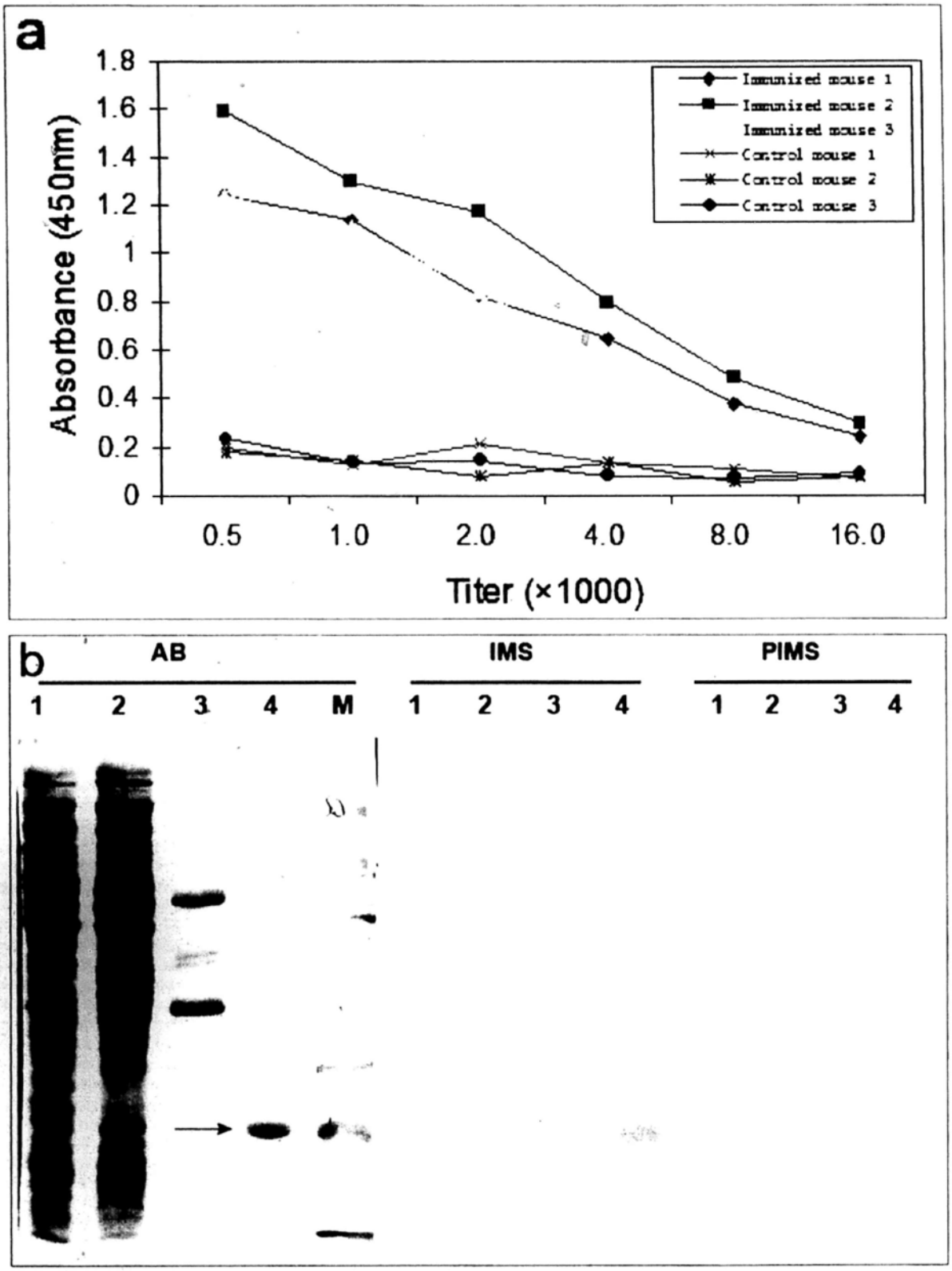

Fig.4.2 Anti-rSj16 antibody production and detection by western-blot and ELISA. **a.** Determining anti-rSj16 antibody titers. Two-fold dilutions of the sera were used; the titer values are defined as the dilutions which give optical density readings at least two-fold higher than the mean background of pre-immunized mouse serum (control

mouse serum); data were averages of triplicate wells. **b.** Western blot analysis of recombinant protein using mouse serum immunized with rSj16. **AB**, amido black stained membrane; **IMS**, immunized mouse serum; **PIMS**, pre-immunized mouse serum. Lane 1, total cell lysate of *E. coli* BL21(DE3) cells before IPTG induction; lane 2, total cell lysate of *E. coli* BL21(DE3) cells after IPTG induction; lane 3, recombinant fusion protein purified by affinity purification; lane 4, purified rSj16; lane M, molecular mass standards (BSA, Glutamic Dehydrogenase, Alcohol Dehydrogenase, Carbonic Anhydrase, Myoglobin Red, Lysozyme, Aprotinin). The sera were used at 1:3,000 dilution. Arrow indicates the rSj16 band.

4.3 Detection of anti-Sj16 antibody in *S. japonicum*-infected rabbits

Purified rSj16 was probed with sera collected from rabbits 45 days post infection with *S. japonicum*. The quality of the sera was verified by Western blot (Fig.4.3a) and ELISA (titer > 1,600) (Fig.4.3c) for their immune reactivity to SWAP. Sera from uninfected rabbits were used as negative controls. The results show that *S. japonicum*-infected sera could not recognize rSj16 as evaluated by Western blot (Fig.4.3a) and ELISA (titer < 1: 50) (Fig.4.3b). This result indicated that native Sj16 may fail to induce circulating antibodies in rabbits during *S. japonicum* infection.

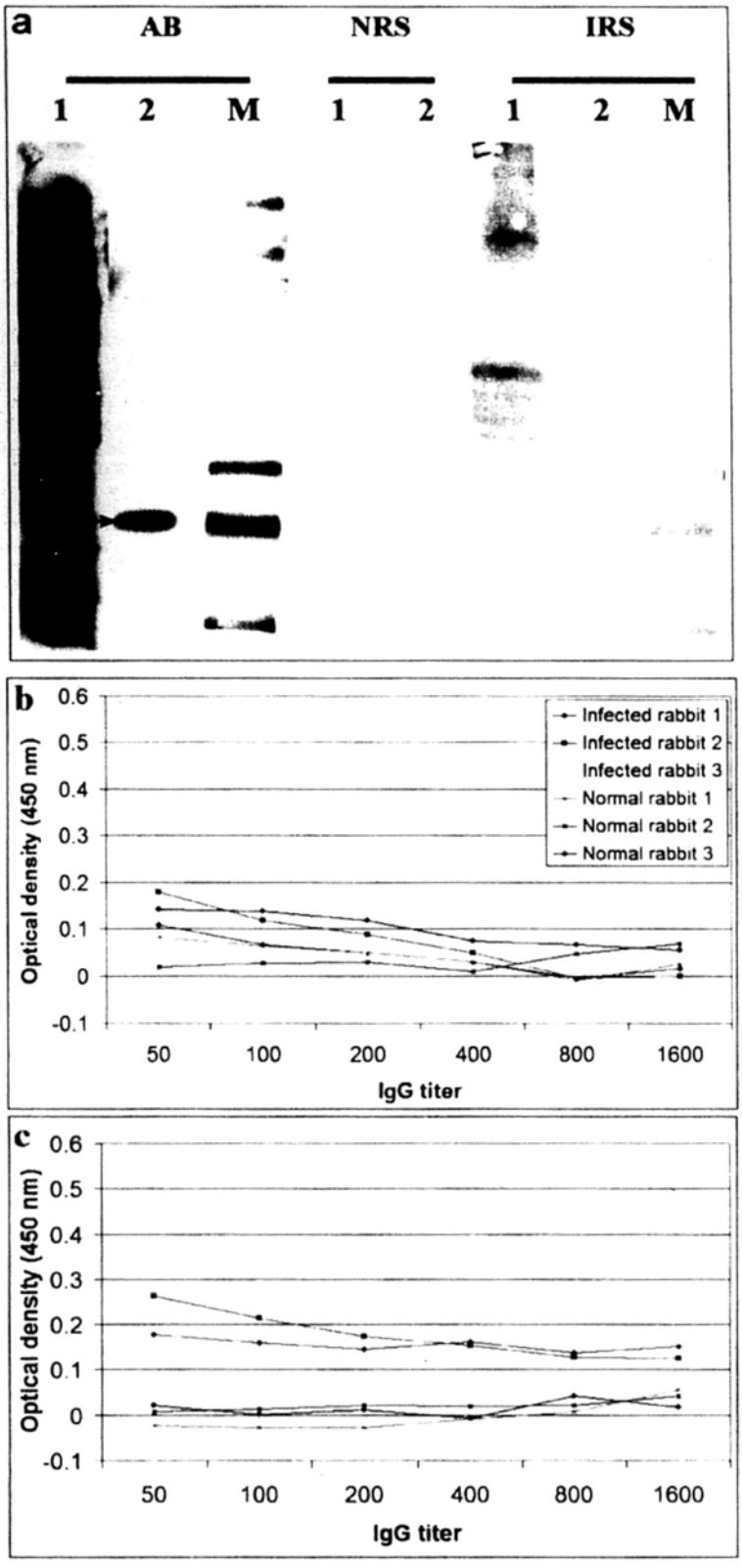

Fig.4.3 Detection of anti-Sj16 antibody in rabbit serum. a. Western blot used to detect anti-Sj16 antibodies in infected rabbit serum. AB, amido black stained membrane; NRS, probed with normal rabbit serum; IRS, probed with *Schistosoma japonicum*-infected rabbit serum. Lane 1, *S. japonicum* soluble worm antigen

preparation (SWAP); lane 2, purified rSj16; lane M, pre-stained protein standard (BSA, Glutamic Dehydrogenase, Alcohol Dehydrogenase, Carbonic Anhydrase, Myoglobin Red, Lysozyme, Aprotinin). The sera were used at 1:1,000 dilution. Arrow indicates the rSj16 band. **b-c.** ELISA for detecting anti-Sj16 antibodies (b) or anti-SWAP antibodies (c). Two-fold dilutions of the sera were used; the titer values are defined as the dilutions which give optical density readings at least two-fold higher than the mean background of un-infected normal serum; data were averages of triplicate wells.

4.4 Evaluation of the anti-inflammatory activity of rSj16

4.4.1 Characterization of the inflammatory model

Before evaluating the anti-inflammatory activity of rSj16, an initial experiment was performed to characterize the inflammatory responses of BALB/c mice to TG (Fig.4.4.1). Peritoneal injection with 3% TG induced a time-dependent accumulation of leukocytes into the peritoneal cavity, with a maximum infiltration at 24 h, and retained a high level at 72 h. A differential cell count indicated that the extravasation of polymorphonuclear cells (PMN) rapidly reached its maximum within 3 hours after injection, and declined sharply to a basal level at 72 hours. In contrast, the infiltration of macrophages was not apparent until 12 hours after injection, but gradually increased for at least 72 hours.

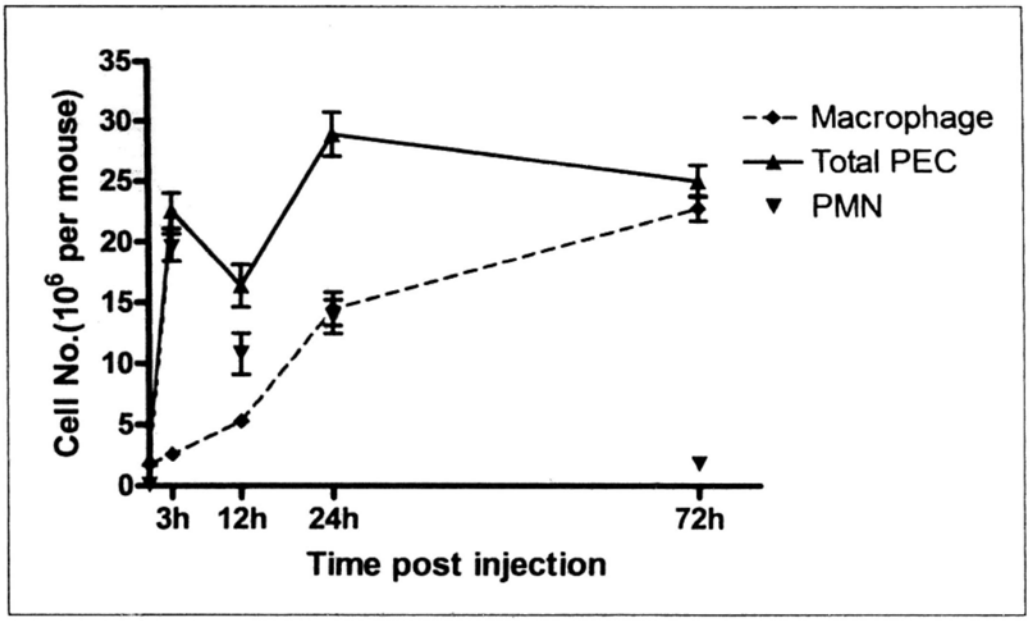

Fig.4.4.1 Time dependency of 3% Brewer thioglycollate medium (TG)-induced polymorphonuclear cell (PMN) and macrophage infiltration. Mice were treated i.p. with 1 ml 3% TG at time zero. Untreated mice were used as controls (time zero in the figure). Total peritoneal exudate cells (PECs) were collected at indicated time points, total cell, PMN and macrophage numbers were counted as described in Materials and Methods. Data are expressed as mean ± S.E.M. of six mice per group.

4.4.2 Inhibition of TG-induced leukocyte accumulation

To evaluate the anti-inflammatory activity of rSj16, mice were injected i.p. with different concentrations of rSj16 (1 ml per mouse) 1 hour before the injection of 3% TG. The PECs were isolated and counted 3 days post-TG injection. Results showed that rSj16 could dramatically inhibit the accumulation of thioglycollate-induced leukocytes in the peritoneal cavity, and this inhibition was dose-dependent (Fig.4.4.2a). rSj16 showed a maximum suppressive effect when its concentration reached 0.5 μg/ml (1 ml per mouse) or more. rGST did not show a significant effect on the recruitment of thioglycollate-induced leukocytes. Peritoneal injection of rSj16 or rGST alone did not induce a significant accumulation of leukocytes into the

peritoneal cavity (data not shown).

Because the number of PMNs had declined to basal level and most leukocytes in the peritoneal cavity are macrophages at 3 days post-TG injection, a time-course analysis of the role of rSj16 on the thioglycollate-induced PMN and macrophage influx was further assessed. Fig.4.4.2b-d show that rSj16 suppresses both PMN and macrophage accumulation at the beginning of TG-induced inflammation.

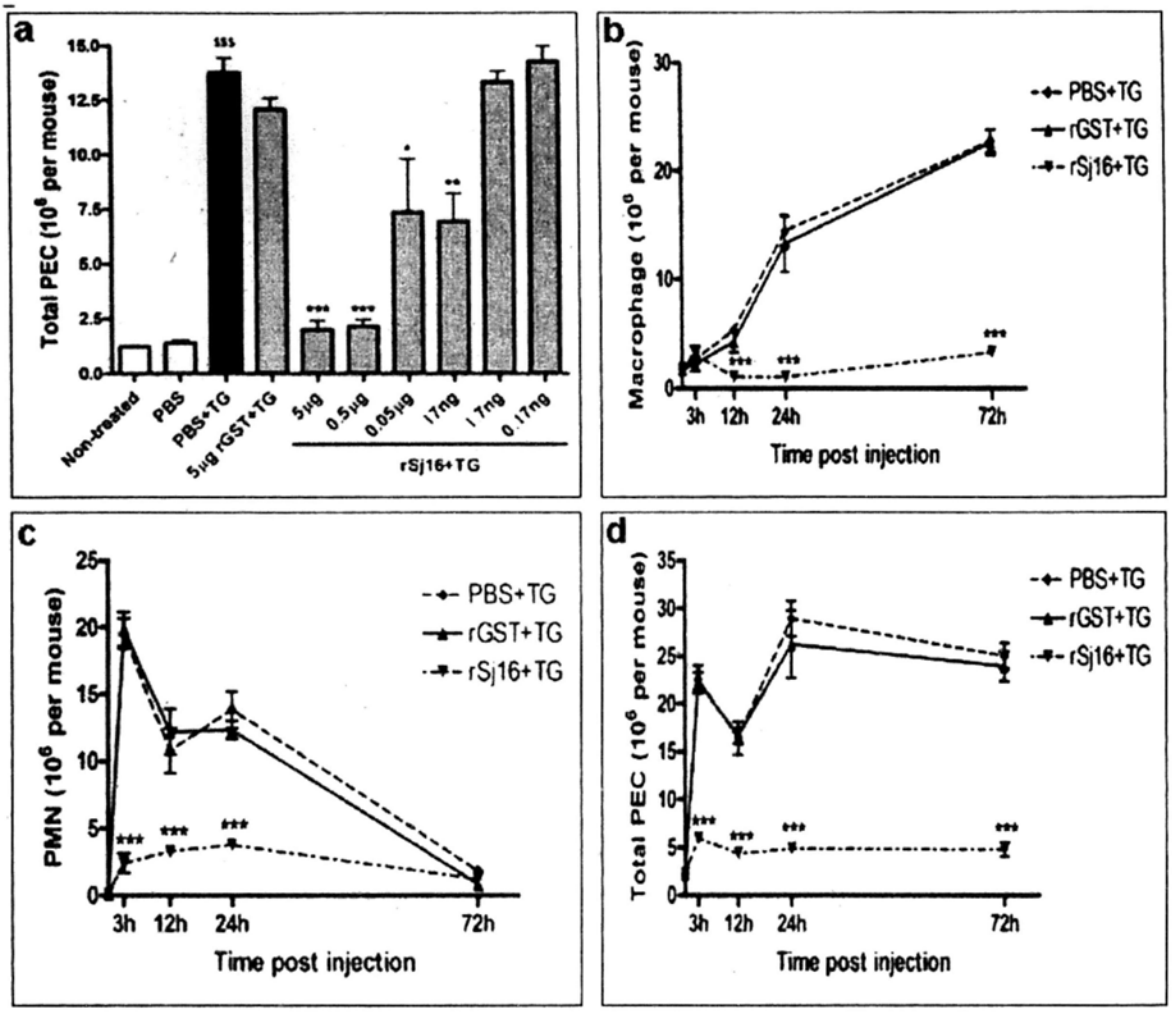

Fig.4.4.2 Recombinant anti-inflammatory protein Sj16 (rSj16) suppresses the recruitment of leukocytes into the peritoneal cavity induced by thioglycollate. Each BALB/c mice was pre-treated i.p. with 1 ml of sterile PBS, 0.5 μg/ml (b-d) or indicated concentration (a) of rSj16, or 5 μg/ml rGST (a) or 0.5 μg/ml rGST (b-d). The mice were then injected i.p. with 1 ml 3% Brewer thioglycollate medium (TG) or sterile PBS. The total peritoneal exudate cells (PECs) were isolated and counted for 3 days (a) or differentially counted at indicated times (b-d) post-TG injection. Data are the mean ± S.E.M. of six mice/group. Since i.p. injection of PBS alone didn't cause significant changes in the peritoneal cell population, the data from this group are not shown in the time-course analysis. *, $P < 0.1$; **, $P < 0.01$; ***, $P < 0.001$ as compared with the PBS + TG group. $$$, $P < 0.001$ as compared with the PBS group.

In order to test whether the suppression of leukocyte accumulation by rSj16 was due to its cytotoxic effect on the leukocytes, total PECs were incubated *in vitro* with rSj16 for 24 hours and cell cytotoxicity was assessed as described in Materials and methods. The results indicated that rSj16 was not cytotoxic to resident PECs (0.05% ± 0.89% cytotoxicity; $P > 0.5$), 3 hours PECs (1.88% ± 2.34%; $P > 0.5$) or 3 day PECs (1.51% ± 1.58%; $P > 0.4$). In addition, a WBC count of whole blood performed 48 hours following rSj16 injection showed that circulating WBC numbers were unaffected by rSj16 administration ($8.66 \times 10^6 \pm 0.29 \times 10^6$ WBCs/ml whole blood versus $8.68 \times 10^6 \pm 0.58 \times 10^6$; rSj16 injection versus PBS; $P > 0.5$).

4.4.3 Effect of rSj16 on the maturation of peritoneal macrophages

It is well documented that macrophage maturation plays an important role in inducing specialized cellular functions(119). During the maturation process, cells undergo several morphological changes that include the lower nucleus/cytoplasm ratio, decreasing cytoplasmic granules, increasing cell size, round nucleus eccentrically placed, and a large amount of cytoplasm containing vacuoles (119, 120). In the present study, the maturation of macrophages was determined morphologically according to the above criteria. No accumulation of mature macrophages was found in untreated mice (Fig.4.4.3b), PBS, rSj16 alone or rGST alone treated mice (data not shown). As expected, i.p. administration of 3% TG resulted in a rapid accumulation of mature peritoneal macrophages (Fig.4.4.3a, 4.4.3c). The mature macrophages began to appear in the peritoneal cavity as early as 3 hours post injection, and most of the cells had matured (85.7%) by the end of day 1 (Fig.4.4.3a). A significant reduction in macrophage maturation was obtained at 12 hours in mice pretreated with rSj16, and the percentage of mature macrophages was reduced from 87.0% ± 5.0% to 27.0% ± 1.7% at 72 hours (Fig.4.4.3a, 4.4.3e). Pretreatment of mice with rGST did not suppress TG-induced macrophage maturation (Fig.4.4.3a, 4.4.3d).

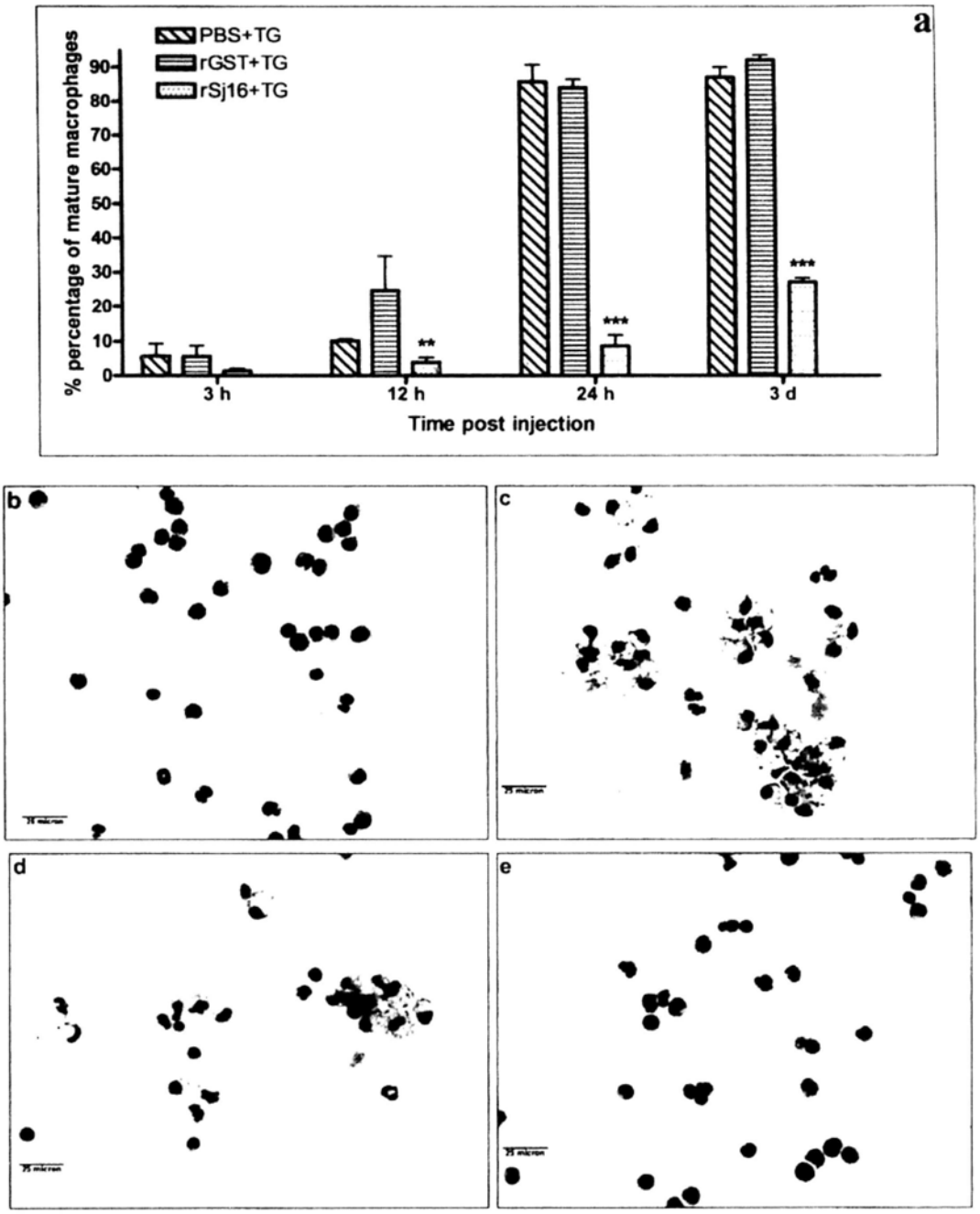

Fig.4.4.3 Recombinant anti-inflammatory protein Sj16 (rSj16) modulated 3% Brewer thioglycollate medium (TG)-mediated macrophage maturation. Mice were treated as mentioned in Fig. 5b. At indicated times the peritoneal cells were collected and transferred onto glass slides by cytospin centrifuge. The slides were stained with modified Wright-Giemsa staining and the cells were morphologically analyzed under a light microscope. a. Data are the mean ± S.E.M. of six mice/group. At least 500 cells were counted for each sample. **, $P < 0.01$; ***, $P < 0.001$ versus the PBS + TG group. b-e. Wright-Giemsa staining of total peritoneal exudate cells

(PECs). The total PECs were isolated from untreated mouse (b), or from mice treated for 3 days with 3% TG (c), with 0.5 μg/ml rGST and 3% TG (d), or with 0.5 μg/ml rSj16 and 3% TG (e) (magnification, ×400). The black bars represent 25 micrometers. The photos are representatives of six individual experiments.

4.4.4 Modulation of TG-induced cytokine and chemokine gene expression by rSj16

The role of rSj16 in the expression of cytokine and chemokine induced by TG was assessed using quantitative RT-PCR. Initial studies showed that expression of pro-inflammatory cytokines IL-1α, IL-1β, TNF-α, IL-12 and chemokines macrophage-inflammatory protein-2 (MIP-2), keratinocyte chemoattractant (KC), MIP-1α were markedly increased in the PECs of mice 3 hours after i.p. delivery of PBS and 3% TG (PBS + TG group, Fig.4.4.4). However, pre-treatment of mice with 0.5 ug/ml rSj16 1 hour before TG showed that by 3 hours there was a 3.3-fold reduction in IL-1β transcript and 1.9-fold reduction in MIP-2 transcript (Fig.4.4.4b, 4.4.4e). Although rSj16 did not show any significant effect on the IL-12p40 transcript (Fig.4.4.4h), it did suppress the transcription of IL-12p35 to the basal level at 3 hours (Fig.4.4.4d). In contrast, no significant modulation was observed for TNF-α, KC, and MIP-1α mRNA levels in the PEC pellets of rSj16 pre-treated mice (Fig.4.4.4c, Fig.4.4.4f, Fig.4.4.4g). Moreover, pre-injection with rSj16 produced an unexpected 3.7-fold increase in IL-1α transcript (Fig.4.4.4a).

Subsequent analysis of IL-10 and IL-1RA gene expression at 3 and 24 hours showed that rSj16 caused an 8.2-fold up-regulation of the mRNA level of IL-10 by 3 hours or 34.6-fold at 24 hours (Fig.4.4.4i), and 2.5-fold up-regulation of IL-1RA by 24 hours (Fig.4.4.4j). In this set of experiments, the mRNA level of IL-1RA in mouse peritoneal membranes were also measured, and again a 4.9-fold increase was

found at 24 hours in rSj16 pre-treated mice (Fig.4.4.4k).

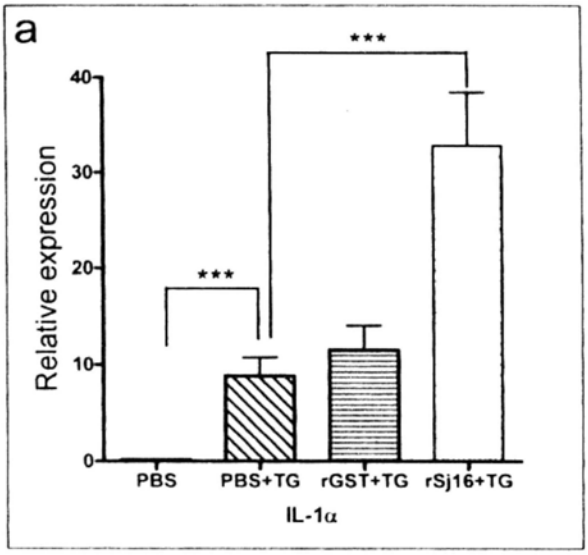

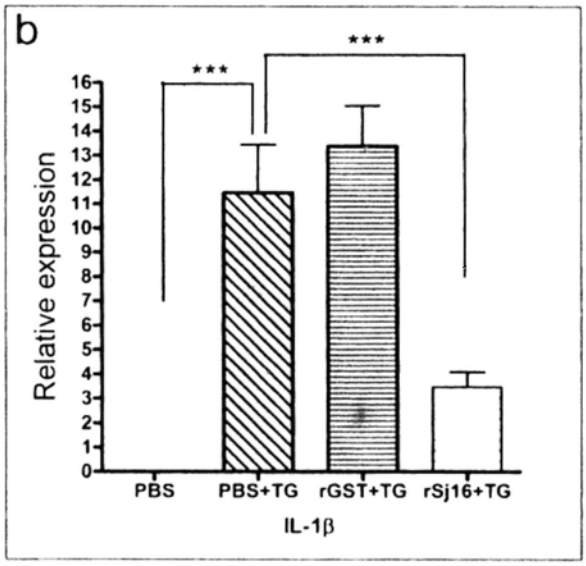

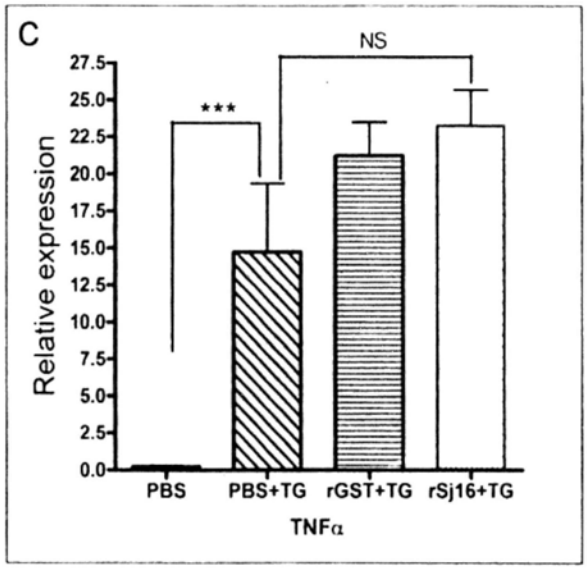

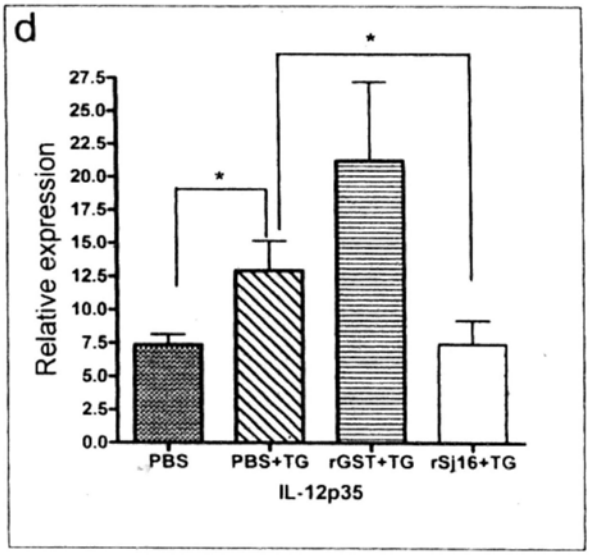
d
Relative expression
27.5
25.0
22.5
20.0
17.5
15.0
12.5
10.0
7.5
5.0
2.5
0.0
*
*
PBS
PBS+TG
rGST+TG
rSj16+TG
IL-12p35

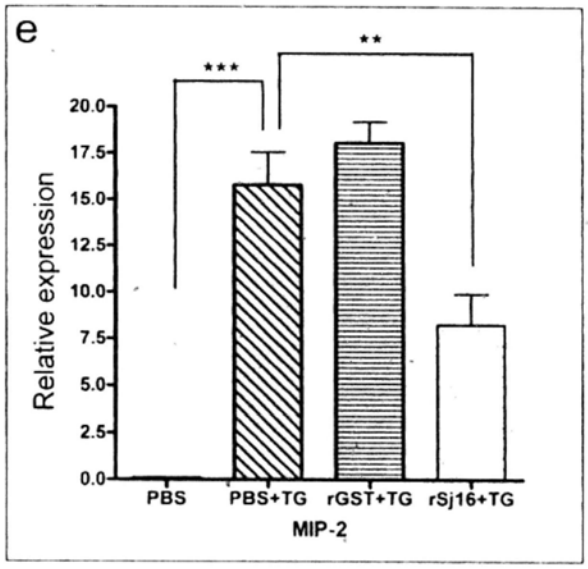
e
Relative expression
20.0
17.5
15.0
12.5
10.0
7.5
5.0
2.5
0.0
***
**
PBS
PBS+TG
rGST+TG
rSj16+TG
MIP-2

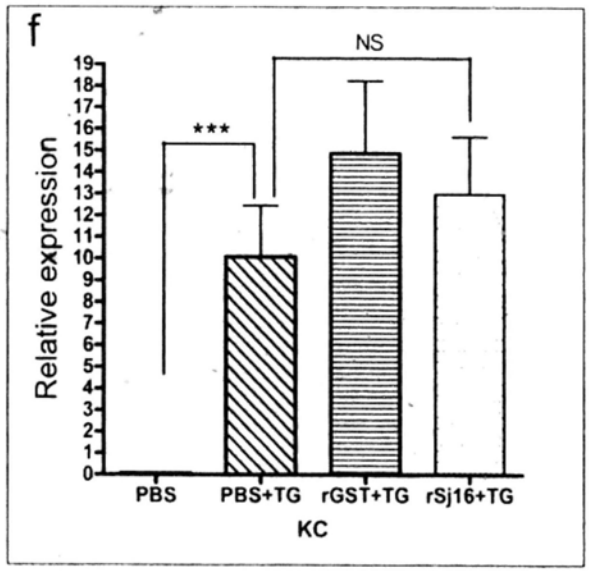
f
Relative expression
19
18
17
16
15
14
13
12
11
10
9
8
7
6
5
4
3
2
1
0
NS
***
PBS
PBS+TG
rGST+TG
rSj16+TG
KC

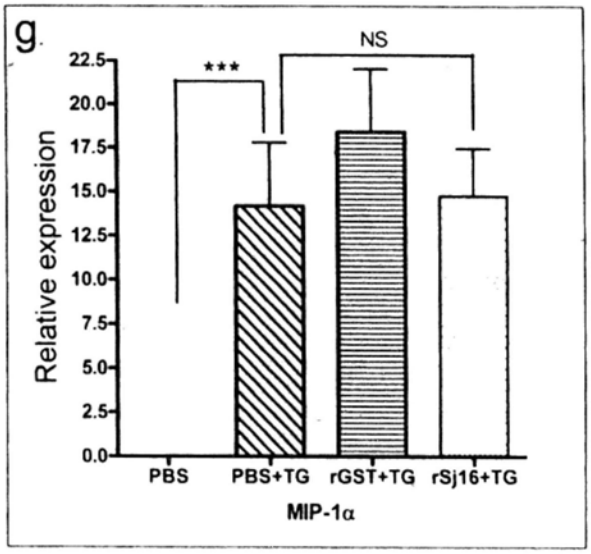
g
NS
***
22.5
20.0
17.5
15.0
12.5
10.0
7.5
5.0
2.5
0.0
Relative expression
PBS
PBS+TG
rGST+TG
rSj16+TG
MIP-1α

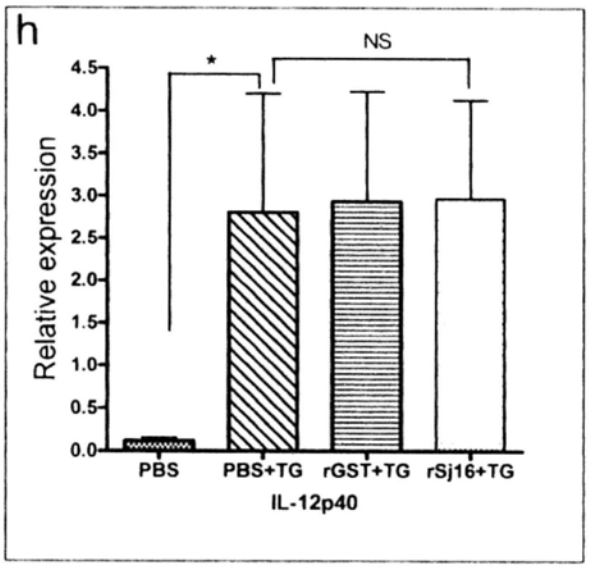
h
NS
*
4.5
4.0
3.5
3.0
2.5
2.0
1.5
1.0
0.5
0.0
Relative expression
PBS
PBS+TG
rGST+TG
rSj16+TG
IL-12p40

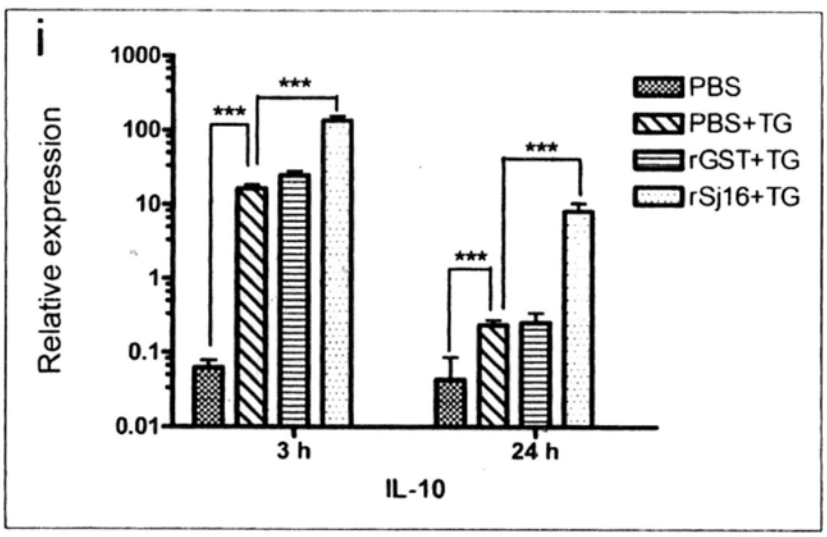
i
1000
100
10
1
0.1
0.01
***
***
***
***
Relative expression
PBS
PBS+TG
rGST+TG
rSj16+TG
3 h
24 h
IL-10

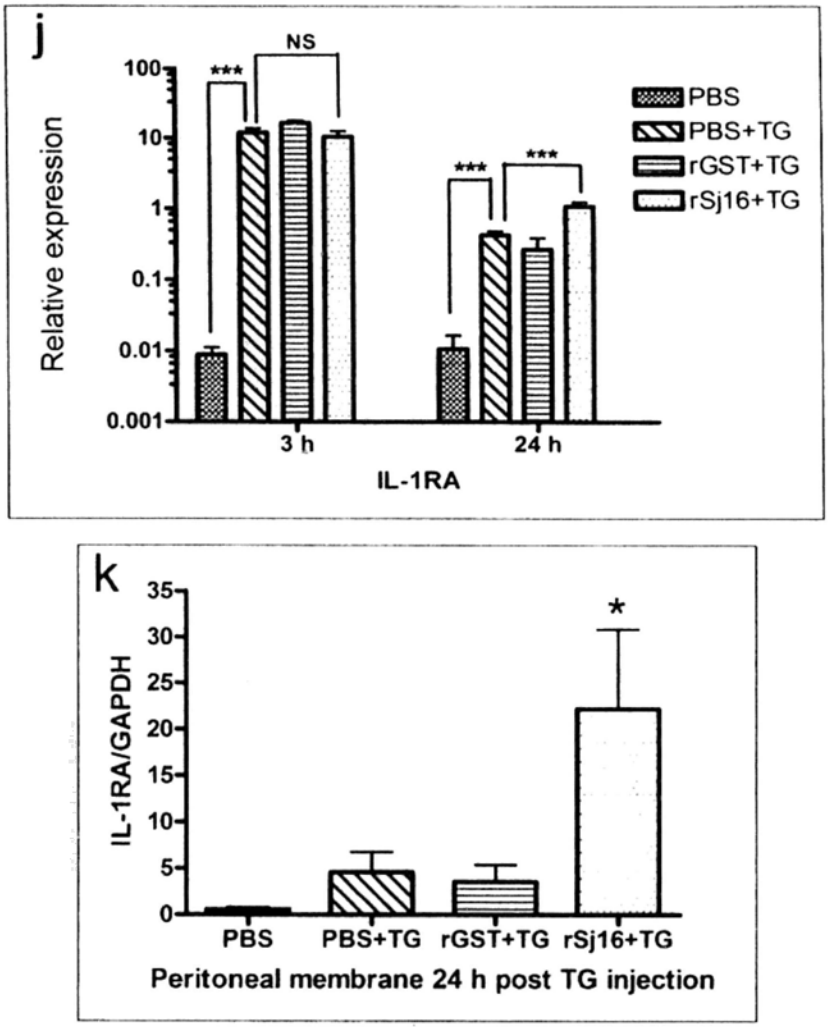

Fig.4.4.4 Quantitative reverse transcriptase (RT)-PCR analysis of cytokine and chemokine transcription. Mice were treated as described in Materials and Methods. The total peritoneal exudate cells (PECs) (or peritoneal membrane as indicated) were collected at 3 hours post 3% Brewer thioglycollate medium (TG) injection except where indicated. The total RNAs were then isolated and subjected to cDNA synthesis and quantitative RT-PCR analysis. The mRNA expression was determined as the ratio of the each gene to glyceraldehyde 3-phosphate dehydrogenase (GAPDH). Data are the mean ± S.E.M. of six mice/group. *, $P < 0.1$; **, $P < 0.01$; ***, $P < 0.001$; NS, not significant.

4.5 Suppression of adaptive immune responses to heterologous antigens by rSj16

4.5.1 Suppression of antibodies production to heterologous antigens in the presence of LPS as adjuvant

Following i.p. immunization with LPS-HSA, BALB/c mice displayed a significant increase in HSA-specific IgM (Fig.4.5.1.1a), IgG (Fig.4.5.1.1b), IgG2a (Fig.4.5.1.1c) and IgG1 (Fig.4.5.1.1d) production as compared with those immunized with HSA alone. The production of anti-HSA IgG, IgG1 and IgG2a was observed following primary immunization, and was further enhanced with boosting. The production of HSA-specific IgM in the sera of LPS-HSA immunized mice were not significant increased following primary immunization, but reached a high level following boosting, and was still higher than the levels in HSA alone-immunized mice after challenge. In addition, small amounts of HSA-specific IgA were seen after boosting and challenge in the LPS-HSA-immunized mice, but not detectable at any time point in the mice immunized with HSA alone (Fig.4.5.1.1e). Mice pretreated with rSj16 1 hour before or along with the immunization of LPS-HSA displayed reduced levels of anti-HSA IgM (Fig.4.5.1.1a), IgG (Fig.4.5.1.1b), IgG2a (Fig.4.5.1.1c) after boosting and challenge. The productions of anti-HSA IgA and IgG1 were not affected by the rSj16 treatment (Fig.4.5.1.1d-4.5.1.1e). Mice pretreated with rGST 1 hour before the immunization of LPS-HSA did not display any difference in the production of anti-HSA IgM (Fig.4.5.1.1a), IgG (Fig.4.5.1.1b), IgG2a (Fig.4.5.1.1c), IgA (Fig.4.5.1.1e) and IgG1 (Fig.4.5.1.1d). HSA-specific IgE is not detectable in any groups of the mice at any time point throughout the course of the experiment (data not shown). Mice only i.p. injected with Dulbecco's PBS did not display any HSA-specific antibodies (Data not shown).

Next we sought to determine whether the suppressive effect of rSj16 on adaptive immunity to heterologous antigens was antigen specific. Groups of four BALB/c mice were immunized i.p. with PSA (50 μg), LPS (25 μg)-PSA (50 μg), 0.5 μg rSj16

followed 1 hour later by LPS-PSA, or 0.5 μg rGST followed 1 hour later by LPS-PSA as described in Methodology 3.4.1. The antibodies levels in serum were then determined by ELISA as described in Methodology 3.4.1. The results indicated that BALB/c mice immunized with LPS-PSA also displayed a significant increase in anti-PSA IgM (Fig.4.5.1.2a), IgG (Fig.4.5.1.2b), IgG2a (Fig.4.5.1.2c) production. Furthermore, mice pretreated with rSj16 1 hour before the immunization of LPS-HSA also displayed reduced levels of anti-PSA IgM (Fig.4.5.1.2a), IgG (Fig.4.5.1.2b), IgG2a (Fig.4.5.1.2c).

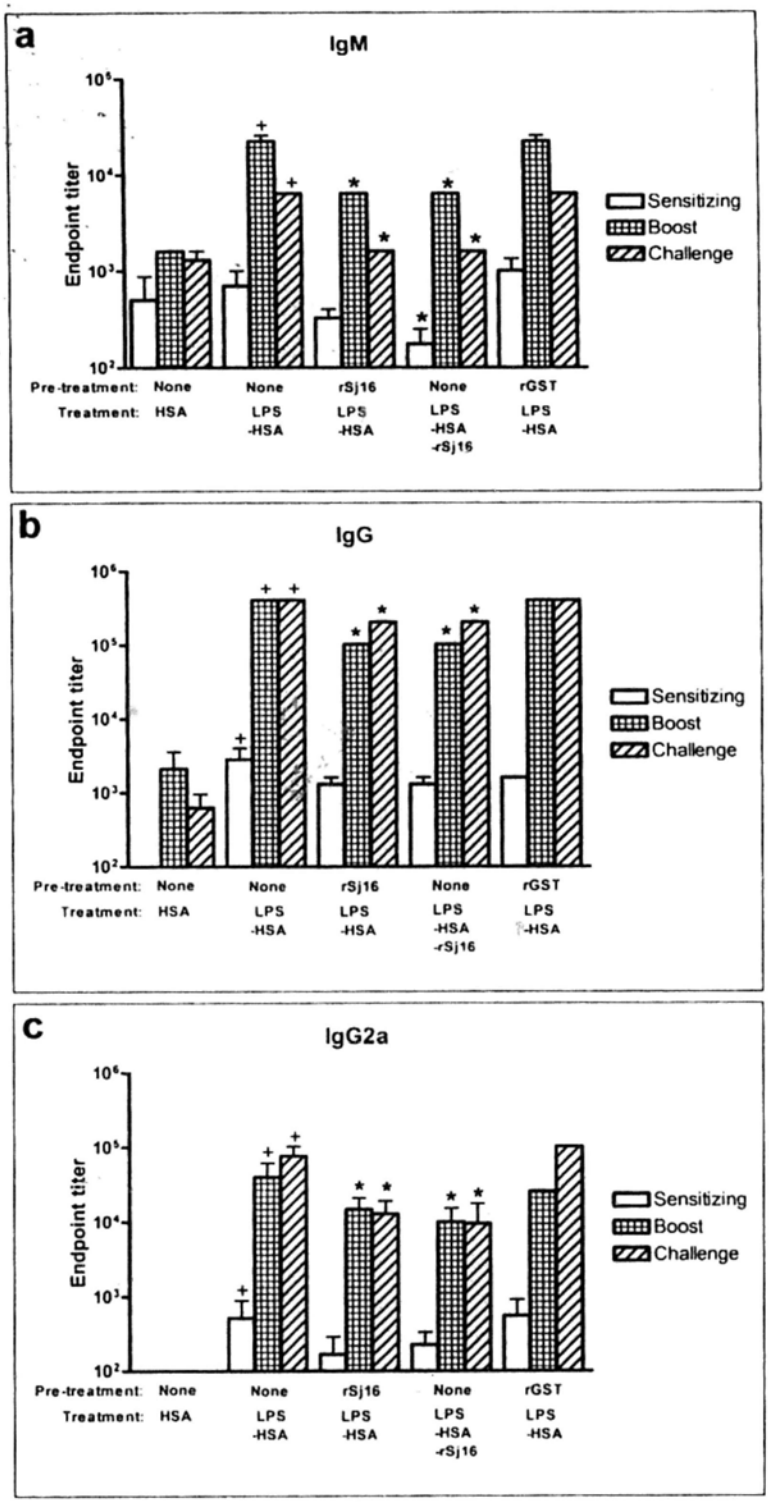
a
IgM
Endpoint titer
Sensitizing
Boost
Challenge
Pre-treatment: None None rSj16 None rGST
Treatment: HSA LPS -HSA LPS -HSA LPS -HSA -rSj16 LPS -HSA
b
IgG
Endpoint titer
Sensitizing
Boost
Challenge
Pre-treatment: None None rSj16 None rGST
Treatment: HSA LPS -HSA LPS -HSA LPS -HSA -rSj16 LPS -HSA
c
IgG2a
Endpoint titer
Sensitizing
Boost
Challenge
Pre-treatment: None None rSj16 None rGST
Treatment: HSA LPS -HSA LPS -HSA LPS -HSA -rSj16 LPS -HSA

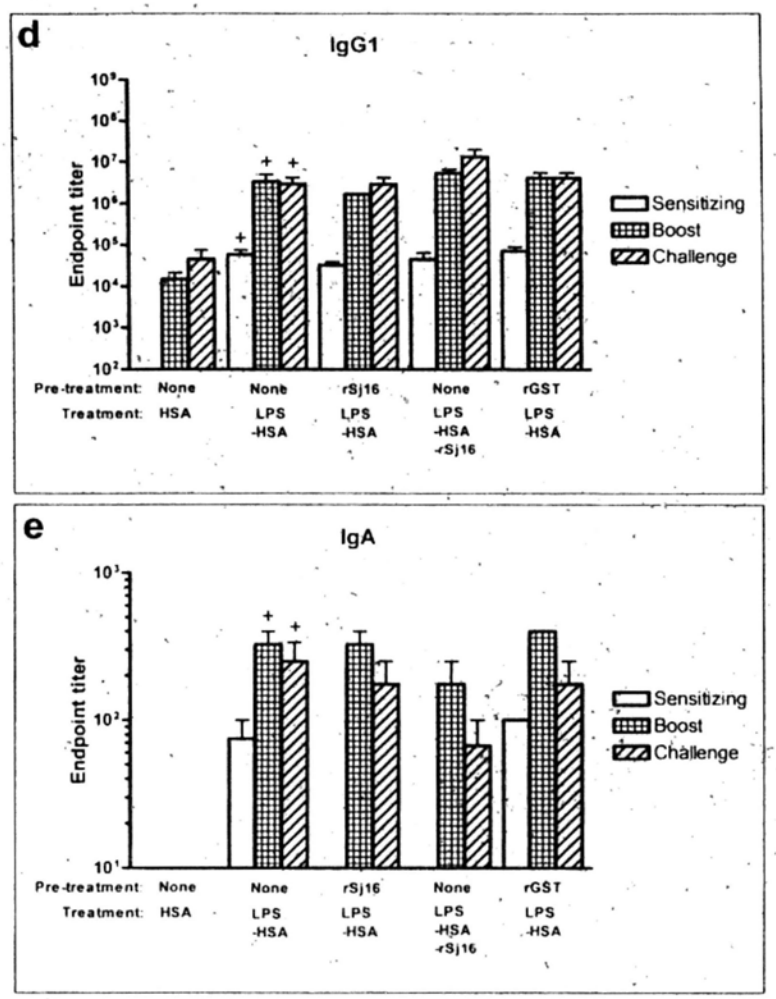

Fig.4.5.1.1 rSj16 suppressed antibody production to heterologous antigen HSA in the presence of LPS as adjuvant. Groups of BALB/c mice were treated i.p. with rSj16, or PBS (labeled as **None**, served as control), or recombinant GST (rGST) (served as control) for 1 hour. The mice were then immunized i.p. with human serum albumin (HSA) in the presence of lipopolysacchride (LPS) as adjuvant. Two weeks later, the mice were boosted with the same antigens as used in the sensitization. All mice were then challenged i.p. with HAS after the booster injection. Serum samples were collected for antibody determination after sensitization, booster, and last challenge. The antibody levels in the sera were determined using ELISA. Data were expressed as mean ± S.E.M. of 4 mice per group. +, $P < 0.1$ V.S. those immunized with HSA alone; *, $P < 0.1$ V.S. those immunized with LPS + HSA as analyzed with Mann-Whitney U test.

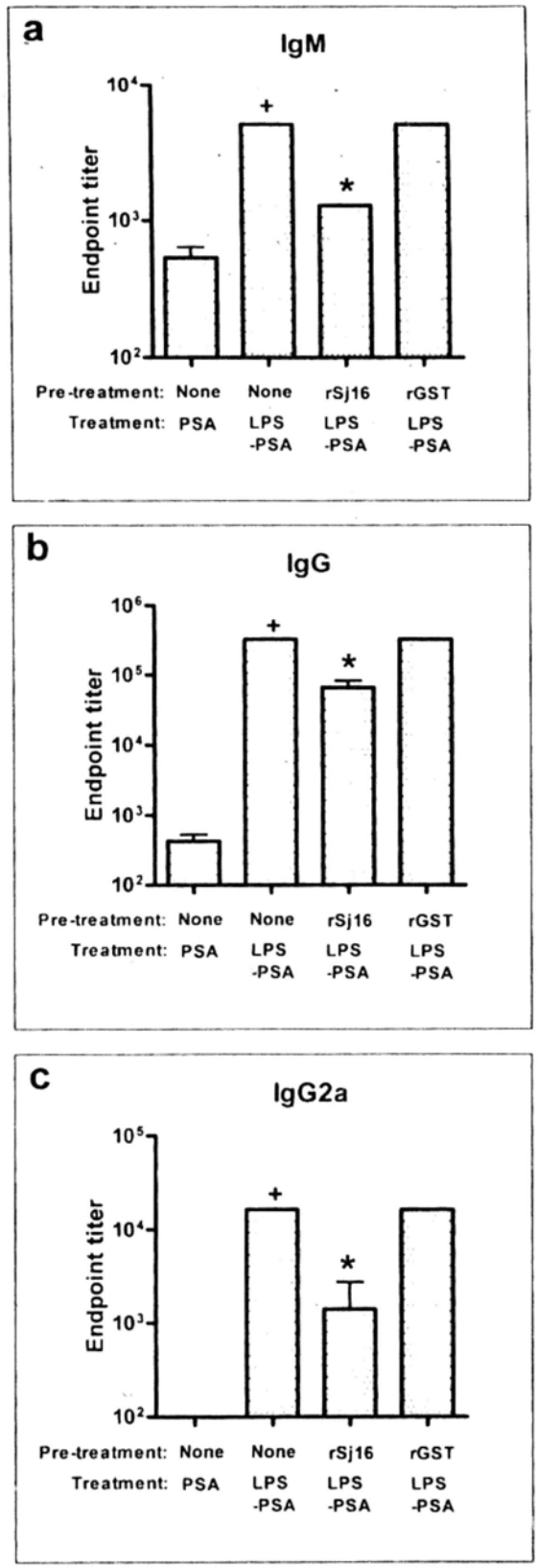

Fig.4.5.1.2 rSj16 suppressed antibody production to heterologous antigen PSA in the presence of LPS as adjuvant. Groups of BALB/c mice were treated i.p. with rSj16, or PBS (labeled **None**, served as control), or recombinant GST (rGST) (served as control) for 1 hour. The mice were then immunized i.p. with pig serum

albumin (PSA) in the presence of lipopolysacchride (LPS) as adjuvant. Two weeks later, the mice were boosted with the same antigens as used in the sensitization. All mice were then challenged i.p. with HSA. Serum samples were collected for antibody determination after the last challenge. The antibody levels in the sera were determined using ELISA. Data were expressed as mean ± S.E.M. of 4 mice per group. +, $P < 0.1$ V.S. those immunized with PSA alone; *, $P < 0.1$ V.S. those immunized with LPS + PSA as analyzed with Mann-Whitney U test.

4.5.2 Suppression of antibodies production to heterologous antigen in the presence of alum as adjuvant

Previous studies suggest that high dosage of LPS induce Th1 type immune responses(121), while alum is a classical Th2 inducing adjuvant(122). We were therefore interested to investigate the effect of rSj16 on the antibodies production to HSA in the presence of alum as adjuvant. The results showed that following i.p. immunization with alum-HSA, BALB/c mice displayed a significant increase in HSA-specific IgM (Fig.4.5.2.1a), IgG (Fig.4.5.2.1b), IgG2a (Fig.4.5.2.1c), IgE (Fig.4.5.2.1d), IgG1 (Fig.4.5.2.1e) and IgA (Fig.4.5.2.1f) production as compared with those immunized with HSA alone. The production of anti-HSA IgG, IgG1, IgG2a and IgA were observed following primary immunization, and were further enhanced with boosting. The production of HSA-specific IgM in the sera of alum-HSA immunized mice were not significant increased following primary immunization, but reached a high level following boosting, and was still higher than the levels in HSA alone-immunized mice after challenge. It should be mentioned that, although the BALB/c mice immunized with both LPS along with HSA and alum along with HSA displayed increased levels of anti-HSA IgG1 and IgG2a in their sera, the ratio of IgG2a/IgG1 in LPS along with HSA-immunized mice sera is

much higher than those in alum along with HSA-immunized mice sera (Fig.4.5.2.2). Mice pretreated with rSj16 1 hour before or along with the immunization of LPS-HSA displayed reduced levels of anti-HSA IgM (Fig.4.5.2.1a), IgG (Fig.4.5.2.1b), IgG1 (Fig.4.5.2.1e), IgA (Fig.4.5.2.1f), and IgE (Fig.4.5.2.1d).

The productions of anti-HSA IgA and IgG2a were not affected by the rSj16 treatment (Fig.4.5.2.1c, 4.5.2.1f). Mice pretreated with rGST 1 hour before the immunization of LPS-HSA did not display any difference in the production of anti-HSA IgM (Fig.4.5.2.1a), IgG (Fig.4.5.2.1b), IgG2a (Fig.4.5.2.1c), IgA (Fig.4.5.2.1f), IgE (Fig.4.5.2.1d) and IgG1 (Fig.4.5.2.1e).

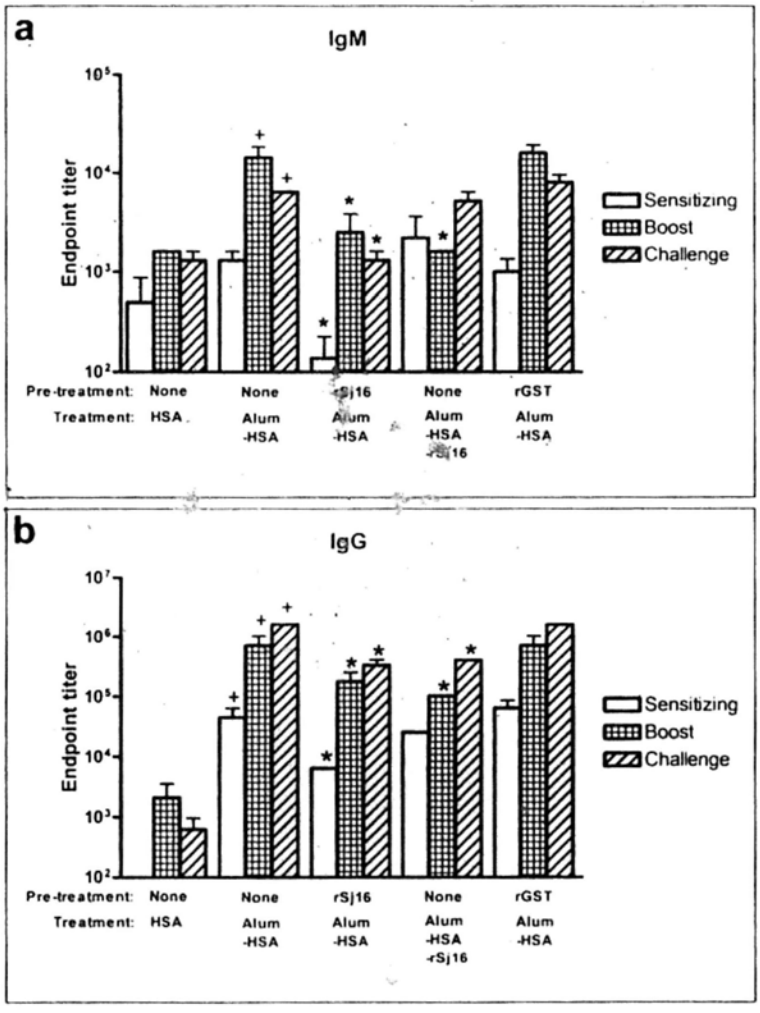

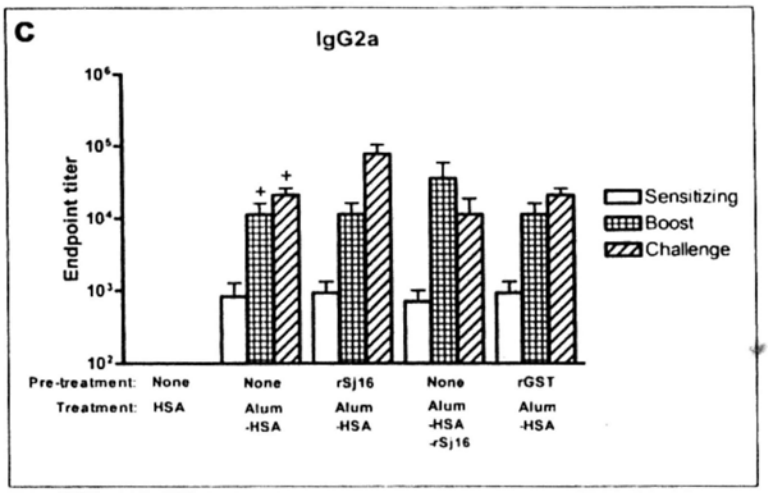
c
IgG2a
Endpoint titer
Sensitizing
Boost
Challenge
Pre-treatment: None None rSj16 None rGST
Treatment: HSA Alum -HSA Alum -HSA Alum -HSA -rSj16 Alum -HSA

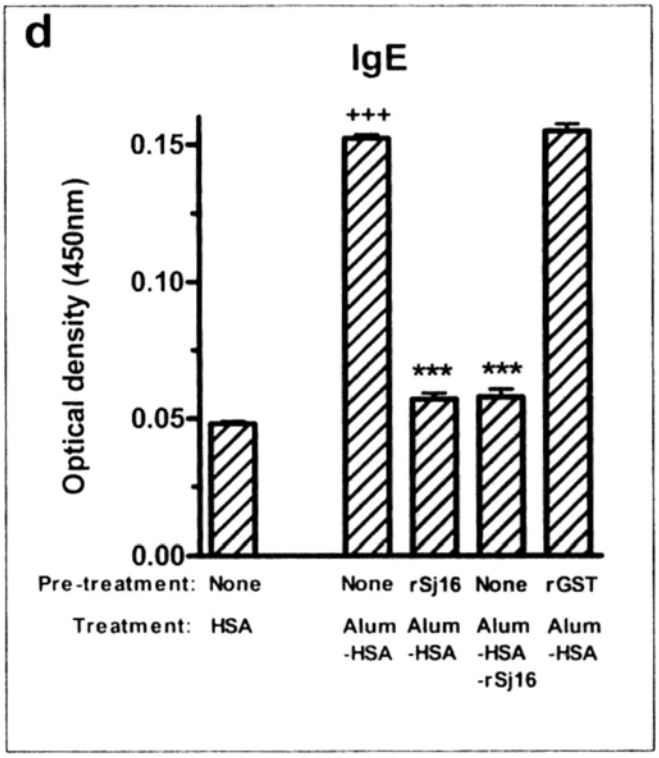
d
IgE
Optical density (450nm)
0.15
0.10
0.05
0.00
+++
***
***
Pre-treatment: None None rSj16 None rGST
Treatment: HSA Alum -HSA Alum -HSA Alum -HSA -rSj16 Alum -HSA

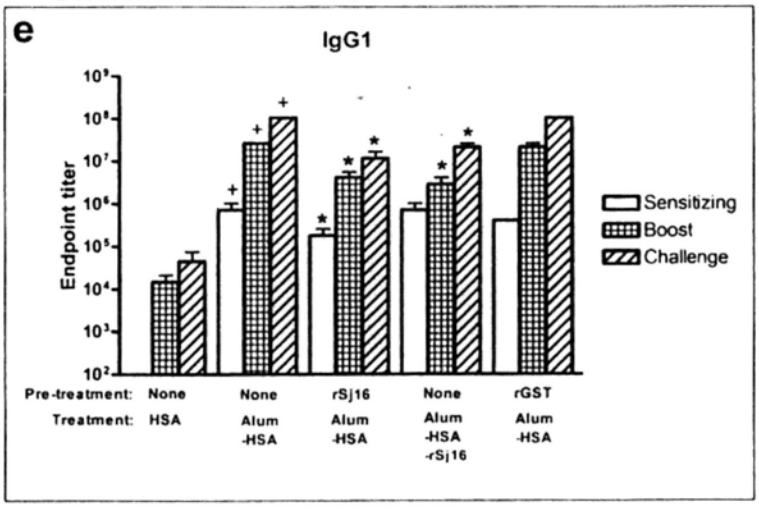
e
IgG1
Endpoint titer
Sensitizing
Boost
Challenge
Pre-treatment: None None rSj16 None rGST
Treatment: HSA Alum -HSA Alum -HSA Alum -HSA -rSj16 Alum -HSA

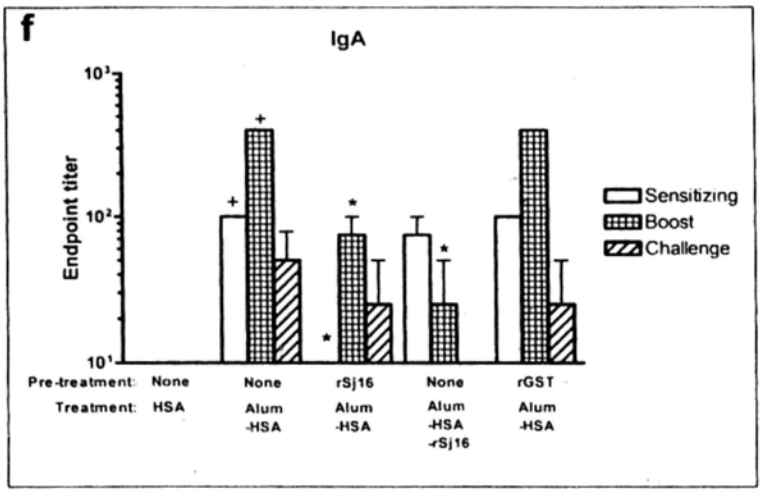

Fig.4.5.2.1 rSj16 suppressed antibody production to heterologous antigen HSA in the presence of alum as adjuvant. Groups of BALB/c mice were treated i.p. with rSj16, or PBS (labeled as **None**, served as control), or recombinant GST (rGST) (served as control) for 1 hour. The mice were then immunized i.p. with human serum albumin (HSA) in the presence of alum as adjuvant. Two weeks later, the mice were boosted with the same antigens as used in the sensitization. All mice were then challenged i.p. with HSA. Serum samples were collected for antibody determination after sensitization, booster, and last challenge. The antibody levels in the sera were determined using ELISA. Data were expressed as mean ± S.E.M. of 4 mice per group. +, $P < 0.1$ V.S. those immunized with HSA alone; *, $P < 0.1$ V.S. those immunized with LPS + HSA as analyzed with student t test (for IgE) or Mann-Whitney U test (for IgG, IgM, IgG2a, IgG1, and IgA).

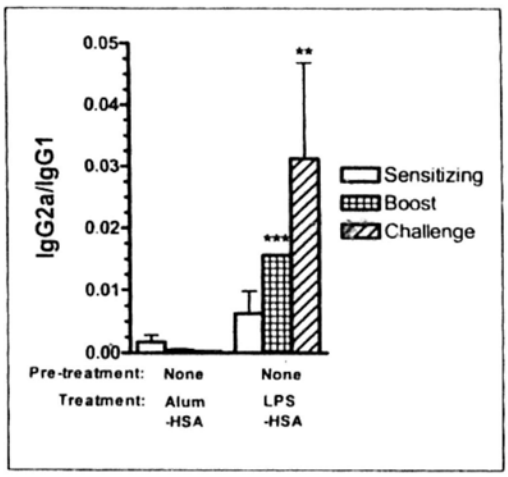

Fig.4.5.2.2 Compare the ratio of HSA-specific IgG2a/IgG1 in the sera of mice immunized with LPS-HSA and mice immunized with alum-HSA. Groups of BALB/c mice were immunized with HSA in the presence of LPS as adjuvant, or HSA in the presence of alum as adjuvant, and then boosted and challenged as described in Methodology 3.4.1. Serum samples were collected for antibody determination after sensitization, booster, and last challenge. The sera levels of IgG2a and IgG1 were determined using ELISA, and the ratio of IgG2a/IgG1 for each serum sample was calculated. Data were expressed as mean ± S.E.M. of 4 mice per group. **, $P < 0.01$; ***, $P < 0.001$ V.S. those of alum + HSA group.

4.5.3 Spleen cells from mice treated with rSj16 display a lower proliferative response to HSA

One day after last challenge, the mice were sacrificed and the spleens were isolated. Spleen cell suspension was prepared from each spleen and stimulated with 5 μg/ml HSA for 3 days. The spleen cell proliferation was then analyzed by BrdU cell proliferation ELISA. The results showed that spleen cells from both rSj16 treated groups exhibited less proliferative potential to the HSA stimulation as compared with those immunized with LPS-HSA (Fig.4.5.3.1a) or with those immunized with alum-HSA (Fig.4.5.3.1b). Spleen cells from rGST pre-treated mice

did not show significant difference in the proliferation as compared with those immunized with LPS-HSA (Fig.4.5.3.1a) or with those immunized with alum-HSA (Fig.4.5.3.1b).

In order to study whether the suppressed spleen cell proliferativity in rSj16-treated groups due to directly inhibitory effect of rSj16 on the spleen cell proliferation, spleen cell suspension prepared from naïve mice or LPS-HSA primed mice was pre-treated with 0.5 μg/ml rSj16, 0.5 μg/ml rGST or PBS for 1 hour, followed by the stimulation with 5 μg/ml ConA or 5 μg/ml HSA for 72 hours as described in Methodology 3.4.5. The cell proliferation was then assessed as mentioned above. The results showed that neither rSj16 nor rGST pre-treatment caused any significant changes in the ConA or HSA stimulated spleen cell proliferation (Fig.4.5.3.2, Fig.4.5.3.3).

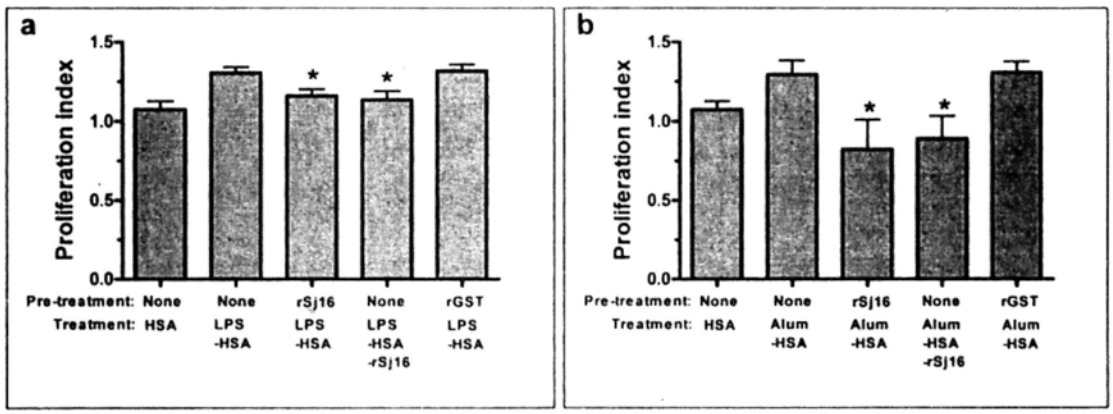

Fig.4.5.3.1 Spleen cells from rSj16-treated mice exhibited less proliferative response to HSA stimulation. Mice were treated as described in **Fig.4.5.1.1** and **Fig.4.5.2.1**. 24 hour after last challenge, the mice were sacrificed, and the spleens cells from each mouse were isolated and stimulated with HSA at 37°C for 72 hours. The spleen cells proliferation was then evaluated with BrdU cell proliferation ELISA. Data were expressed as mean ± S.E.M. of 4 mice per group. *, $P < 0.05$ V.S. those immunized with LPS + HSA or alum + HSA.

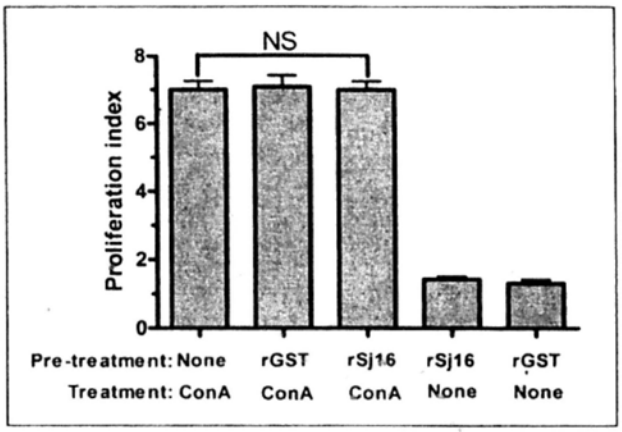

Fig.4.5.3.2 Effects of rSj16 on ConA-stimulated spleen cell proliferation. Spleen cells from non-treated BALB/c mouse were isolated, pre-treated with or without rSj16, and stimulated with ConA at 37°C for 72 hours. The spleen cells proliferation was then evaluated with BrdU cell proliferation ELISA. Data were expressed as mean ± S.E.M. of 4 mice per group. NS, not significant.

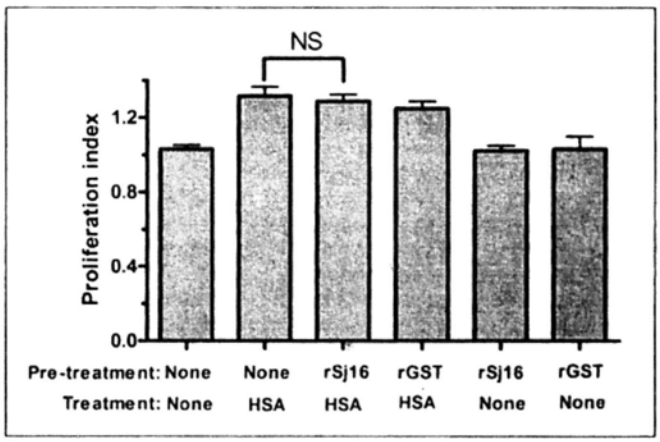

Fig.4.5.3.3 Effect of rSj16 on HSA-stimulated spleen cell proliferation. Mice were treated as described in **Fig.4.5.1.1**. 24 hour after last challenge, the mice were sacrificed. The spleens cells from LPS + HSA group were isolated, pre-treated with ot without rSj16, and stimulated with HSA at 37°C for 72 hours. The spleen cells proliferation was then evaluated with BrdU cell proliferation ELISA. Data were expressed as mean ± S.E.M. of 4 mice per group. NS, not significant.

4.5.4 Spleen cells from rSj16-treated mice produce less cytokines in response to HSA stimulation

Mice were primed, boosted, and challenged with HSA as described in Methodology 3.4.1. Spleen cells were isolated 24 hours after final challenge, and cultured with or without HSA for for 48 hour. Cytokine levels in these supernatants were determined by Sandwich ELISA or FlowCytomix. Following *in vitro* stimulation with HSA, spleen cells from LPS-HSA immunized mice produced significantly more IL-2 (Fig.4.5.4.1a), IL-4 (Fig.4.5.4.1b), IL-10 (Fig.4.5.4.1c), IL-17 (Fig.4.5.4.1d), and IFN-γ (Fig.4.5.4.1e) as compared with those from HSA alone-immunized mice. However, if the mice were treated with rSj16 1 hour before or along with the immunization of LPS-HSA, rSj16 could significantly suppress the production of IL-2 (Fig.4.5.4.1a), IL-4 (Fig.4.5.4.1b), IL-10 (Fig.4.5.4.1c), IL-17 (Fig.4.5.4.1d), and IFN-γ (Fig.4.5.4.1e).

The same effect was observed when alum was used as the immunization adjuvant. Following stimulation with HSA, spleen cells from alum-HSA immunized mice produced significantly more IL-4 (Fig.4.5.4.2a), IL-6 (Fig.4.5.4.2b), and IL-10 (Fig.4.5.4.2c) as compared with those from HSA alone-immunized mice. Again, rSj16 could significantly suppress the production of IL-4 (Fig.4.5.4.2a), IL-6 (Fig.4.5.4.2b), and IL-10 (Fig.4.5.4.2c) when it was i.p. injected 1 hour before or along with the alum-HSA.

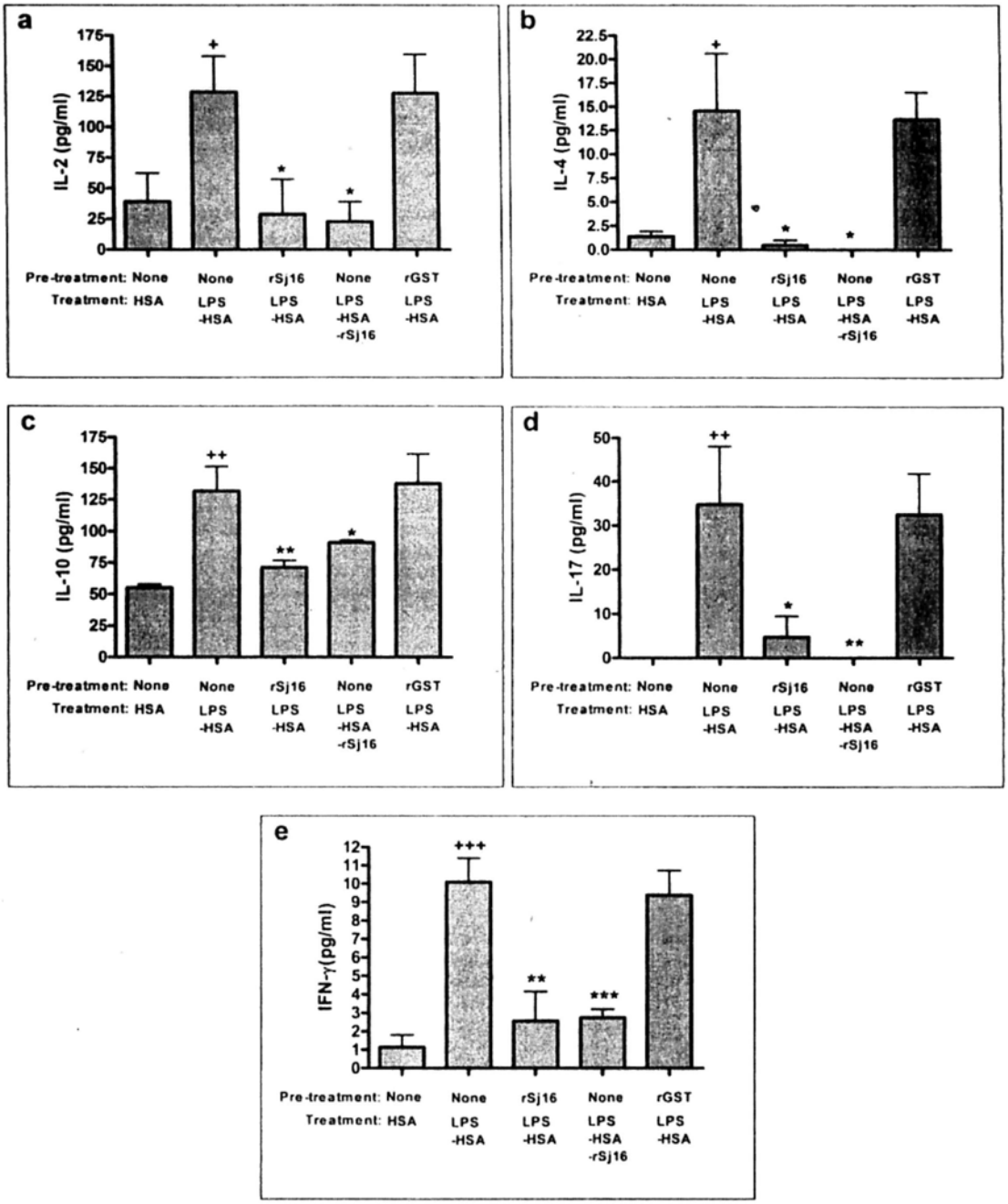

Fig.4.5.4.1 rSj16 suppressed cytokine production by spleen cells from mice immunized with HSA in the presence of LPS as adjuvant. Mice were treated as described in **Fig.4.5.1.1** in the presence of LPS as adjuvant. 24 hour after last challenge, the mice were sacrificed, and the spleens from each mouse were isolated and stimulated with HSA at 37°C for 48 hours. The cytokine levels in the culture supernatants were measured with Sandwich ELISA. Data were expressed as mean ± S.E.M. of 4 mice per group. +, $P < 0.1$; ++, $P < 0.01$; +++, $P < 0.001$ V.S. those immunized with HSA alone; *, $P < 0.1$; **, $P < 0.01$; ***, $P < 0.001$ V.S. those immunized with LPS + HSA.

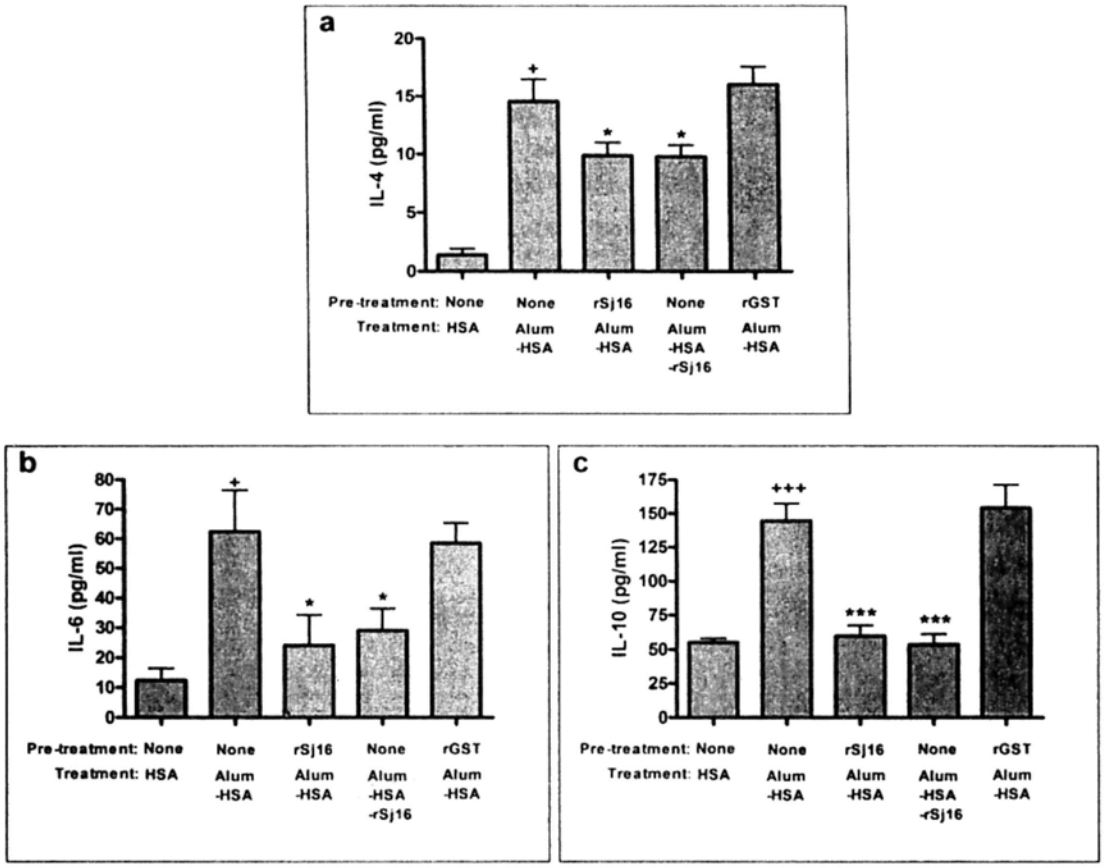

Fig.4.5.4.2 rSj16 suppressed cytokine production by spleen cells from mice immunized with HSA in the presence of alum as adjuvant. Mice were treated as described in **Fig.4.5.2.1** in the presence of alum as adjuvant. 24 hour after last challenge, the mice were sacrificed, and the spleens from each mouse were isolated and stimulated with HSA at 37°C for 48 hours. The cytokine levels in the culture supernatants were measured with Sandwich ELISA. Data were expressed as mean ± S.E.M. of 4 mice per group. +, $P < 0.1$; ++, $P < 0.01$; +++, $P < 0.001$ V.S. those immunized with HSA alone; *, $P < 0.1$; **, $P < 0.01$; ***, $P < 0.001$ V.S. those immunized with alum+ HSA.

4.6 Effects of rSj16 on the differentiation of JCS cell and hematopoiesis of mouse bone marrow cells

4.6.1 rSj16 inhibited JCS cell proliferation

The anti-proliferative effect of rSj16 was evaluated by MTT assay. Data were

expressed as the percentage inhibition by the ratio of each absorbance relative to the absorbance of the non-treated control, multiplied by 100%. A concentration- (Fig.4.6.1a) and time- (Fig.4.6.1b) dependent inhibition of rSj16 on JCS cell growth was observed at 48 hours (more than 10% inhibition) and persisted until 72 hours. rSj16 inhibited the proliferation of JCS cells at a maximal effect of more than 40% at 72 hours, and reached this maximal effect at the concentration of 0.5 μg/ml or higher (Fig.4.6.1a). Thus, in the following part of this study, 0.5 μg/ml of rSj16 was used. rGST didn't show significant effect on the proliferation of JCS cells when be used as high as 5 μg/ml (data not shown).

In order to test whether the suppression of JCS proliferation by rSj16 is due to its cytotoxic effect on the cells, JCS cells were incubated with rSj16 for up to 72 hours and the cell viability was assessed as described in Methodology 3.5.2. The results indicated that the viability of JCS cells was not affected after 0.5 μg/ml rSj16 treatment for 24 hours (98.51% ± 0.14% vs. 98.86% ± 0.28% viability, $P>0.2$; rSj16 treatment vs. untreated; n=4), 48 hours (97.80% ± 0.35% vs. 97.36 ± 0.43%, $p>0.2$; n=4) and 72 hours (96.48% ± 0.57% vs. 97.43% ± 0.51%, $p>0.2$; n=4). 0.5 μg/ml rGST didn't cause significant effects on JCS viability (data not shown).

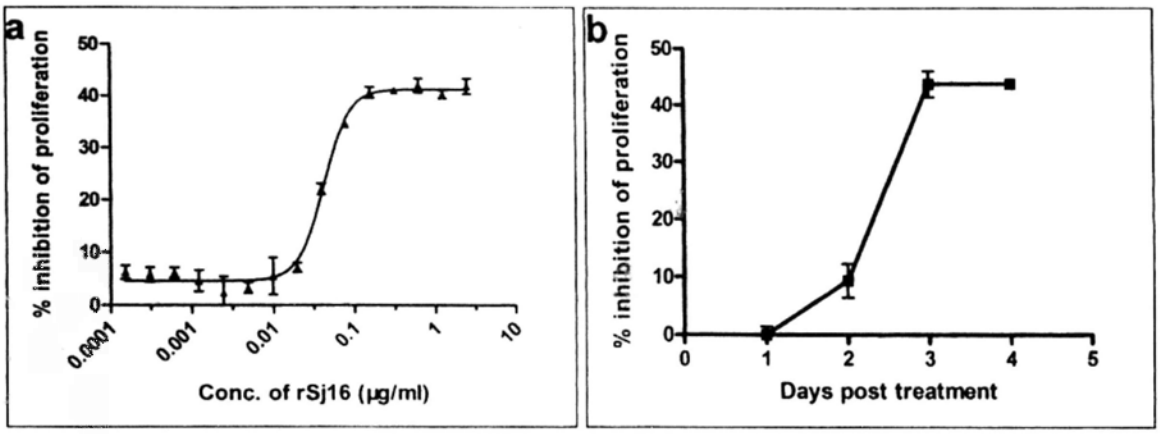

Fig.4.6.1 Anti-proliferative effect of rSj16 on JCS cells. JCS cells were incubated with 0.2 ml of medium containing different doses of rSj16 for 72 hours (a), or containing 0.5 μg/ml rSj16 for up to 96 hours (b). The proliferation was quantified by MTT assay.

4.6.2 Effect of rSj16 on the JCS cell cycle

Because rSj16 exerted significant effect on JCS cells proliferation, while didn't affect the viability of the cells, we were interested in studying the pattern of cell cycle distribution of rSj16-treated cells. The cell cycle distribution was assessed by flow cytometry after treatment with rSj16 for various times.

A significant accumulation of JCS cells in the G1/G0 phase of the cell cycle occurred at 24 hours (Fig.4.6.2a) and reached the peak at 72 hours (Fig.4.6.2c) after treatment with 0.5 μg/ml rSj16, companied with a concomitant decrease in the proportion of those in S phase. A significant accumulation of JCS cells in the G2/M phase of the cell cycle also occurred at 48 hours (Fig.4.6.2b) and reached the peak at 72 hours (Fig.4.6.2c) after treatment with 0.5 μg/ml rSj16. After 72 hours, the accumulation of G1/G0 and G2/M population didn't increase anymore even exposure for longer time (Fig.4.6.2d). rGST had no effect on the cell cycle distribution of JCS cells (Fig. 4.6.2a-4.6.2d).

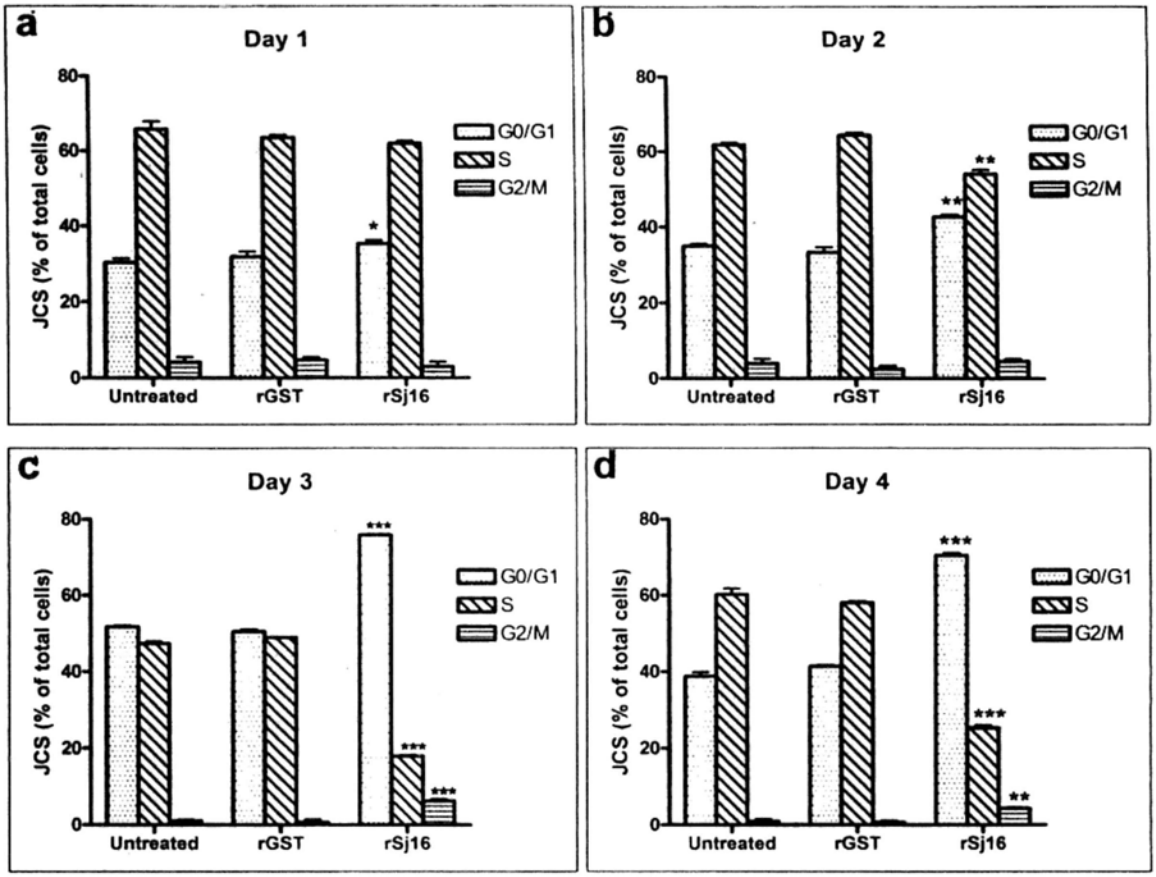

Fig.4.6.2 JCS cell cycle modulation by rSj16. JCS cells were cultured for one day (a), two days (b), three days (c), and four days (d) in the presence of 0.5 μg/ml rSj16 (rSj16), 0.5 μg/ml rGST (rGST) or medium alone (untreated), and the cell cycle status were analyzed using flow cytometry. Data indicate mean ± S.E.M. of three independent experiments. *, $P < 0.1$; **, $P < 0.01$; ***, $P < 0.001$ as compared with that of untreated group.

4.6.3 Morphological study of rSj16-treated JCS cells

The effect of rSj16 on morphology of JCS cells was studied in a time course of 72 hours. The JCS cells became adherent and developed pseudopodia in the presence of rSj16 (0.5 μg/ml) (Fig.4.6.3a- 4.6.3b). Aggregation of the JCS cells to each other followed by the adherence of the cells to the plate was observed within 24 hours of rSj16 exposure. By the time of 48 hours, greater than 50% of the cells attached to the plate and began to form pseudopodia. After 72 hours of rSj16

exposure, 71.28% ± 3.15% of the cells were adherent to the plate, and over 50% of the cells had pseudopodia and cytoplasmic vacuoles. All of these morphological changes indicated that rSj16 may induce monocyte/macrophage-like differentiation of JCS cells, as the abilities to adhere to charged surfaces and to develop prominent pseudopodia are typical features of normal tissue macrophages(123, 124). In contrast, cells exposed with rGST (0.5 μg/ml) didn't developed significant adhesion (only 0.02% ± 0.007% of the cells were adherent at 72 hours) and pseudopodia formation.

To further characterize the morphological changes, cytospin smear of JCS cells treated with rSj16 or rGST were prepared and stained with Wright-Giemsa stain. The result showed that after 72 hours exposure to rSj16, the nuclear:cytoplasmic ratio of the cells reduced, the nuclear chromatin became condensed and eccentrically placed, the cytoplasmic borders were protruded, and cytoplasmic vacuoles were often present (Fig.4.6.3e). These morphological features were similar to those described for mature tissue macrophages (120, 123, 124). JCS cells treated with rGST didn't exhibit significant morphological changes (Fig.4.6.3d).

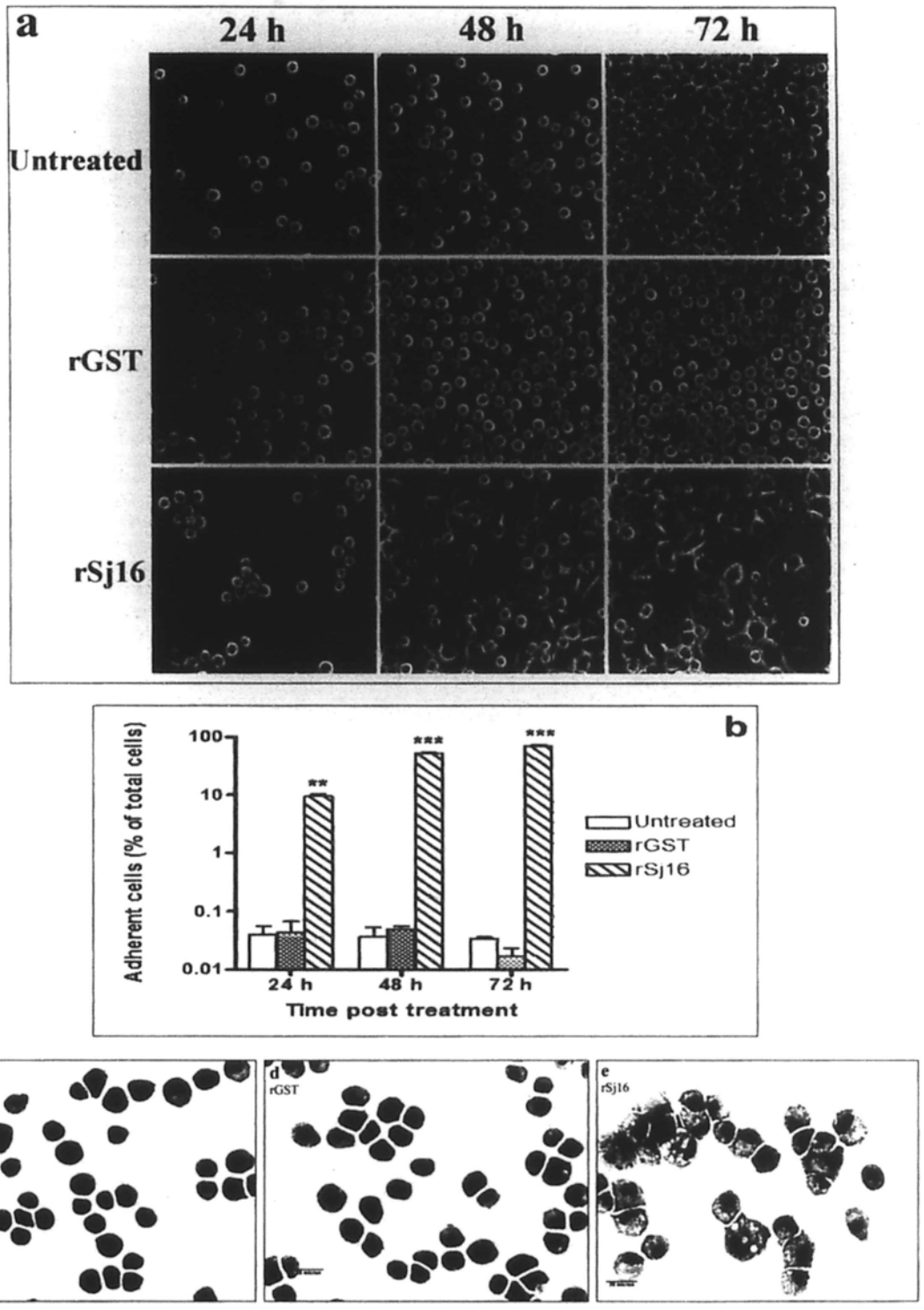

Fig.4.6.3 Effect of rSj16 on adherence and morphology of JCS cells. JCS cells were treated with 0.5 μg/ml rSj16 (rSj16), 0.5 μg/ml rGST (rGST) or medium alone (untreated) for various time periods, and morphological changes were studies using a light microscope (Nikon). **a.** time course morphological changes of JCS cells (magnification, ×200). Black bars represent 50 μm. **b.** Induction of adherence of JCS cells after exposure to rSj16. The data were expressed as mean ± S.E.M., n=3. **, p

< 0.01; ***, $p < 0.001$ as compared with that of untreated group. **c-e.** Wright Giemsa staining of JCS cells 72 hours after exposure (magnification, ×400). Black bars represent 25 μm. Data are representative of three individual experiments.

4.6.4 Effect of rSj16 on the expression of cell surface markers of JCS cells

To confirm the monocyte/macrophage-like differentiation-inducing activity of rSj16 on JCS cells, flow cytometric analysis was carried out to examine for the expression of differentiation antigens by rSj16-treated cells. Untreated JCS cells expressed little $F4/80^+$ and $Gr\text{-}1^+$ (Fig.4.6.4). 72 hours exposure of JCS cells to rSj16 (0.5 μg/ml) resulted in nearly 40% increase in the expression of the antigen $F4/80^+$, while there were no significant changes on the expression of $Gr\text{-}1^+$ (Fig.4.6.4). rGST didn't show significant effect on the expression of these antigens.

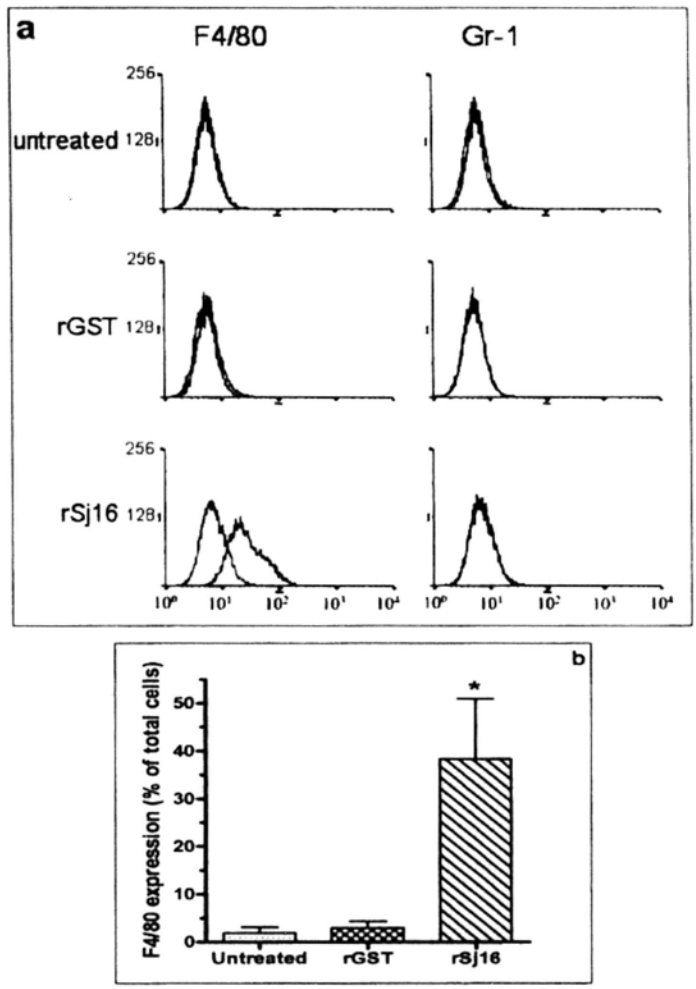

Fig.4.6.4 Induction of cell surface antigens expression on JCS cells by rSj16. JCS cells were treated for 72 hours in the presence of 0.5 μg/ml rSj16 (rSj16), 0.5 μg/ml rGST (rGST) or medium alone (untreated), and then analyzed for expression of F4/80 and Gr-1 using flow cytometry. **a.** Red line indicates isotype-matched control antibody; black line, F4/80 or Gr-1. **b.** Column indicates mean ± S.E.M. of four independent experiments. *, $p < 0.05$ as compared with that of untreated group.

4.6.5 Effect of rSj16 on phagocytic activity of JCS cells

A key function of normal mononuclear phagocytes is ingestion of foreign materials. The biological function of rSj16-treated JCS cells was therefore measured by their capacity of yeast phagocytosis. The results indicated that JCS cells developed the ability to efficiently phagocytose *Saccharomyces cerevisiae* after

rSj16 exposure (Fig.4.6.5a- 4.6.5c). More than 50% of the JCS cells ingested three or more yeast cells after cultured in the presence of 0.5 μg/ml rSj16 for 3 days (Fig.4.6.5d). Less than 2% of the untreated or rGST-treated JCS cells phagocytized yeast cells.

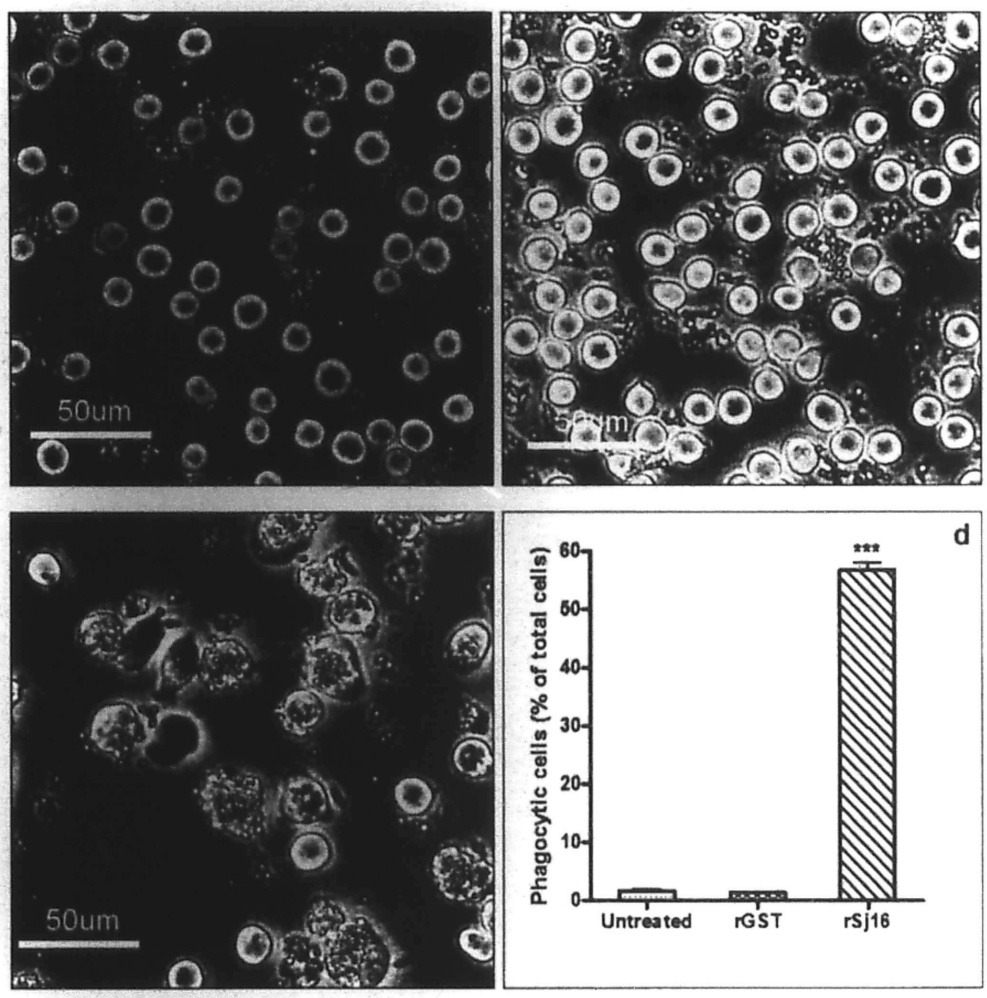

Fig.4.6.5 Effect of rSj16 on phagocytic activity of JCS cells. JCS cells were treated for 72 hours with 0.5 μg/ml rSj16 (rSj16, **c**), 0.5 μg/ml rGST (rGST, **b**) or medium alone (untreated, **a**), and then analyzed for the capacity of yeast-ingesting. **a-c.** Arrows indicate the yeast-ingesting cells. White bars represent 50 μm (magnification, ×400). **d**. Percentage of phagocytic cells after 72 hours treatment. The results are the mean ± S.E.M. of three independent experiments. ***, $p < 0.001$ as compared with that of untreated group.

4.6.6 Up-regulation of IL-1α, IL-1β and TNF-α expression in rSj16-treated JCS cells

Previous studies reported that TNF-α could induce monocytic differentiation of JCS cells(117), and that IL-1α and IL-1β were involved in the differentiation-inducing activity of TNF-α(125). In addition, TNF-α has been identified as the active substance in PMA-induced macrophage differentiation of JCS cells. Thus, we investigated the effects of rSj16 on the expression of IL-1α, IL-1β and TNF-α of JCS cells. Untreated JCS cells expressed little IL-1α and IL-1β (both less than 1 pg/ml in the culture media, Fig.4.6.6b, 4.6.6c), and expressed low level of TNF-α (Fig.4.6.6a). Treatment of JCS cells with rSj16, but not rGST, caused marked time-dependent up-regulation of the expression of these three cytokines (Fig.4.6.6a-4.6.6c). The levels of IL-1α, IL-1β and TNF-α in the culture supernatants increased to 60.77 pg/ml, 8.57 pg/ml, and 97.15 pg/ml respectively after 3 days exposure to rSj16 (Fig.4.6.6a- 4.6.6c).

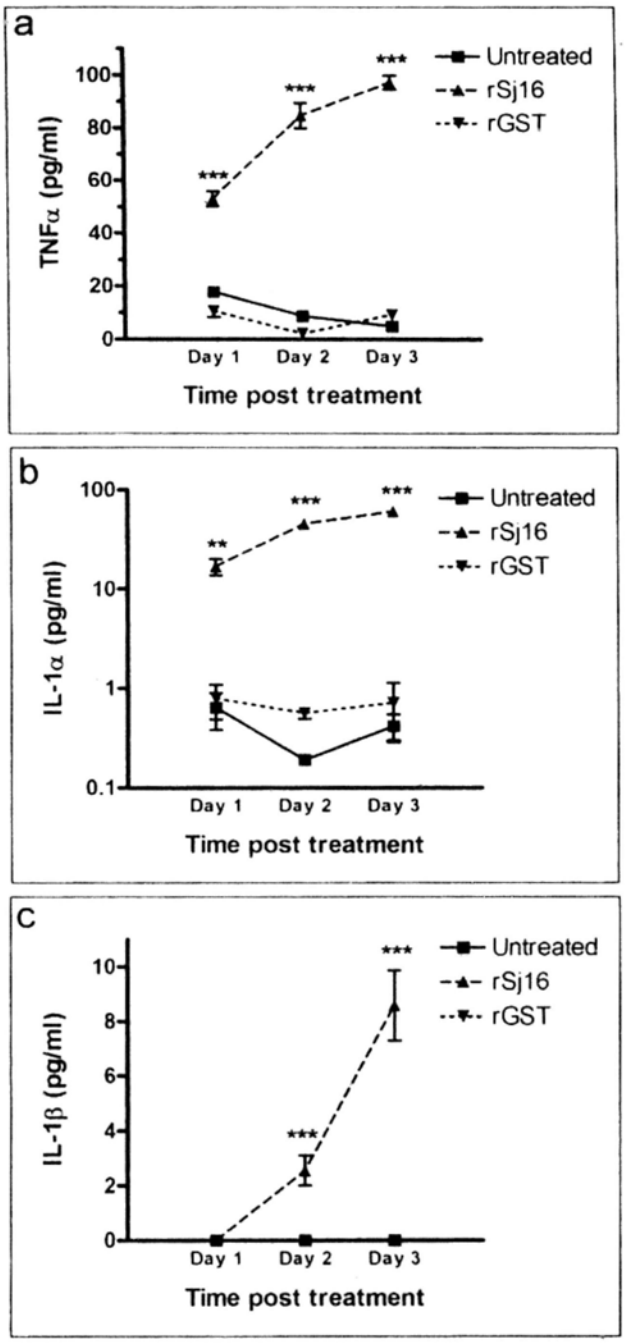

Fig.4.6.6 Effect of rSj16 on IL-1α, IL-1β and TNF-α production in JCS cells. JCS cells were treated with 0.5 μg/ml rSj16 (rSj16), 0.5 μg/ml rGST (rGST) or medium alone (untreated), and then the culture supernatants were collected at different time as indicated for the dectection of IL-1α, IL-1β and TNF-α by Sandwich ELISA. Values represent mean ± S.E.M. of three independent experiments. ***, $p < 0.001$; **, $p < 0.01$, as compared with that of untreated group.

4.6.7 Differentiation-inducing effect of rSj16 on JCS cells is not attributable to endogenous production of IL-1α, IL-1β and TNF-α

To investigate the role of endogenous IL-1α, IL-1β and TNF-α in the rSj16-induced JCS cells differentiation, specific antibodies were adopted to neutralize each cytokine respectively. The neutralizing ability of the antibodies were verified using D10.G4.1 cell proliferation assay for anti-IL-1α and anti-IL-1β, and using L929 cell cytolytic assay for anti-TNF-α. Before evaluating the blocking activity of the antibodies on rSj16-mediated differentiation, an initial experiment was performed to test the effect of each antibody on the proliferation (by MTT assay) and morphological changes of JCS cells, and the results indicated that the effect of each of them neither inhibited the proliferation (Fig.4.6.7.1) nor affected morphological changes (data not shown) of JCS cells when be used as high as 10 μg/ml. The blocking effect of each antibody on rSj16-induced JCS differentiation was evaluated by both MTT assay and morphological studies as described in *Materials and Methods*. The results showed that none of them, no matter be used separately or combined, could block rSj16-mediated morphological changes (data not shown) and anti-proliferation (Fig.4.6.7.2) of JCS cells at the concentration as high as 10 μg/ml. Therefore, it is suggested that rSj16-induced JCS differentiation does not depend on the endogenous production of IL-1α, IL-1β and TNF-α.

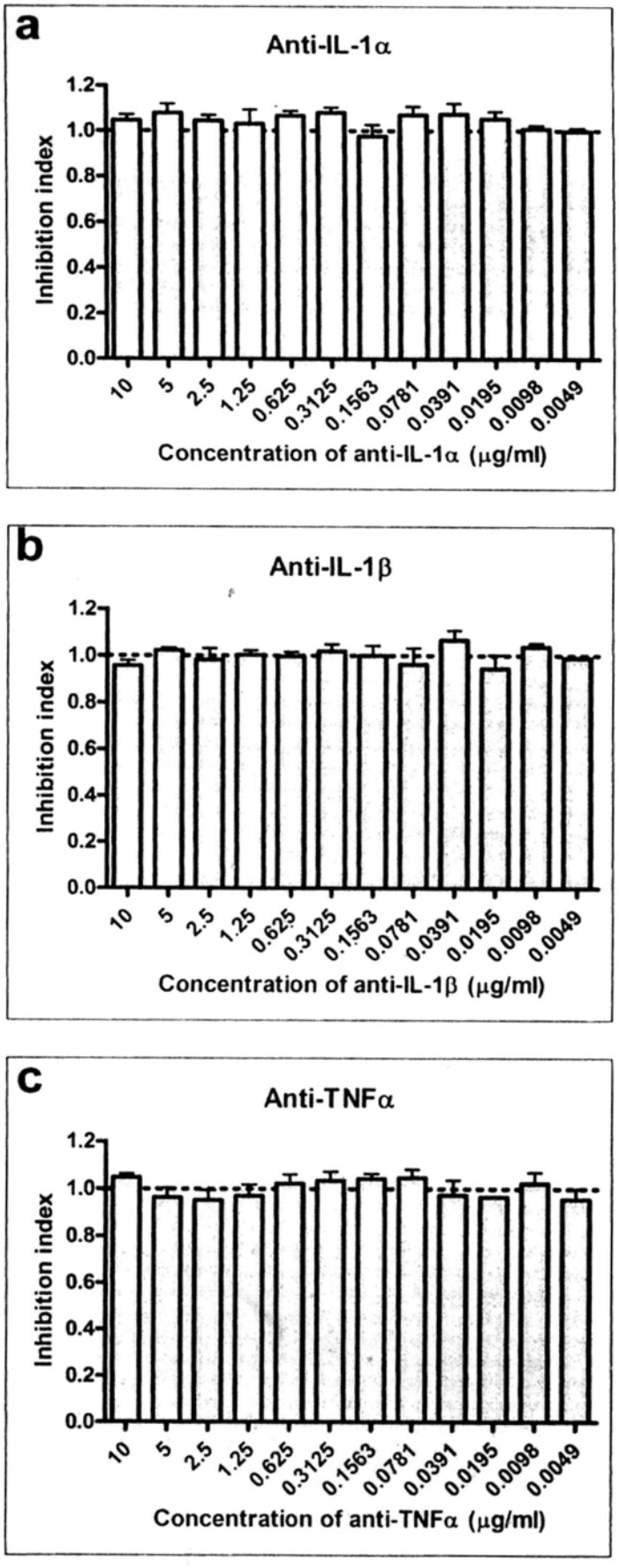

Fig.4.6.7.1 Assessment of anti-proliferative effect of anti-IL-1α antibody, anti-IL-1β antibody and anti-TNF-α antibody on JCS cells. JCS cells were incubated

with 0.2 ml of medium containing serially diluted anti-IL-1α antibody (a), anti-IL-1β antibody (b) and anti-TNF-α antibody (c) for 72 hours. The proliferation was quantified by MTT assay. The results were expressed as inhibition index which equals to mean O.D.570 of triplicate wells with RPMI 1640 medium containing anti-IL-1α, anti-IL-1β or anti-TNF-α antibodies/mean O.D.570 of triplicate wells with RPMI 1640 medium alone.

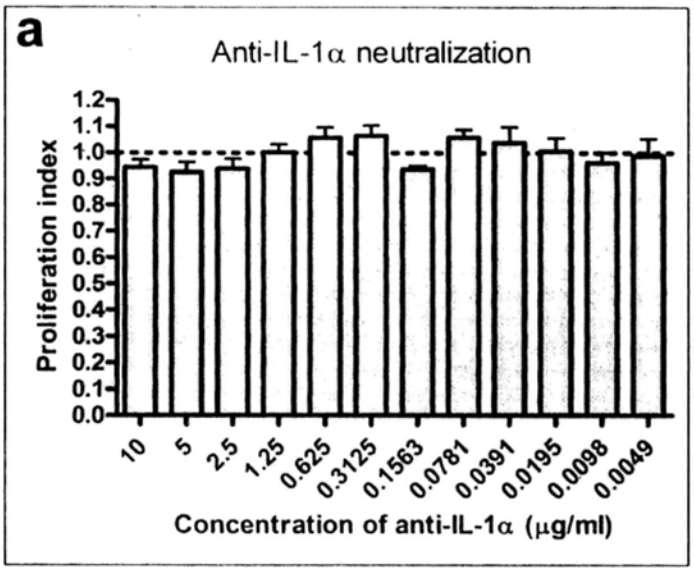

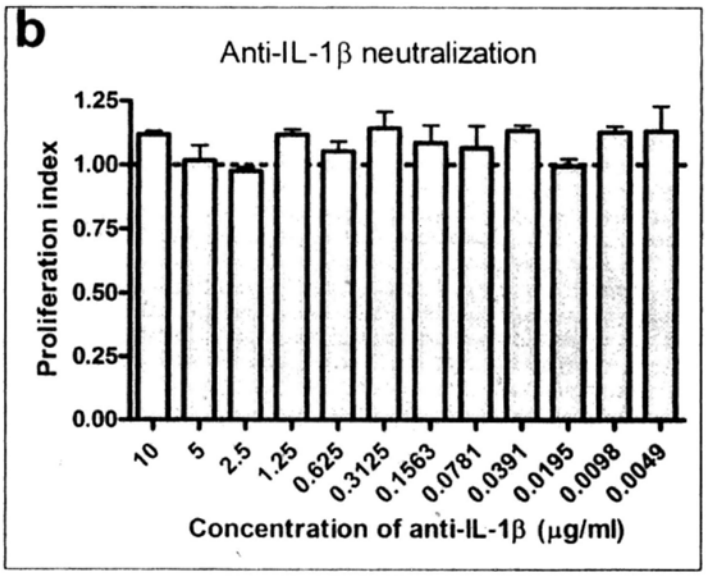

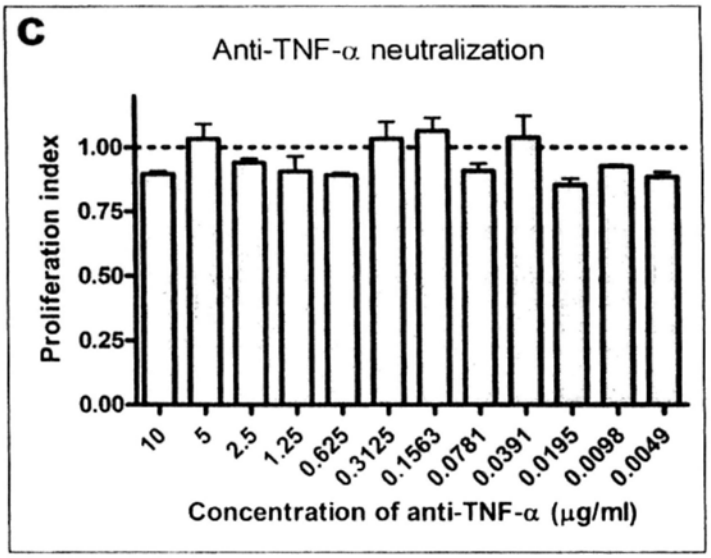

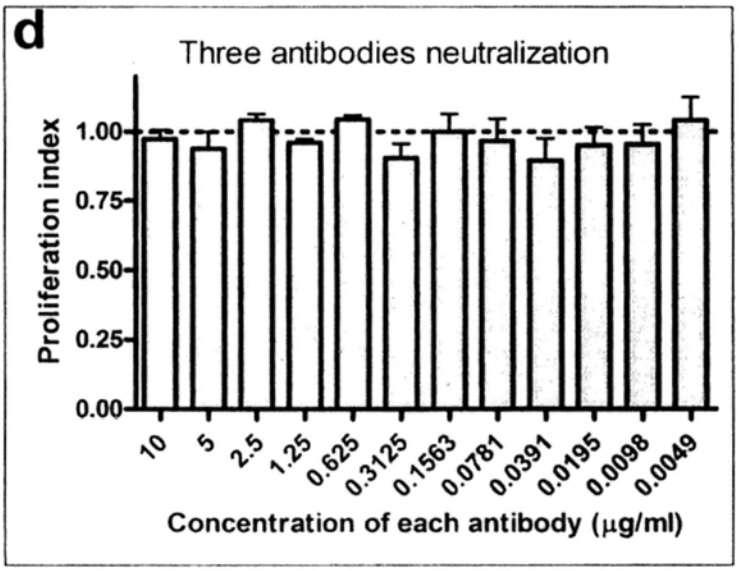

Fig.4.6.7.2 Assessment of the neutralizing effect of anti-IL-1α antibody, anti-IL-1β antibody and anti-TNF-α antibody on rSj16-mediated inhibition of JCS proliferation. JCS cells were incubated with 0.2 ml of medium containing 0.5 μg/ml rSj16 in the presence or absence of serially diluted neutralizing anti-IL-1α antibody (a), anti-IL-1β antibody (b), anti-TNF-α antibody (c), or these three antibodies together (d) for 72 hours. The proliferation was quantified by MTT assay. The results were expressed as proliferation index which equals to mean O.D.570 of triplicate wells containing 0.5 μg/ml rSj16 in the presence of neutralizing anti-IL-1α, anti-IL-1β or anti-TNF-α antibodies/ mean O.D.570 of triplicate wells containing rSj16 in the absence of neutralizing anti-IL-1α, anti-IL-1β or anti-TNF-α antibodies.

4.6.8 Effect of rSj16 on IL-3, M-CSF, or G-CSF induced proliferation and differentiation of mouse bone marrow cells.

As mentioned above, rSj16 could induce macrophage-like differentiation of JCS cells (Fig.4.6.3-4.6.5). Since the WEHI-3B JCS cells are derived from bone marrow progenitors (93), it raised a question whether rSj16 can also affect normal hematopoiesis of bone marrow cells. It is well characterized that hematopoietic growth factors such as G-CSF, M-CSF, and IL-3 can regulate the proliferation and differentiation of bone marrow cells and stimulate related colony formation (126, 127). To test the effects of rSj16 on normal hematopoiesis, mouse bone marrow cells were cultured in semi-solid agar cultures containing optimal G-CSF, M-CSF, or IL-3 in the presence or absence of 0.5 μg/ml of rSj16.

After treatment with G-CSF or M-CSF, significant increases of CFU-G colonies (Fig.4.6.8.1a) or CFU-M colonies (Fig.4.6.8.1b) were found in the corresponding plates. Addition of rSj16 into the culture before the treatment of G-CSF greatly reduced the colony counts of G-CSF-induced CFU-G (Fig.4.6.8.1a). It is interesting that the presence of rSj16 in the culture didn't affect the number of M-CSF-induced CFU-M colonies (Fig.4.6.8.1b), but only increase the compactness of the cells within the colonies (Fig.4.6.8.2).

As expected, colony forming unit-macrophage (CFU-M), CFU-granulocyte (CFU-G), and CFU-GM were significantly induced following seven days culture with IL-3 (Fig.4.6.8.1c). However, when the culture was pretreated with rSj16 one hour before the IL-3 treatment, the colony counts of CFU-G, CFU-GM and total colonies were significantly decreased, while the colony counts of CFU-M were increased (Fig.4.6.8.1c). Besides, in the presence of rSj16, the cells within CFU-M colonies also become more compact than those treated with IL-3 alone (Fig.4.6.8.3).

There were no colonies induced when the mouse bone marrow cells were treated

with PBS alone, 0.5 μg/ml of rSj16 alone, or 0.5 μg/ml of rGST alone (data not shown).

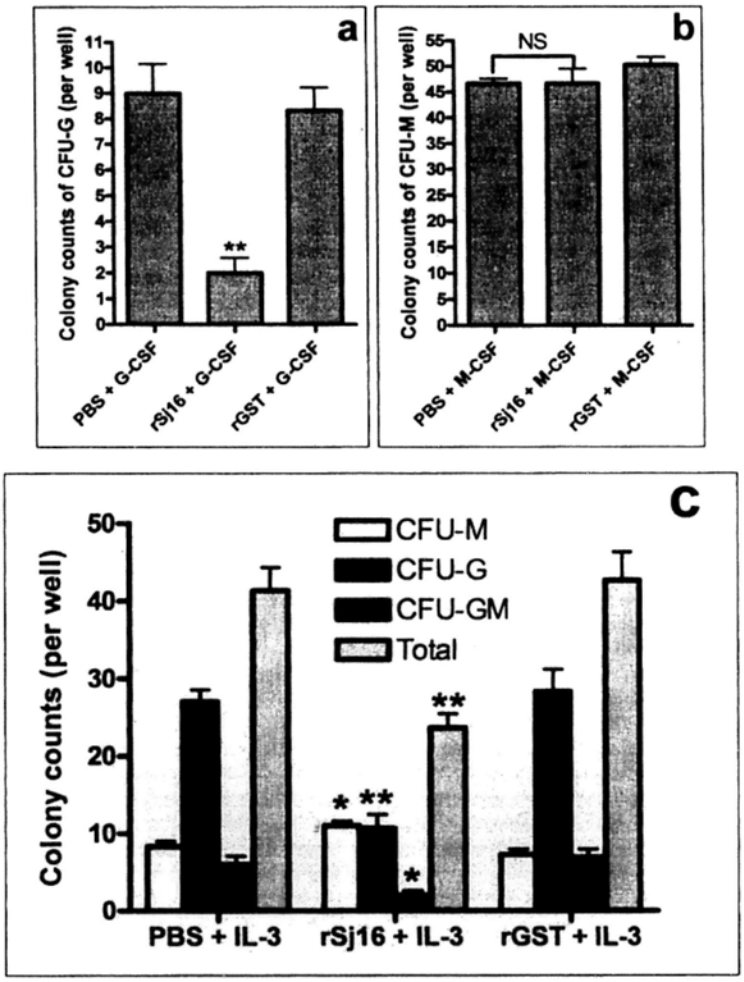

Fig.4.6.8.1 Effect of rSj16 on IL-3, M-CSF, or G-CSF induced colony formation of mouse bone marrow cells. Mouse bone marrow cells were plated in 0.33% agar cultures containing G-CSF (**a**), M-CSF (**b**), or IL-3 (**c**) in the presence of rSj16, rGST, or PBS in 24-well plates. The agar gels were dried and stained with hematoxylin solution following seven days of incubation. Differential colony counts were performed based on the morphology of the cells, and only colonies of greater than 40 cells were counted. Colony counts are indicated as number of colonies per well. Data are mean ± S.E.M. of triplicate wells, and are representatives of three individual experiments. *, $P < 0.05$; **, $P < 0.01$; NS, not significant versus the corresponding data in the PBS + G-CSF/M-CSF/IL-3 group.

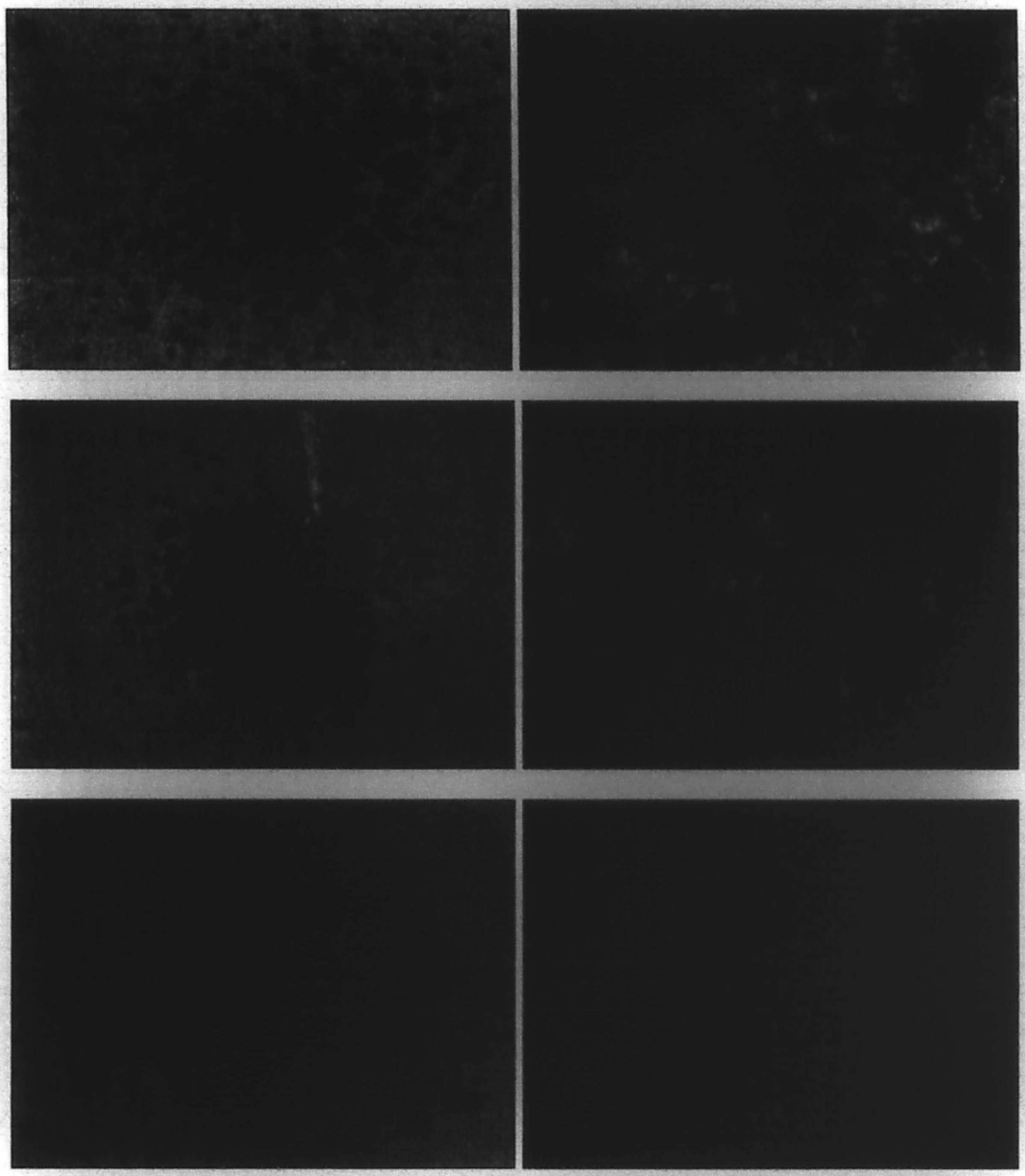

Fig.4.6.8.2 Effect of rSj16 on morphology of M-CSF-induced CFU-M colonies after hematoxylin staining. Mouse bone marrow cells were treated with M-CSF in the presence of rSj16 (b, e), rGST (c, f), or PBS (a, d) as described in Fig.4.6.8.1. Left column: the black bars represent 50 μm (magnification, × 100). Right column: the black bars represent 25 μm (magnification, × 400). The photos are representatives of three individual experiments.

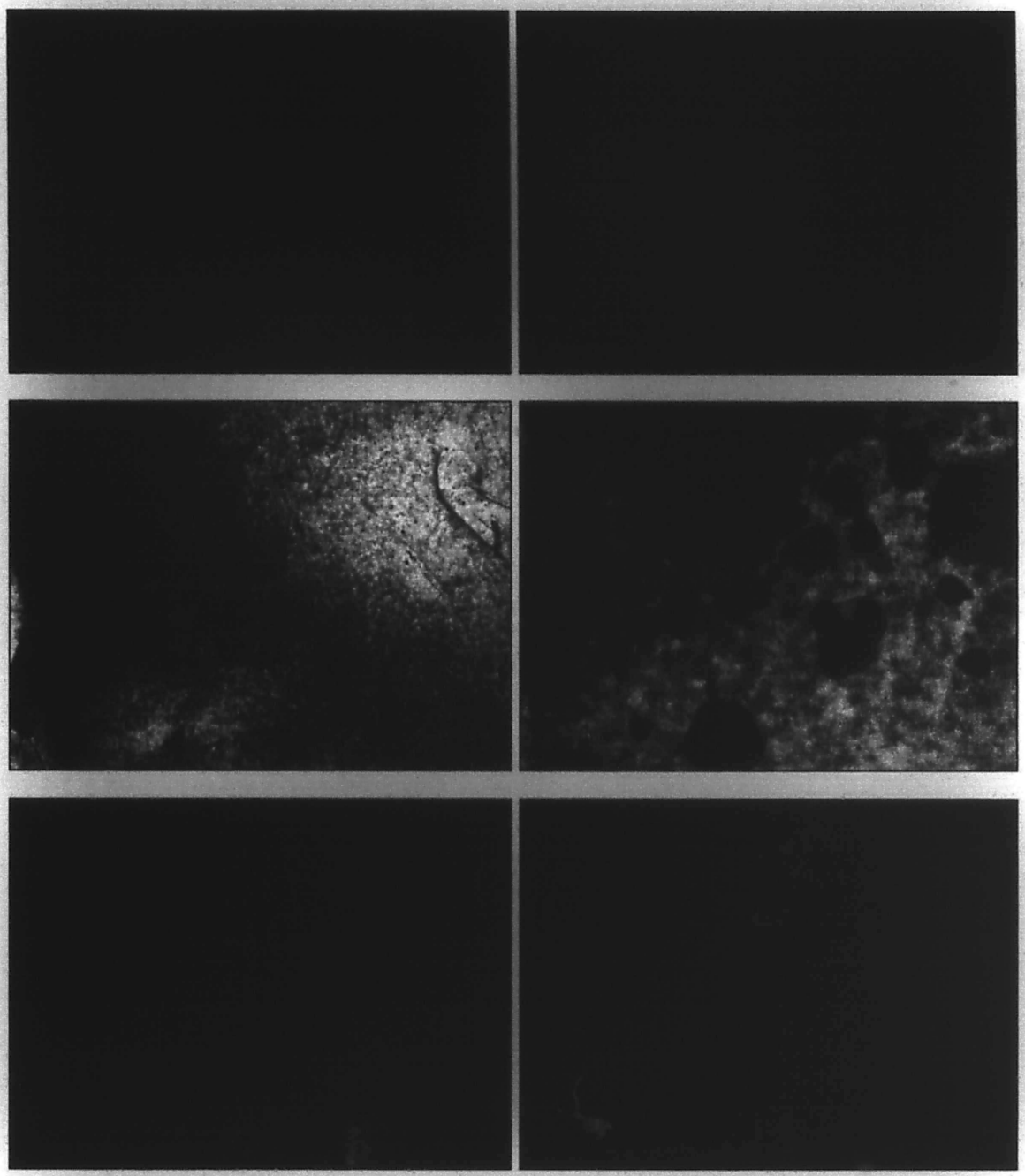

Fig.4.6.8.3 Effect of rSj16 on morphology of IL-3 induced CFU-M colonies after hematoxylin staining. Mouse bone marrow cells were treated with IL-3 in the presence of rSj16 (b, e), rGST (c, f), or PBS (a, d) as described in Fig.4.6.8.1. Left column: the black bars represent 50 μm (magnification, × 100). Right column: the black bars represent 25 μm (magnification, × 400). The photos are representatives of three individual experiments.

4.6.9 Effect of rSj16 on JCS apoptosis

The apoptosis of JCS cells was examined using Annexin-V/PI double staining and analyzed by flow cytometry. Exposure of JCS cells to 0.5 μg/ml rSj16 for 3 days resulted in 22.3% of the cells to undergo apoptosis (Fig.4.6.9). In contrast, rGST didn't induce significant apoptosis (1.3%) as compare with those of untreated cells (2.0%). For all of the cells treated with rSj16, rGST or untreated, no apparent apoptosis could be observed at day 1 and day 2 after treatment (data not shown).

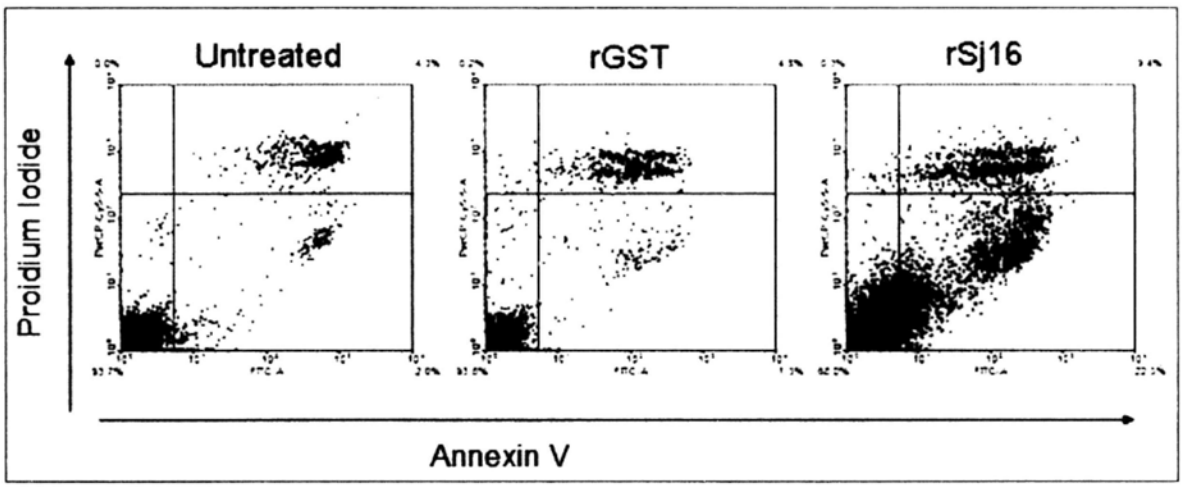

Fig.4.6.9 rSj16-induced apoptosis on JCS cells. JCS cells were treated with 0.5 μg/ml rSj16 (rSj16), 0.5 μg/ml rGST (rGST) or medium alone (untreated) for 3 days and then analyzed for the cells that were Annexin V-FITC$^+$ and PI$^-$, which represent those in the early stage of apoptosis. The percentage of cells in each quadrant was indicated in the figures. The results are representatives of three individual experiments.

5 Discussion

5.1 Expression and purification of recombinant Sj16 (rSj16) and recombinant GST (rGST)

Sj16 has 100% identity with the protein sequence of Sm16 which was identified from *S. mansoni* (Fig.4.1.1.1). Previous studies (85-88) reported that Sm16 could suppress the host immune responses by inhibiting the antigen-induced lymphoproliferation and suppressing the IL-2 production from lymphocytes. Sm16 could also suppress LPS-induced neutrophil infiltration and down-regulate production of the pro-inflammatory cytokines.

As it is difficult to obtain sufficient amount of native Sj16 protein from *S. japonicum*, we chose to express and purify rSj16 from *E. coli*. Previously, Rao et al. (2000) tried to express recombinant Sm16 in the *E. coli* and baculovirus systems. Although apparent recombinant proteins could be detected by Western blot using a Sm16 antibody, sufficiently purified recombinant Sm16 could not be obtained in a soluble form in their study (128). In addition, Valle et al. (1999) reported their attempt to express SmSLP in bacteria, yeast and insect systems, but invariably obtained very low yields of the recombinant protein (129). These studies indicated that this protein is difficult to be expressed in the usual prokaryotic or eukaryotic systems. In order to obtain sufficient soluble rSj16, we also tried several prokaryotic expression vectors using the *E. coli* system. Firstly, three types of pET vectors, pET28, pET30, pET32 (Novagen, USA), and pTYB4 (New England Biolabs, USA) were used, but no apparent recombinant protein could be detected (data no shown). Then, the coding region of Sj16 was inserted into *cspA* promoter-containing vector pCold TF (Takara, Japan) and the expression of rSj16 was induced at 15°C. Using this approach, rSj16 fusion protein could be produced as analyzed by SDS-PAGE (Fig.4.1.5). However, when we attempted to purify the recombinant protein, very low

yields of soluble protein were obtained. Finally, we used the vector pGEX-4T-1 (Amersham, USA) and obtained sufficient soluble rSj16 although the yields were still quite low (Fig.4.1.6). However, in all cases except using vector pCold TF, evident inhibition of host cell growth was observed during the induction of rSj16 expression (Fig.4.1.9 for using pGEX-4T-1, data no shown for other vectors), which corresponded with Valle's observation on SmSLP (129).

Amino acid sequence analysis of Sj16 suggested that Sj16 also shares partial similarities (~ 50%) with stathmins from several species. Stathmin is a protein that is known to play an important role in the process of mitotic arrest (130, 131). Stathmin can regulate microtubule dynamics by sequestering unpolymerized tubulin through binding two α/β-tubulin heterodimers (132, 133), and by increasing the rate of catastrophe through inducing a conformational change that promotes microtubule depolymerization (134). Previous studies on SmSLP demonstrated that it inhibits tubulin assembly and causes the depolymerization of preassembled microtubules (129). However, a subsequent report has failed to detect any functional similarities between Sm16 and stathmin, while they demonstrated that Sm16 resulted in a caspase-dependent apoptotic response of the host human cells (135). Although the exact role of rSj16 in microtubule dynamics is still waiting to be evaluated in the present study, the inhibition of bacteria growth (Fig.4.1.9) may suggest that it has a potential cell-cycle regulatory effect. For all of the vectors we used, rSj16 was highly expressed and no apparent inhibition of host cell growth was observed during the induction only when pCold TF was used. This may be interpreted as the activity of expressed rSj16 being suppressed at low temperature (15°C) as pCold TF is a cold shock expression vector. Also, pCold TF vector expresses a 48 kDa Trigger Factor (TF) chaperone as a fusion tag which may cover some active sites of rSj16. The low

level expression of rSj16 by the vector pGEX-4T-1 may be due to the blocking of active sites by GST tag.

As mentioned above, we chose the plasmid pGEX-4T-1 as the vector in this study to express rSj16 from *E. coli*. Since a rGST tag will be co-expressed with the rSj16 as a fusion protein, we need to remove the rGST tag to release the free rSj16 before it could be subjected to functional assay. However, the real situation is that traces of rGST may still exist in the rSj16 solution even after removing process. So we further expressed and purified rGST from *E. coli* and used it as a control protein (Fig.4.1.7).

5.2 Evaluation of immunogenicity of rSj16 and detection of Sj16-specific antibody in *S. japonicum*-infected rabbits

Previous studies by Rao et al. (2002) suggested that intradermal delivery of Sm16 eukaryotic expression plasmid failed to induce circulating antibodies in mice (88). Ramaswamy et al. (2002) also reported their attempts to immunize mice with Sm16 protein but were unsuccessful (88). In the present study, we evaluated the levels of Sj16-specific antibodies in sera of rabbits infected with *S. japonicum* by Western blot and ELISA, and the results indicated that infected rabbit sera did not show antibodies against rSj16 (Fig.4.3). Therefore, out studies further confirm that Sj16 is less immunogenic and does not elicit specific antibodies during *S. japonicum* infection, although denatured rSj16 could provoked specific antibody production in BALB/c mice (Fig.4.2). This low immunogenicity, together with its anti-inflammatory activity, suggests that Sj16 may be developed as an anti-inflammatory agent for the treatment of certain inflammatory diseases.

5.3 Evaluation of the anti-inflammatory activity of rSj16

Since TG has been widely used as an agitator of acute peritoneal inflammation in mice, we used a TG-mediated peritoneal inflammation model to investigate the anti-inflammatory activity of rSj16 (136, 137). The i.p. injection of TG induced a rapid

and long lasting accumulation of PMNs and macrophages in the peritoneal cavity (Fig.4.4.1). Pre-administration of rSj16 markedly blunted leukocyte infiltration in a dose-dependent manner at day 3 (Fig.4.4.2a), thereby indicating an anti-inflammatory function of rSj16. Subsequent analysis of the kinetics of PMN and macrophage influx indicated that rSj16 suppresses peritoneal inflammation as early as 3 h (Fig.4.4.2b-d). It is important to note that reduced leukocyte accumulation in rSj16-treated mice was not attributable to a cytotoxic effect or systemic leukopenia, because PECs were not sensitive to rSj16 and the number of circulating WBCs in rSj16-treated mice was comparable with that of PBS-treated mice at 48 h. Previous studies indicated that resident macrophages play a key role in acute peritoneal inflammation and PMN infiltration (137). Also, the ability of macrophages to induce immune responses differentially depends on their maturation stage (120). We therefore monitored the effect of rSj16 on the maturation profile of peritoneal macrophages during TG-induced inflammation. The result showed that rSj16 dramatically suppressed TG-induced macrophage maturation (Fig.4.4.3). All together, these results may suggest that rSj16 inhibit TG-induced inflammation by suppressing resident macrophage maturation.

To extend the studies of rSj16-mediated anti-inflammatory effect, we investigated whether pro-inflammatory cytokine generation could also be modulated by rSj16. Our data revealed that rSj16 pre-treatment selectively inhibited IL-1β transcription (Fig.4.4.4b), without affecting TNF-α transcription (Fig.4.4.4c), and unexpectedly increased the IL-1α transcription (Fig.4.4.4a) in the PECs. As IL-1α and IL-1β are under separate transcriptional control (138, 139), it is not surprising that these two genes were differentially modulated by rSj16. Rao et al. (2002) also reported that delivery of the Sm16 gene into mouse skin reduced IL-1β transcripts while it increased IL-1α transcripts (88). However, the underlying mechanism in this up-

regulation of IL-1α transcription is still not clear. Previous studies by Ramaswamy et al. (1996) indicated an important role of IL-1RA in the Sm16-mediated anti-inflammatory effect (86). In this study we also found that the transcription of IL-1RA was markedly up-regulated by rSj16 pre-treatment in PECs (2.5-fold) and in peritoneal membrane cells (4.9-fold) at 24 h post-TG injection (Fig.4.4.4j, 4.4.4k). However, no apparent difference in IL-1RA transcription was observed between rSj16 pretreatment mice (rSj16+TG group) and PBS pretreatment mice (PBS+TG group) at 3 h (Fig.4.4.4j). It should be mentioned that Ramaswamy *et al.* evaluated the IL-1RA-inducing effect of Sm16 using cultured keratinocyte without an inflammatory stimulation(86), while we did it using a TG-induced inflammatory model. Actually it may be the case that rSj16 had exactly induced an increase of IL-1RA transcription at 3 h, but this inductive effect was masked by TG because TG is a stronger inducer of IL-1RA. Even so, based on the data presented in this study it is obviously that at the early stage the anti-inflammatory effect of rSj16 may not rely on IL-1RA production.

Chemokine has been well documented as playing a role in orchestrating leukocyte recruitment in TG-induced peritonitis (140, 141). We examined the effect of rSj16 on the transcription of CXC and CC chemokines in this model. Our results suggest that inhibition of PMN infiltration is mediated by suppressing MIP-2 production but not KC because rSj16 pre-treatment reduced TG-induced MIP-2 transcripts (Fig.4.4.4e), without affecting KC (Fig.4.4.4f). This is reasonable since MIP-2 has been shown to be more potent than KC in PMN infiltration in TG peritonitis (137). However, there was no inhibition of MIP-1α (Fig.4.4.4g) transcripts in rSj16 pre-treated mice which suggests that macrophage infiltration may be modulated by other mechanisms.

We also examined the modulation of IL-12 and IL-10 transcription by rSj16. IL12 is a pro-inflammatory cytokine that is produced by phagocytic cells and antigen-presenting cells as a result of non-antigen-specific stimulation (142, 143). IL12 is composed of two disulfide-bonded subunits p40 and p35 [p70], and the disulfide-linked p40 dimer [(p40)2] can antagonize its activity (144). It has been suggested that p40 expression controls the level of bioactive IL12, as this subunit is highly regulated, whereas p35 is expressed ubiquitously (145). However, other studies suggested that p35 is the limiting factor in bioactive IL12 production, as p40 remained elevated despite the down-regulation of the p70 (146). In this study, our data suggest that: i) p40 determines IL-12 activity during the TG-induced inflammatory process, as p40 transcription was 23.7-fold (Fig.4.4.4h) up-regulated while p35 was only 1.5-fold (Fig.4.4.4d); ii) p35 is the limiting factor of IL-12 activity during rSj16-mediated anti-inflammation, as the p35 transcripts reduced to basal level while p40 remained elevated (Fig.4.4.4d, 4.4.4h). These findings lend weight to other reports that the biological activity of IL12 may be determined by the ratio of p40 to p70 (144, 147). IL-10 has been well documented to be critical in limiting inflammatory responses (148). Previous studies found that IL-10 is induced early after exposure to schistosome cercariae (149-151). Interestingly, radiation-attenuated cercariae, which induce high levels of protective immunity in mice, either fail to induce IL-10 production (72) or elicit a delayed response relative to normal larvae (152). Further studies showed that IL-10-deficient mice have an enhanced inflammatory response and enhanced Th1-type responses when exposed to schistosome cercariae (72, 150). Therefore, it appears that IL-10 is one of the key regulatory mediators of immune responsiveness during schistosome infection. In our study, as expected, we found that IL-10 transcript was greatly increased in rSj16-pretreated mice at 3 h and continued to be highly up-regulated at 24 h (Fig.4.4.4i),

thereby suggesting that Sj16 may be the key stimulator of IL-10 production during schistosome infection.

5.4 Suppression of adaptive immune responses to heterologous antigens by rSj16

As mentioned above, rSj16 has been demonstrated to suppress the TG-induced peritoneal macrophage maturation in BALB/c mice (Fig.4.4.3), and up-regulate the expression of IL-10, while down-regulate the expression of IL-12p35 in peritoneal cells (Fig.4.4.4). It is well known that IL-12 is an important cytokine to induce the expression of IFN-γ, to induce the differentiation Th1 cells, and to enhance the production of Th1-associated classes of immunoglobulin (143, 153). IL-10 was first recognized for its ability to inhibit activation and function of T cells, monocytes, and macrophages(148). It plays a key role in limiting inflammatory responses and in differentiation and function of regulatory T cells. Besides, IL-10 inhibits the production of IL-12, and suppresses the activation and cytokine production by Th1 cells(154). Because of the crucial roles of IL-10 and IL-12 in regulation of T cell responses, together with that rSj16 inhibited macrophage maturation (Fig.4.4.3), it is reasonable to hypothesize that rSj16 may also suppress T-cell responses and adaptive immunity.

To test the effects of rSj16 on T-cell responses and adaptive immunity, an animal model of adaptive immunity is needed. LPS has been widely used to be an adjuvant for inducing adaptive immunity. Previous studies showed that LPS used in high dosage induces Th1 immune responses, while used in low dosage induces Th2 immune responses(121). Other studies indicated that LPS from different bacteria activate dendritic cell subsets to produce different cytokines, and induce distinct types of adaptive immunity in vivo (155). In this study, LPS was used as an adjuvant in the BALB/c mouse model of adaptive immunity. The LPS were used as 100

μg/ml, 250 μl per injection. After immunization with LPS along with HSA, there was a significant increase of anti-HSA IgM (Fig.4.5.1.1a), IgG (Fig.4.5.1.1b), IgG2a (Fig.4.5.1.1c), IgG1 (Fig.4.5.1.1d), and IgA (Fig.4.5.1.1e) levels in the immunized mouse serum as compared with those immunized with HSA alone, while there was no anti-HSA IgE (data not shown) detected in all of the mice.

It also has been widely accepted that alum is a classical Th2-inducing adjuvant (156). By i.p. injecting BALB/c and C57BL/6 mice with HSA absorbed alum, Okano, et al. (2001) has demonstrated the successful induction of Th2 responses in the mice as displayed with high levels of HSA-specific IgE and IgG1 in the sera (122). In this study, after immunization with HSA along with alum, the mice displayed a significant increase in HSA-specific IgM (Fig.4.5.2.1a), IgG (Fig.4.5.2.1b), IgG2a (Fig.4.5.2.1c), IgG1 (Fig.4.5.2.1e), and IgA (Fig.4.5.2.1f), and also IgE (Fig.4.5.2.1d), as compared with those immunized with HSA alone. It should noticed that, although the BALB/c mice immunized with both LPS along with HSA and alum along with HSA displayed increased levels of anti-HSA IgG1 and IgG2a in their sera, the ratio of IgG2a/IgG1 in LPS along with HSA-immunized mice sera is much higher than those in alum along with HSA-immunized mice sera (Fig.4.5.2.2). As we have known, IgG has several isotypes, such as IgG1, IgG2a, IgG2b, IgG3, etc, and IgG1 is Th2 associated while IgG2a is Th1 associated (157). Together with that mice immunized alum along with HSA raised anti-HSA IgE (Fig.4.5.2.1d) in the sera while those immunized with LPS along with HSA raised no anti-HSA IgE (data not shown), the data indicated that, in this study, the LPS along with HSA induced more preferred Th1 responses, while alum along HSA induced more preferred Th2 responses in the BALB/c mice.

The observations presented in this study clearly demonstrated that rSj16, either i.p. injected one hour before or along with the administration of LPS-HSA,

suppressed the LPS-HSA induced anti-HSA IgM (Fig.4.5.1.1a), IgG (Fig.4.5.1.1b), IgG2a (Fig.4.5.1.1c) in mice sera. We also revealed that rSj16 suppressed the alum-HSA induced HSA-specific IgM (Fig.4.5.2.1a), IgG (Fig.4.5.2.1b), IgG1 (Fig.4.5.2.1e), IgA (Fig.4.5.2.1f), and IgE (Fig.4.5.2.1d) in mice sera. Our data therefore indicated that rSj16 suppressed both Th1 and Th2 responses, and also humoral responses to heterologous antigen. So, it suggests that, unlike some other immunomodulaors produced by the parasite which prefer to induce a biased Th2 response (158), rSj16 is general suppressor. This adaptive immunity-suppressive effect of rSj16 was obviously not antigen specific, as it could inhibit the antibody production to PSA in the presence of LPS as adjuvant (Fig.4.5.1.2).

To further confirm the suppressive effect of rSj16 on adaptive immunity, we investigated the role of rSj16 on lymphocyte proliferation and cytokine production. As mentioned above, the spleen cells isolated from BALB/c mice treated with rSj16 displayed lower proliferation (Fig.4.5.3.1) and produced less cytokines (Fig.4.5.4.1, 4.5.4.2) in response to HSA stimulation, as compared with those immunized with LPS along with HSA, or those immunized with alum along with HSA. Obviously, this subdued splenocyte proliferation was not due to directly inhibitory effect of rSj16 on the spleen cells, but because of the less spleen cell activation, since rSj16 pre-treatment inhibited neither the ConA-stimulated naïve spleen cell proliferation (Fig.4.5.3.2) nor the HSA-stimulated LPS-HSA-primed spleen cell proliferation (Fig.4.5.3.3).

Schistosomes appear to have evolved to modulate the host's immune response in order to promote their own survival. Many studies have demonstrated that the infection of schistosome is characterized by a state of immune hyporesponsiveness exhibited as a reduced ability of host immune cells to activate and proliferate, and therefore as suppressed T cell response and antibody production (8, 78-80, 159-161).

This schistosome-induced hyporesponsiveness has been well documented to impede not only the capacity of infected host to cope with concurrent infections, but also their capacity to amount protective immune responses to vaccination (18, 162-166). In the course of a schistosome infection, the immune response progresses through at least three phases(79). In the first 3–5 weeks, during which the host is exposed to migrating immature parasites, the dominant response is Th1-like. However, this Th1-like response is usually not significant and quickly resolved (167). As the parasites mature, mate and begin to produce eggs at weeks 5–6, the response alters markedly; the Th1 component decreases and this is associated with the emergence of a strong Th2 response. This response is induced primarily by egg antigens. During the chronic phase of infection (infections are long lived and worms continue to produce eggs — ~300 per day in the case of each *S. mansoni* female), the Th2 response is modulated and granulomas that form around newly deposited eggs are smaller than at earlier times during infection. Since rSj16 showed general suppressive effect on adaptive immunity and studies have suggested that Sj16 is secreted by the skin-penetrating schistosomulae (Wu, et al. unpublished data, (85)), the results from this data may indicate that the subdued inflammatory and Th1 responses at the skin stage of schistosome infection may be at least partially due to the Sj16 secretion.

In the other hand, previous studies revealed that schistosome have also adopted some strategies, including antigen variation, antigen shedding and coating their surfaces with host antigens to evade from host's immune system. These mechanisms make it hardly to amount protective immune by surface antigens during schistosome infection. However, as these evasive mechanisms (antigen variation, antigen shedding and coating their surfaces with host antigens) seldom happen at the right beginning of the infection(59), and even the parasite will secret some materials (e.g.

proteases) at this stage to facilitate its penetration, it is questionary about why those antigens, which have direct contact with host immune system before those evasive mechanisms happen, also cannot amount a protective immune during schistosome infection. Based on the data presented in this study, it may be interpreted, but just partly, as the results of Sj16 secretion. Of course, some other substances, e.g. PGE2 and PGD2, may also take some similar roles as Sj16 during this process(59).

5.5 Effects of rSj16 on the differentiation of JCS and hematopoiesis of mouse bone marrow cells

In this study, we first investigated the effects of rSj16 on the proliferation and differentiation of a leukemia cell line JCS. Our data indicated that rSj16 could inhibit the growth of JCS cells (Fig.4.6.1). It is obvious that the rSj16-mediated anti-proliferation is not attributable to its cytotoxic effects, since the viability of the JCS cells was not affected by the rSj16 treatment (as mentioned in *Results 4.6.1*). It should be noted that, although early stage of apoptosis was detected in the JCS cells treated with rSj16 for 3 days (Fig.4.6.9), at least at the early stage, apoptosis should also not be the main causes of rSj16-induced anti-proliferation, since more than 10% inhibition of JCS growth was already observed at day 2 after rSj16 treatment while no significant apoptosis was detected during this stage (data not shown). Further studies indicated that rSj16 also induced macrophage-like differentiation of the JCS cells (Fig.4.6.3), companied with markedly decrease of the cells in the S phases and concomitant accumulation in the proportion of those in G1/G0 and G2/M phase (Fig.4.6.2).

Membrane antigens serve as excellent markers of murine macrophage differentiation *in vivo* and *in vitro*(168). To confirm macrophage-like differentiation of the JCS cells, we analyzed the membrane antigens by flow cytometry. Among the two antigens be analyzed, the F4/80 is expressed by a majority of mature

macrophages and is the best marker for this population of cells(169), Gr-1 is expressed by bone marrow granulocytes as well as on peripheral neutrophils(170). As expected, our data showed that rSj16 could stimulate the expression of F4/80 on the JCS cells surface but not Gr-1 (Fig.4.6.4), thus supported the macrophage-like differentiation of the cells. Subsequently, this differentiated JCS cells have been verified to acquire the yeast-phagocytizing activity after rSj16 treatment (Fig.4.6.5).

It is well known that LPS could induce macrophage differentiation of certain leukemia cells(171, 172). In order to exclude the possible contamination of endotoxin during preparation of rSj16, the purified proteins were passed through a Detoxi-Gel AffinityPak™ polymyxin B column (Pierce) to eliminate endotoxin. The absence of endotoxin in the protein samples was confirmed by *Limulus* amebocyte lysate test (sensitivity 0.25 EU/ml, Associates of Cape Cod). Besides, the rGST prepared as the same way as rSj16 were served as negative control in the whole study. Thus, in this study, the rSj16-induced macrophage-like differentiation should not due to endotoxin contamination.

Cytokines, such as IL-l, Leukaemia Inhibitory Factor (LIF), TNF-α, and IL-4, have been shown to regulate the growth and differentiation of hematopoietic cells(173, 174). Previous studies reported that PMA-induced macrophage differentiation of JCS cells was mediated by endogenous production of TNF-α, as the differentiation-inducing effect of PMA could be prevented by neutralizing anti-TNF-α antibodies(117). Further studies showed that macrophage differentiation of JCS cells could also induced by TNF-α, IL-1α or IL-1β. We were thereby interested in whether rSj16-induced JCS cells differentiation was results of endogenous production of TNF-α, IL-1α or IL-1β. Unexpectedly, although the production of these three cytokines has been upregulated (Fig.4.6.6), they were obviously not involved in the rSj16-induced JCS differentiation, as none of the anti-IL-1α, anti-IL-

1β and anti-TNF-α antibodies could prevented the activity of rSj16 (Fig.4.6.7.2). Thus, these results indicated that rSj16 induce JCS cells differentiation through some other mechanisms. However, currently we don't have information about the mechanisms. This will be addressed in our following studies.

The JCS cell line is a subclone isolated from the murine myelomonocytic leukemia WEHI-3B cell line, and therefore possesses some certain features of myelomonocytic progenitor cells(92). This cell line has been widely used to be a useful model in the study of hematopoietic cell differentiation(92, 93, 116, 175, 176). In the present study, we have demonstrated that rSj16 could induce macrophage-like differentiation of the JCS cell (Fig.4.6.3-4.6.5). It is thus reasonable to investigate the regulatory effect of rSj16 on mouse hematopoiesis. Our results showed that rSj16 could suppress G-CSF induced CFU-G colony formation (Fig.4.6.8.1a), and suppress IL-3 induced CFU-G and CFU-GM colony formation (Fig.4.6.8.1c). On the other hand, although rSj16 alone did not induce any colony formation of the mouse bone marrow cells, we revealed that rSj16 could increase the number of IL-3 induced CFU-M colony formation (Fig.4.6.8.1). This result corresponded with our previous observation that rSj16 induces macrophage-like differentiation of JCS cell (Fig.4.6.3-4.6.5). However, unexpectedly, the addition of rSj16 into the culture didn't affect the number of M-CSF-induced CFU-M colonies (Fig.4.6.8.1b). A possible interpretation is that M-CSF is a potent inducer of macrophage differentiation which may mask the inducing effect of rSj16.

Furthermore, it is very interesting that the macrophages within the CFU-M colonies induced by IL-3 along with rSj16 (Fig.4.6.8.3b, 4.6.8.3e) and M-CSF along with rSj16 (Fig. 4.6.8.2b, 4.6.8.2e) became more compact than those induce with IL-3 (Fig.4.6.8.3a, 4.6.8.3d) or M-CSF (Fig. 4.6.8.2a, 4.6.8.2d) alone, which suggested that the differentiated macrophages may possess less ability of migration. This result,

together with the observation that rSj16 at the late stage of treatment caused apoptosis of WEHI-3B JCS cells (Fig.4.6.9), may indicate that, although rSj16 induced macrophage differentiation of WEHI-3B JCS cell and increased the number of IL-3 induced CFU-M colony formation of mouse bone marrow cells, the differentiated macrophage cells may not display full functions as normal mature macrophages. This postulation is reasonable as our previous studies indicated that rSj16 inhibited the 3% TG induced mouse peritoneal inflammation and suppressed peritoneal macrophage maturation(177). However, further studies are needed to support the postulation and explore the potential mechanisms.

6 Conclusion

In this study, we have successfully expressed and purified soluble rSj16 protein from bacterial expression system, and revealed that rSj16 suppressed 3% TG-induced peritoneal inflammation in BALB/c mice. Furthermore, we demonstrated that the potential mechanisms of Sj16-mediated anti-inflammation involve suppressing peritoneal macrophage maturation and regulating the cytokine production by peritoneal cells. Besides, our results showed that rSj16 could also modulate humoral and cellular immunity to heterologous antigens in BALB/c mouse model. In addition, we demonstrated that rSj16 induced the macrophage-like differentiation of the murine myeloid leukemia cell line JCS, and modulated mouse hematopoiesis towards macrophage lineage. However, the rSj16-induced macrophages may not be fully functional since the macrophages displayed less ability of migration. Finally, our study also suggested that Sj16 is less immunogenic and can not elicit specific anti-bodies during *S. japonicum* infection. This is the first study to successfully purify sufficient soluble rSj16, and investigate the anti-inflammatory and immunomodulatory effects of the rSj16 on host's immune responses. Our study will contribute to the knowledge about the role of Sj16 during schistosome infection and the underlying mechanism, which is important in the development of strategies to combat the schistosomiasis.

7 References

1. Gryseels, B., K. Polman, J. Clerinx, and L. Kestens. 2006. Human schistosomiasis. *Lancet* 368:1106-1118.
2. KE Mott, P. D., A Moncayo, P Ranque and P de Raadt. 1990. Parasitic diseases and urban development. In *Bull World Health Organ 68*. 691-698.
3. John, D. T., and Petri, W.A. Jr. 2006. The trematodes. In *Markell and Voge's Medical Parasitology*, 9th ed. L. Wilson, ed. Saunders Elsevier, St. Louis.
4. McKerrow, J. H., and J. Salter. 2002. Invasion of skin by Schistosoma cercariae. *Trends in Parasitology* 18:193-195.
5. Curwen, R. S., and R. A. Wilson. 2003. Invasion of skin by schistosome cercariae: some neglected facts. *Trends in Parasitology* 19:63-66; discussion 66-68.
6. Ruppel, A., K. Chlichlia, and M. Bahgat. 2004. Invasion by schistosome cercariae: neglected aspects in Schistosoma japonicum. *Trends in Parasitology* 20:397-400.
7. Whitfield, P. J., A. Bartlett, M. B. Brown, and C. Marriott. 2003. Invasion by schistosome cercariae: studies with human skin explants. *Trends in Parasitology* 19:339-340.
8. Jenkins, S. J., J. P. Hewitson, G. R. Jenkins, and A. P. Mountford. 2005. Modulation of the host's immune response by schistosome larvae. *Parasite Immunology* 27:385-393.
9. Chitsulo, L., D. Engels, A. Montresor, and L. Savioli. 2000. The global status of schistosomiasis and its control. *Acta Tropica* 77:41-51.
10. Bergquist, N. R. 2002. Schistosomiasis: from risk assessment to control. *Trends in Parasitology* 18:309-314.
11. McManus, D. P., and A. Loukas. 2008. Current status of vaccines for schistosomiasis. *Clinical Microbiology Reviews* 21:225-242.
12. King, C. H., K. Dickman, and D. J. Tisch. 2005. Reassessment of the cost of chronic helmintic infection: a meta-analysis of disability-related outcomes in endemic schistosomiasis. *Lancet* 365:1561-1569.
13. Brown, M., P. A. Mawa, S. Joseph, J. Bukusuba, C. Watera, J. A. Whitworth, D. W. Dunne, and A. M. Elliott. 2005. Treatment of Schistosoma mansoni infection increases helminth-specific type 2 cytokine responses and HIV-1 loads in coinfected Ugandan adults. *The Journal of Infectious Diseases* 191:1648-1657.
14. Brown, M., G. Miiro, P. Nkurunziza, C. Watera, M. A. Quigley, D. W. Dunne, J. A. Whitworth, and A. M. Elliott. 2006. Schistosoma mansoni, nematode infections, and progression to active tuberculosis among HIV-1-infected

Ugandans. *The American Journal of Tropical Medicine and Hygiene* 74:819-825.

15. Kallestrup, P., R. Zinyama, E. Gomo, A. E. Butterworth, G. J. van Dam, C. Erikstrup, and H. Ullum. 2005. Schistosomiasis and HIV-1 infection in rural Zimbabwe: implications of coinfection for excretion of eggs. *The Journal of Infectious Diseases* 191:1311-1320.
16. Kallestrup, P., R. Zinyama, E. Gomo, A. E. Butterworth, G. J. van Dam, J. Gerstoft, C. Erikstrup, and H. Ullum. 2006. Schistosomiasis and HIV in rural Zimbabwe: efficacy of treatment of schistosomiasis in individuals with HIV coinfection. *Clinical Infectious Diseases* 42:1781-1789.
17. Kjetland, E. F., P. D. Ndhlovu, E. Gomo, T. Mduluza, N. Midzi, L. Gwanzura, P. R. Mason, L. Sandvik, H. Friis, and S. G. Gundersen. 2006. Association between genital schistosomiasis and HIV in rural Zimbabwean women. *Aids* 20:593-600.
18. Kamal, S. M., and K. El Sayed Khalifa. 2006. Immune modulation by helminthic infections: worms and viral infections. *Parasite Immunology* 28:483-496.
19. Eberl, M., J. A. Langermans, P. A. Frost, R. A. Vervenne, G. J. van Dam, A. M. Deelder, A. W. Thomas, P. S. Coulson, and R. A. Wilson. 2001. Cellular and humoral immune responses and protection against schistosomes induced by a radiation-attenuated vaccine in chimpanzees. *Infection and Immunity* 69:5352-5362.
20. Elias, D., H. Akuffo, and S. Britton. 2006. Helminthes could influence the outcome of vaccines against TB in the tropics. *Parasite Immunology* 28:507-513.
21. Elias, D., H. Akuffo, A. Pawlowski, M. Haile, T. Schon, and S. Britton. 2005. Schistosoma mansoni infection reduces the protective efficacy of BCG vaccination against virulent Mycobacterium tuberculosis. *Vaccine* 23:1326-1334.
22. Elias, D., H. Akuffo, C. Thors, A. Pawlowski, and S. Britton. 2005. Low dose chronic Schistosoma mansoni infection increases susceptibility to Mycobacterium bovis BCG infection in mice. *Clinical and Experimental Immunology* 139:398-404.
23. Booth, M., B. J. Vennervald, A. E. Butterworth, H. C. Kariuki, C. Amaganga, G. Kimani, J. K. Mwatha, A. Otedo, J. H. Ouma, and D. W. Dunne. 2004. Exposure to malaria affects the regression of hepatosplenomegaly after treatment for Schistosoma mansoni infection in Kenyan children. *BMC Medicine* 2:36.
24. Briand, V., L. Watier, L. E. H. JY, A. Garcia, and M. Cot. 2005. Coinfection

with Plasmodium falciparum and schistosoma haematobium: protective effect of schistosomiasis on malaria in senegalese children? *The American Journal of Tropical Medicine and Hygiene* 72:702-707.

25. Diallo, T. O., F. Remoue, A. M. Schacht, N. Charrier, J. P. Dompnier, S. Pillet, O. Garraud, A. N'Diaye A, A. Capron, M. Capron, and G. Riveau. 2004. Schistosomiasis co-infection in humans influences inflammatory markers in uncomplicated Plasmodium falciparum malaria. *Parasite Immunology* 26:365-369.
26. Lyke, K. E., A. Dabo, L. Sangare, C. Arama, M. Daou, I. Diarra, C. V. Plowe, O. K. Doumbo, and M. B. Sztein. 2006. Effects of concomitant Schistosoma haematobium infection on the serum cytokine levels elicited by acute Plasmodium falciparum malaria infection in Malian children. *Infection and Immunity* 74:5718-5724.
27. Pierrot, C., S. Wilson, H. Lallet, S. Lafitte, F. M. Jones, W. Daher, M. Capron, D. W. Dunne, and J. Khalife. 2006. Identification of a novel antigen of Schistosoma mansoni shared with Plasmodium falciparum and evaluation of different cross-reactive antibody subclasses induced by human schistosomiasis and malaria. *Infection and Immunity* 74:3347-3354.
28. Vennervald, B. J., M. Booth, A. E. Butterworth, H. C. Kariuki, H. Kadzo, E. Ireri, C. Amaganga, G. Kimani, L. Kenty, J. Mwatha, J. H. Ouma, and D. W. Dunne. 2005. Regression of hepatosplenomegaly in Kenyan school-aged children after praziquantel treatment and three years of greatly reduced exposure to Schistosoma mansoni. *Transactions of the Royal Society of Tropical Medicine and Hygiene* 99:150-160.
29. Ganley-Leal, L. M., P. N. Mwinzi, C. B. Cetre-Sossah, J. Andove, A. W. Hightower, D. M. Karanja, D. G. Colley, and W. E. Secor. 2006. Correlation between eosinophils and protection against reinfection with Schistosoma mansoni and the effect of human immunodeficiency virus type 1 coinfection in humans. *Infection and Immunity* 74:2169-2176.
30. Karanja, D. M., A. W. Hightower, D. G. Colley, P. N. Mwinzi, K. Galil, J. Andove, and W. E. Secor. 2002. Resistance to reinfection with Schistosoma mansoni in occupationally exposed adults and effect of HIV-1 co-infection on susceptibility to schistosomiasis: a longitudinal study. *Lancet* 360:592-596.
31. Spear, R. C., A. Hubbard, S. Liang, and E. Seto. 2002. Disease transmission models for public health decision making: Toward an approach for designing intervention strategies for Schistosomiasis japonica. *Environmental Health Perspectives* 110:907-915.
32. Minggang, C., and F. Zheng. 1999. Schistosomiasis control in China.

Parasitology International 48:11-19.

33. Chen, M. G. 1989. Schistosomiasis control program in the People's Republic of China: a review. *The Southeast Asian Journal of Tropical Medicine and Public Health* 20:511-517.
34. 1998. An introduction of a nationwide sampling survey on schistosomiasis in China. *Zhongguo Ji Sheng Chong Xue Yu Ji Sheng Chong Bing Za Zhi* 16:84-88.
35. Bottieau, E., J. Clerinx, M. R. de Vega, E. Van den Enden, R. Colebunders, M. Van Esbroeck, T. Vervoort, A. Van Gompel, and J. Van den Ende. 2006. Imported Katayama fever: clinical and biological features at presentation and during treatment. *The Journal of Infection* 52:339-345.
36. Salvana, E. M., and C. H. King. 2008. Schistosomiasis in travelers and immigrants. *Current Infectious Disease Reports* 10:42-49.
37. Hatz, C. F. 2005. Schistosomiasis: an underestimated problem in industrialized countries? *Journal of Travel Medicine* 12:1-2.
38. Cheever, A. W., K. F. Hoffmann, and T. A. Wynn. 2000. Immunopathology of schistosomiasis mansoni in mice and men. *Immunology Today* 21:465-466.
39. Yuan, Y., X. J. Xu, H. F. Dong, M. S. Jiang, and H. G. Zhu. 2005. Transmission control of schistosomiasis japonica: implementation and evaluation of different snail control interventions. *Acta Tropica* 96:191-197.
40. Yang, G. J., P. Vounatsou, X. N. Zhou, M. Tanner, and J. Utzinger. 2005. A Bayesian-based approach for spatio-temporal modeling of county level prevalence of Schistosoma japonicum infection in Jiangsu province, China. *International Journal for Parasitology* 35:155-162.
41. Yang, G. J., P. Vounatsou, X. N. Zhou, J. Utzinger, and M. Tanner. 2005. A review of geographic information system and remote sensing with applications to the epidemiology and control of schistosomiasis in China. *Acta Tropica* 96:117-129.
42. Baiandina, D. G., A. I. Krotov, and A. I. Cherniaeva. 1981. [Praziquantel, a new broad-spectrum anthelmintic (review of the literature)]. *Meditsinskaia Parazitologiia I Parazitarnye Bolezni* 50:62-70.
43. Farid, Z., B. Trabolsi, and M. Stek. 1984. Schistosomiasis and praziquantel. *Annals of Internal Medicine* 101:881-882.
44. Groll, E. 1984. Praziquantel. *Advances in Pharmacology and Chemotherapy* 20:219-238.
45. Bergquist, N. R., and D. G. Colley. 1998. Schistosomiasis vaccines: Research to development. *Parasitology Today* 14:99-104.
46. Hagan, P., and O. Sharaf. 2003. Schistosomiasis vaccines. *Expert Opinion on Biological Therapy* 3:1271-1278.

47. Wilson, R. A., and P. S. Coulson. 1998. Why don't we have a schistosomiasis vaccine? *Parasitology Today* 14:97-99.

48. Fallon, P. G., R. F. Sturrock, C. M. Niang, and M. J. Doenhoff. 1995. Short Report - Diminished Susceptibility to Praziquantel in a Senegal Isolate of Schistosoma-Mansoni. *American Journal of Tropical Medicine and Hygiene* 53:61-62.

49. Ismail, M., A. Metwally, A. Farghaly, J. Bruce, L. F. Tao, and J. L. Bennett. 1996. Characterization of isolates of Schistosoma mansoni from Egyptian villagers that tolerate high doses of praziquantel. *American Journal of Tropical Medicine and Hygiene* 55:214-218.

50. Stelma, F. F., I. Talla, S. Sow, A. Kongs, M. Niang, K. Polman, A. M. Deelder, and B. Gryseels. 1995. Efficacy and Side-Effects of Praziquantel in an Epidemic Focus of Schistosoma-Mansoni. *American Journal of Tropical Medicine and Hygiene* 53:167-170.

51. Ruppel, A., Y. E. Shi, and N. A. Moloney. 1990. Schistosoma-Mansoni and Schistosoma-Japonicum - Comparison of Levels of Ultraviolet-Irradiation for Vaccination of Mice with Cercariae. *Parasitology* 101:23-26.

52. Bennett, J. L. 2000. Schistosomiasis vaccines: What parasitology can do for immunology. *Parasitology Today* 16:356-356.

53. Cox, F. E. G. 1985. Parasitology - Towards Schistosomiasis Vaccines. *Nature* 314:402-403.

54. Gryseels, B. 2000. Schistosomiasis vaccines: The devils' advocate's final plea. *Parasitology Today* 16:357-358.

55. Hagan, P., and S. Sharaf. 2003. Schistosomiasis vaccines. *Expert Opinion on Biological Therapy* 3:1271-1278.

56. Katz, N. 1999. Schistosomiasis vaccines: The need for more research before clinical trials. *Parasitology Today* 15:165-166.

57. Amiri, P., R. M. Locksley, T. G. Parslow, M. Sadick, E. Rector, D. Ritter, and J. H. McKerrow. 1992. Tumour necrosis factor alpha restores granulomas and induces parasite egg-laying in schistosome-infected SCID mice. *Nature* 356:604-607.

58. Harrison, R. A., and M. J. Doenhoff. 1983. Retarded development of Schistosoma mansoni in immunosuppressed mice. *Parasitology* 86 (Pt 3):429-438.

59. Forrester, S. G., and Pearce E.J. 2006. Immunobiology of schistosomes. In *Parasitic Flatworms: Molecular Biology, Biochemistry, Immunology and Physiology*. A. G. Maule, and Marks, N.J., ed. CAB International, Oxfordshire. 175-179.

60. Wolowczuk, I., O. Roye, S. Nutten, M. Delacre, F. Trottein, and C. Auriault.

1999. Role of interleukin-7 in the relation between Schistosoma mansoni and its definitive vertebrate host. *Microbes and Infection* 1:545-551.

61. Cheever, A. W., R. W. Poindexter, and T. A. Wynn. 1999. Egg laying is delayed but worm fecundity is normal in SCID mice infected with Schistosoma japonicum and S. mansoni with or without recombinant tumor necrosis factor alpha treatment. *Infection and Immunity* 67:2201-2208.
62. Davies, S. J., C. B. Shoemaker, and E. J. Pearce. 1998. A divergent member of the transforming growth factor beta receptor family from Schistosoma mansoni is expressed on the parasite surface membrane. *The Journal of Biological Chemistry* 273:11234-11240.
63. Forrester, S. G., P. W. Warfel, and E. J. Pearce. 2004. Tegumental expression of a novel type II receptor serine/threonine kinase (SmRK2) in Schistosoma mansoni. *Molecular and Biochemical Parasitology* 136:149-156.
64. Beall, M. J., and E. J. Pearce. 2001. Human transforming growth factor-beta activates a receptor serine/threonine kinase from the intravascular parasite Schistosoma mansoni. *The Journal of Biological Chemistry* 276:31613-31619.
65. Osman, A., E. G. Niles, and P. T. LoVerde. 2004. Expression of functional Schistosoma mansoni Smad4 - Role in Erk-mediated transforming growth factor beta (TGF-beta) down-regulation. *Journal of Biological Chemistry* 279:6474-6486.
66. Verjovski-Almeida, S., R. DeMarco, E. A. L. Martins, P. E. M. Guimaraes, E. P. B. Ojopi, A. C. M. Paquola, J. P. Piazza, M. Y. Nishiyama, J. P. Kitajima, R. E. Adamson, P. D. Ashton, M. F. Bonaldo, P. S. Coulson, G. P. Dillon, L. P. Farias, S. P. Gregorio, P. L. Ho, R. A. Leite, L. C. C. Malaquias, R. C. P. Marques, P. A. Miyasato, A. L. T. O. Nascimento, F. P. Ohlweiler, E. M. Reis, M. A. Ribeiro, R. G. Sa, G. C. Stukart, M. B. Soares, C. Gargioni, T. Kawano, V. Rodrigues, A. M. B. N. Madeira, R. A. Wilson, C. F. M. Menck, J. C. Setubal, L. C. C. Leite, and E. Dias-Neto. 2003. Transcriptome analysis of the acoelomate human parasite Schistosoma mansoni. *Nature Genetics* 35:148-157.
67. Wilson, R. A. 1987. Cercariae to liver worms: development and migration in the mammalian host. In *The Biology of Schistosomes*. D. Rollinson, and Simpson, A.J.G., ed. Academic Press, London. 115-146.
68. Samuelson, J. C., and J. P. Caulfield. 1986. Cercarial glycocalyx of Schistosoma mansoni activates human complement. *Infection and Immunity* 51:181-186.
69. Marikovsky, M., M. Parizade, R. Arnon, and Z. Fishelson. 1990. Complement regulation on the surface of cultured schistosomula and adult

worms of Schistosoma mansoni. *European Journal of Immunology* 20:221-227.

70. Angeli, V., C. Faveeuw, P. Delerive, J. Fontaine, Y. Barriera, N. Franchimont, B. Staels, M. Capron, and F. Trottein. 2001. Schistosoma mansoni induces the synthesis of IL-6 in pulmonary microvascular endothelial cells: role of IL-6 in the control of lung eosinophilia during infection. *European Journal of Immunology* 31:2751-2761.
71. Herve, M., V. Angeli, E. Pinzar, R. Wintjens, C. Faveeuw, S. Narumiya, A. Capron, Y. Urade, M. Capron, G. Riveau, and F. Trottein. 2003. Pivotal roles of the parasite PGD2 synthase and of the host D prostanoid receptor 1 in schistosome immune evasion. *European Journal of Immunology* 33:2764-2772.
72. Ramaswamy, K., P. Kumar, and Y. X. He. 2000. A role for parasite-induced PGE2 in IL-10-mediated host immunoregulation by skin stage schistosomula of Schistosoma mansoni. *Journal of Immunology* 165:4567-4574.
73. Chen, L., K. V. Rao, Y. X. He, and K. Ramaswamy. 2002. Skin-stage schistosomula of Schistosoma mansoni produce an apoptosis-inducing factor that can cause apoptosis of T cells. *The Journal of Biological Chemistry* 277:34329-34335.
74. Trottein, F., S. Nutten, V. Angeli, P. Delerive, E. Teissier, A. Capron, B. Staels, and M. Capron. 1999. Schistosoma mansoni schistosomula reduce E-selectin and VCAM-1 expression in TNF-alpha-stimulated lung microvascular endothelial cells by interfering with the NF-kappa B pathway. *European Journal of Immunology* 29:3691-3701.
75. Damian, R. T. 1967. Common Antigens between Adult Schistosoma Mansoni and Laboratory Mouse. *Journal of Parasitology* 53:60-64.
76. Smithers, S. R., R. J. Terry, and D. J. Hockley. 1969. Host Antigens in Schistosomiasis. *Proceedings of the Royal Society of London Series B-Biological Sciences* 171:483-494.
77. Pearce, E. J., P. F. Basch, and A. Sher. 1986. Evidence That the Reduced Surface Antigenicity of Developing Schistosoma-Mansoni Schistosomula Is Due to Antigen Shedding Rather Than Host Molecule Acquisition. *Parasite Immunology* 8:79-94.
78. Salzet, M., A. Capron, and G. B. Stefano. 2000. Molecular crosstalk in host-parasite relationships: schistosome- and leech-host interactions. *Parasitology Today* 16:536-540.
79. Pearce, E. J., and A. S. MacDonald. 2002. The immunobiology of schistosomiasis. *Nature Reviews Immunology* 2:499-511.
80. Wynn, T. A., R. W. Thompson, A. W. Cheever, and M. M. Mentink-Kane.

2004. Immunopathogenesis of schistosomiasis. *Immunological Reviews* 201:156-167.

81. Stadecker, M. J., H. Asahi, E. Finger, H. J. Hernandez, L. I. Rutitzky, and J. Sun. 2004. The immunobiology of Th1 polarization in high-pathology schistosomiasis. *Immunological Reviews* 201:168-179.

82. Ramaswamy, K., Y. X. He, and B. Salafsky. 1997. ICAM-1 and iNOS expression increased in the skin of mice after vaccination with gamma-irradiated cercariae of Schistosoma mansoni. *Experimental Parasitology* 86:118-132.

83. Teixeira, M. M., M. J. Doenhoff, C. McNeice, T. J. Williams, and P. G. Hellewell. 1993. Mechanisms of the inflammatory response induced by extracts of Schistosoma mansoni larvae in guinea pig skin. *Journal of Immunology* 151:5525-5534.

84. Mulvihill, C. A., and J. W. Burnett. 1990. Swimmer's itch: a cercarial dermatitis. *Cutis* 46:211-213.

85. Rao, K. V., and K. Ramaswamy. 2000. Cloning and expression of a gene encoding Sm16, an anti-inflammatory protein from Schistosoma mansoni. *Molecular and Biochemical Parasitology* 108:101-108.

86. Ramaswamy, K., B. Salafsky, S. Potluri, Y. X. He, J. W. Li, and T. Shibuya. 1996. Secretion of an anti-inflammatory, immunomodulatory factor by schistosomulae of Schistosoma mansoni. *Journal of Inflammation* 46:13-22.

87. Ramaswamy, K., Potluri, S., Ramaswamy, P., et al. 1998. Immune evasion by Schistosoma mansoni: characterization of Sm 16.8 an anti-inflammatory protein produced by the skin stage schistosomulum. In *Proceedings of the Ninth International Conference on Parasitology*. 597-603.

88. Rao, K. V. N., Y. X. He, and K. Ramaswamy. 2002. Suppression of cutaneous inflammation by intradermal gene delivery. *Gene Therapy* 9:38-45.

89. Ram, D., F. Lantner, E. Ziv, V. Lardans, and I. Schechter. 1999. Cloning of the SmSPO-1 gene preferentially expressed in sporocyst during the life cycle of the parasitic helminth Schistosoma mansoni1. *Biochim Biophys Acta* 1453:412-416.

90. Valle, C., A. Festucci, A. Calogero, P. Macri, B. Mecozzi, P. Liberti, and D. Cioli. 1999. Stage-specific expression of a Schistosoma mansoni polypeptide similar to the vertebrate regulatory protein stathmin. *The Journal of Biological Chemistry* 274:33869-33874.

91. Holmfeldt, P., K. Brannstrom, M. E. Sellin, B. Segerman, S. R. Carlsson, and M. Gullberg. 2007. The Schistosoma mansoni protein Sm16/SmSLP/SmSPO-1 is a membrane-binding protein that lacks the proposed microtubule-regulatory activity. *Molecular and Biochemical*

Parasitology 156:225-234.

92. Mak, N. K., M. C. Fung, K. N. Leung, and A. J. Hapel. 1993. Monocytic differentiation of a myelomonocytic leukemic cell (WEHI 3B JCS) is induced by tumour necrosis factor-alpha (TNF-alpha). *Cellular Immunology* 150:1-14.

93. Fung, M. C., Y. Y. Szeto, K. N. Leung, Y. L. Wong-Leung, and N. K. Mak. 1997. Effects of biochanin A on the growth and differentiation of myeloid leukemia WEHI-3B (JCS) cells. *Life Sciences* 61:105-115.

94. Hanahan, D. 1985. Techniques for Transformation of E. coli. In *DNA Cloning: A Practical Approach. Volume 1.* D. M. Dlover, and B. D. Hames, eds. IRL Press Limited, Oxford, England. 109-135.

95. Sambrook, J., and D. W. Russell. 2001. Quantitation of nucleic acids. In *Molecular cloning: a laboratory manual. Volume 3.*, Third ed. Cold Spring Harbor Laboratory Press, Cold Spring Harbor, New York, USA. A8.19-A18.24.

96. Sambrook, J., and D. W. Russell. 2001. The basic polymerase chain reaction. In *Molecular cloning: a laboratory manual. Volume 2.*, Third ed. Cold Spring Harbor Laboratory Press, Cold Spring Harbor, New York, USA. 8.18-18.24.

97. Sambrook, J., and D. W. Russell. 2001. The Hanahan method for preparation and transformation of cpmpetent E. coli: high efficiency transformation. In *Molecular cloning: a laboratory manual. Volume 1.*, Third ed. Cold Spring Harbor Laboratory Press, Cold Spring Harbor, New York, USA. 1.105-101.111.

98. Sambrook, J., and D. W. Russell. 2001. Expression of cloned genes in Escherichia coli. In *Molecular cloning: a laboratory manual. Volume 3.*, Third ed. Cold Spring Harbor Laboratory Press, Cold Spring Harbor, New York, USA. 15.11-15.60.

99. Piedra, P. A., S. G. Cron, A. Jewell, N. Hamblett, R. McBride, M. A. Palacio, R. Ginsberg, C. M. Oermann, and P. W. Hiatt. 2003. Immunogenicity of a new purified fusion protein vaccine to respiratory syncytial virus: a multi-center trial in children with cystic fibrosis. *Vaccine* 21:2448-2460.

100. Sambrook, J., E. F. Fritsch, and T. Maniatis. 1989. Detection and analysis of proteins expressed from cloned genes. In *Molecular cloning: a laboratory manual. Volume 3.*, Second ed. Cold Spring Harbor Laboratory Press, Cold Spring Harbor, New York, USA. 18.11-18.88.

101. Fujita, S., F. Matsubara, and T. Matsuda. 1986. Enzyme-linked immunosorbent assay measurement of fluctuations in antibody titer and antigenemia in cancer patients with and without candidiasis. *Journal of*

Clinical Microbiology 23:568-575.

102. Carneiro, C. R., and J. D. Lopes. 1986. Surface antigen detected by a Schistosoma mansoni monoclonal antibody in worm extracts and kidney deposits of infected mice and hamsters. *Infection and Immunity* 52:230-235.

103. da Silva, L. C., and R. G. Ferri. 1968. Schistosoma mansoni homogenate for active immunization of mice. *The American Journal of Tropical Medicine and Hygiene* 17:369-371.

104. Pearce, E. J., S. L. James, S. Hieny, D. E. Lanar, and A. Sher. 1988. Induction of protective immunity against Schistosoma mansoni by vaccination with schistosome paramyosin (Sm97), a nonsurface parasite antigen. *Proceedings of the National Academy of Sciences of the United States of America* 85:5678-5682.

105. Hirsch, E., V. L. Katanaev, C. Garlanda, O. Azzolino, L. Pirola, L. Silengo, S. Sozzani, A. Mantovani, F. Altruda, and M. P. Wymann. 2000. Central role for G protein-coupled phosphoinositide 3-kinase gamma in inflammation. *Science* 287:1049-1053.

106. Falcone, D. J., K. M. Khan, T. Layne, and L. Fernandes. 1998. Macrophage formation of angiostatin during inflammation. A byproduct of the activation of plasminogen. *The Journal of Biological Chemistry* 273:31480-31485.

107. Melnicoff, M. J., P. K. Horan, and P. S. Morahan. 1989. Kinetics of changes in peritoneal cell populations following acute inflammation. *Cellular Immunology* 118:178-191.

108. Cuesta, N., C. A. Salkowski, K. E. Thomas, and S. N. Vogel. 2003. Regulation of lipopolysaccharide sensitivity by IFN regulatory factor-2. *Journal of Immunology* 170:5739-5747.

109. Honma, K., H. Udono, T. Kohno, K. Yamamoto, A. Ogawa, T. Takemori, A. Kumatori, S. Suzuki, T. Matsuyama, and K. Yui. 2005. Interferon regulatory factor 4 negatively regulates the production of proinflammatory cytokines by macrophages in response to LPS. *Proceedings of the National Academy of Sciences of the United States of America* 102:16001-16006.

110. Lentschat, A., H. Karahashi, K. S. Michelsen, L. S. Thomas, W. Zhang, S. N. Vogel, and M. Arditi. 2005. Mastoparan, a G protein agonist peptide, differentially modulates TLR4- and TLR2-mediated signaling in human endothelial cells and murine macrophages. *Journal of Immunology* 174:4252-4261.

111. Millington, O. R., C. Di Lorenzo, R. S. Phillips, P. Garside, and J. M. Brewer. 2006. Suppression of adaptive immunity to heterologous antigens during Plasmodium infection through hemozoin-induced failure of dendritic cell function. *Journal of Biology* 5:5.

112. Mosmann, T. 1983. Rapid colorimetric assay for cellular growth and survival: application to proliferation and cytotoxicity assays. *Journal of Immunological Methods* 65:55-63.

113. Kan, S. F., C. H. Yu, H. F. Pu, J. M. Hsu, M. J. Chen, and P. S. Wang. 2007. Anti-proliferative effects of evodiamine on human prostate cancer cell lines DU145 and PC3. *Journal of Cellular Biochemistry* 101:44-56.

114. Strober, W. 1997. Trypan blue exclusion test of cell viability. In *Current Protocols in Immunology*. R. Coico, ed. John Wiley & Sons, New York. A.3B1-A.3B2.

115. Chaves, M. M., and E. G. Kallas. 2004. Cell cycle distribution of CD4+ lymphocytes in HIV-1-infected subjects. *Cytometry. Part B, Clinical cytometry* 62:46-51.

116. Mak, N. K., Y. Y. Szeto, M. C. Fung, K. N. Leung, and S. K. Kwan. 1997. Effects of midazolam on the differentiation of murine myeloid leukemia cells. *Chemotherapy* 43:272-281.

117. Mak, N. K., M. C. Fung, K. N. Leung, and A. J. Hapel. 1993. Monocytic Differentiation of a Myelomonocytic Leukemic-Cell (Wehi 3b Jcs) Is Induced by Tumor-Necrosis-Factor-Alpha (Tnf-Alpha). *Cellular Immunology* 150:1-14.

118. Fung, M. C., Y. Y. Szeto, K. N. Leung, Y. L. WongLeung, and N. K. Mak. 1997. Effects of biochanin A on the growth and differentiation of myeloid leukemia WEHI-3B (JCS) cells. *Life Sciences* 61:105-115.

119. Jim A. Turpin, G. L.-B. 1993. Differentiation, Maturation, and Activation of Monocytes and Macrophages: Functional Activity is Controlled by a Continuum of Maturation In *Mononuclear phagocytes in cell biology* J. K. Gabriel Lopez-Berestein, ed. CRC Press Boca Raton. 71-99.

120. Oliveira, M. A. P., G. M. A. C. Lima, M. T. Shio, P. J. M. Leenen, and I. A. Abrahamsohn. 2003. Immature macrophages derived from mouse bone marrow produce large amounts of IL-12p40 after LPS stimulation. *Journal of Leukocyte Biology* 74:857-867.

121. Eisenbarth, S. C., D. A. Piggott, J. W. Huleatt, I. Visintin, C. A. Herrick, and K. Bottomly. 2002. Lipopolysaccharide-enhanced, toll-like receptor 4-dependent T helper cell type 2 responses to inhaled antigen. *The Journal of Experimental Medicine* 196:1645-1651.

122. Okano, M., A. R. Satoskar, K. Nishizaki, and D. A. Harn. 2001. Lacto-N-fucopentaose III found on Schitosoma mansoni egg antigens functions as adjuvant for proteins by inducing Th2-type response. *Journal of Immunology* 167:442-450.

123. Hass, R., H. Bartels, N. Topley, M. Hadam, L. Kohler, M. Goppeltstrube, and

K. Resch. 1989. Tpa-Induced Differentiation and Adhesion of U937 Cells - Changes in Ultrastructure, Cytoskeletal Organization and Expression of Cell-Surface Antigens. *European Journal of Cell Biology* 48:282-293.

124. Koeffler, H. P., M. Bareli, and M. C. Territo. 1981. Phorbol Ester Effect on Differentiation of Human Myeloid-Leukemia Cell-Lines Blocked at Different Stages of Maturation. *Cancer Research* 41:919-926.
125. Chan, S. C., M. C. Fung, N. K. Mak, and K. N. Leung. 1997. Involvement of interleukin-1 in the differentiation-inducing activity of tumor necrosis factor-alpha on a murine myeloid leukemia (WEHI-3B JCS). *International Journal of Oncology* 10:821-826.
126. Vrhovac, R., R. Kusec, and B. Jaksic. 1993. Myeloid hemopoietic growth factors. Review article. *Int J Clin Pharmacol Ther Toxicol* 31:241-252.
127. Kaushansky, K., C. B. Brown, and S. Petersdorf. 1991. Hematopoietic colony-stimulating factors. *Biotechnology* 19:365-395.
128. Rao, K. V. N., and K. Ramaswamy. 2000. Cloning and expression of a gene encoding Sm16, an anti-inflammatory protein from Schistosoma mansoni. *Molecular and Biochemical Parasitology* 108:101-108.
129. Valle, C., A. Festucci, A. Calogero, P. Macri, B. Mecozzi, P. Liberti, and D. Ciolio. 1999. Stage-specific expression of a Schistosoma mansoni polypeptide similar to the vertebrate regulatory protein stathmin. *Journal of Biological Chemistry* 274:33869-33874.
130. Rubin, C. I., and G. F. Atweh. 2004. The role of stathmin in the regulation of the cell cycle. *Journal of Cellular Biochemistry* 93:242-250.
131. Sobel, A. 1991. Stathmin - a Relay Phosphoprotein for Multiple Signal Transduction. *Trends in Biochemical Sciences* 16:301-305.
132. Jourdain, L., P. Curmi, A. Sobel, D. Pantaloni, and M. F. Carlier. 1997. Stathmin is a tubulin-sequestering protein which forms a ternary T2S complex with 2 tubulins. *Molecular Biology of the Cell* 8:957-957.
133. Jourdain, L., P. Curmi, A. Sobel, D. Pantaloni, and M. F. Carlier. 1997. Stathmin: A tubulin-sequestering protein which forms a ternary T2S complex with two tubulin molecules. *Biochemistry* 36:10817-10821.
134. Belmont, L. D., and T. J. Mitchison. 1996. Identification of a protein that interacts with tubulin dimers and increases the catastrophe rate of microtubules. *Cell* 84:623-631.
135. Holmfeldt, P., K. Brannstrom, M. E. Sellin, B. Segerman, S. R. Carlsson, and M. Gullberg. 2007. The Schistosoma mansoni protein Sm16/SmSLP/SmSPO-1 is a membrane-binding protein that lacks the proposed microtubule-regulatory activity. *Molecular and Biochemical Parasitology* 156:225-234.

136. Hirsch, E., V. L. Katanaev, C. Garlanda, O. Azzolino, L. Pirola, L. Silengo, S. Sozzani, A. Mantovani, F. Altruda, and M. P. Wymann. 2000. Central role for G protein-coupled phosphoinositide 3-kinase gamma in inflammation. *Science* 287:1049-1053.

137. Cailhier, J. F., M. Partolina, S. Vuthoori, S. J. Wu, K. Ko, S. Watson, J. Savill, J. Hughes, and R. A. Lang. 2005. Conditional macrophage ablation demonstrates that resident macrophages initiate acute peritoneal inflammation. *Journal of Immunology* 174:2336-2342.

138. Telford, J. L., G. Macchia, A. Massone, V. Carinci, E. Palla, and M. Melli. 1986. The Murine Interleukin 1-Beta-Gene - Structure and Evolution. *Nucleic Acids Research* 14:9955-9963.

139. Deustachio, P., S. Jadidi, R. C. Fuhlbrigge, P. W. Gray, and D. D. Chaplin. 1987. Interleukin-1-Alpha and Beta-Genes - Linkage on Chromosome-2 in the Mouse. *Immunogenetics* 26:339-343.

140. Remick, D. G., L. B. Green, D. E. Newcomb, S. J. Garg, G. L. Bolgos, and D. R. Call. 2001. CXC chemokine redundancy ensures local neutrophil recruitment during acute inflammation. *American Journal of Pathology* 159:1149-1157.

141. Call, D. R., J. A. Nemzek, S. J. Ebong, G. L. Bolgos, D. E. Newcomb, and D. G. Remick. 2001. Ratio of local to systemic chemokine concentrations regulates neutrophil recruitment. *American Journal of Pathology* 158:715-721.

142. Trinchieri, G. 1998. Interleukin-12: A cytokine at the interface of inflammation and immunity. *Advances in Immunology, Vol 70* 70:83-243.

143. Trinchieri, G. 2003. Interleukin-12 and the regulation of innate resistance and adaptive immunity. *Nature Reviews Immunology* 3:133-146.

144. Gillessen, S., D. Carvajal, P. Ling, F. J. Podlaski, D. L. Stremlo, P. C. Familletti, U. Gubler, D. H. Presky, A. S. Stern, and M. K. Gately. 1995. Mouse Interleukin-12 (Il-12) P40 Homodimer - a Potent Il-12 Antagonist. *European Journal of Immunology* 25:200-206.

145. Snijders, A., C. M. U. Hilkens, T. C. T. M. V. Kraan, M. Engel, L. A. Aarden, and M. L. Kapsenberg. 1996. Regulation of bioactive IL-12 production in lipopolysaccharide-stimulated human monocytes is determined by the expression of the p35 subunit. *Journal of Immunology* 156:1207-1212.

146. Noone, C. M., E. A. Lewis, A. B. Frawely, R. W. Newman, B. P. Mahon, K. H. Mills, and P. A. Johnson. 2005. Novel mechanism of immunosuppression by influenza virus haemagglutinin: selective suppression of interleukin 12 p35 transcription in murine bone marrow-derived dendritic cells. *Journal of General Virology* 86:1885-1890.

147. Heinzel, F. P., A. M. Hujer, F. N. Ahmed, and R. M. Rerko. 1997. Vivo production and function of IL-12 p40 homodimers. *Journal of Immunology* 158:4381-4388.

148. Moore, K. W., R. D. Malefyt, R. L. Coffman, and A. O'Garra. 2001. Interleukin-10 and the interleukin-10 receptor. *Annual Review of Immunology* 19:683-765.

149. He, Y. X., L. Chen, and K. Ramaswamy. 2002. Schistosoma mansoni, S-haematobium, and S-japonicum: early events associated with penetration and migration of schistosomula through human skin. *Experimental Parasitology* 102:99-108.

150. Hogg, K. G., S. Kumkate, and A. P. Mountford. 2003. IL-10 regulates early IL-12-mediated immune responses induced by the radiation-attenuated schistosome vaccine. *International Immunology* 15:1451-1459.

151. Kumar, P., and K. Ramaswamy. 1999. Vaccination with irradiated cercariae of Schistosoma mansoni preferentially induced the accumulation of interferon-gamma producing T cells in the skin and skin draining lymph nodes of mice. *Parasitology International* 48:109-119.

152. Hogg, K. G., S. Kumkate, S. Anderson, and A. P. Mountford. 2003. Interleukin-12 p40 secretion by cutaneous CD11c+ and F4/80+ cells is a major feature of the innate immune response in mice that develop Th1-mediated protective immunity to Schistosoma mansoni. *Infection and Immunity* 71:3563-3571.

153. Gately, M. K., L. M. Renzetti, J. Magram, A. S. Stern, L. Adorini, U. Gubler, and D. H. Presky. 1998. The interleukin-12/interleukin-12-receptor system: Role in normal and pathologic immune responses. *Annual Review of Immunology* 16:495-521.

154. Braun, M. C., E. Lahey, and B. L. Kelsall. 2000. Selective suppression of IL-12 production by chemoattractants. *Journal of Immunology* 164:3009-3017.

155. Pulendran, B., P. Kumar, C. W. Cutler, M. Mohamadzadeh, T. Van Dyke, and J. Banchereau. 2001. Lipopolysaccharides from distinct pathogens induce different classes of immune responses in vivo. *Journal of Immunology* 167:5067-5076.

156. Brewer, J. M., M. Conacher, A. Satoskar, H. Bluethmann, and J. Alexander. 1996. In interleukin-4-deficient mice, alum not only generates T helper 1 responses equivalent to freund's complete adjuvant, but continues to induce T helper 2 cytokine production. *European Journal of Immunology* 26:2062-2066.

157. Sayeh, E., K. Sterling, E. Speck, J. Freedman, and J. W. Semple. 2004. IgG antiplatelet immunity is dependent on an early innate natural killer cell-

derived interferon-gamma response that is regulated by CD8+ T cells. *Blood* 103:2705-2709.

158. Schramm, G., F. H. Falcone, A. Gronow, K. Haisch, U. Mamat, M. J. Doenhoff, G. Oliveira, J. Galle, C. A. Dahinden, and H. Haas. 2003. Molecular characterization of an interleukin-4-inducing factor from Schistosoma mansoni eggs. *The Journal of Biological Chemistry* 278:18384-18392.

159. Duvaux-Miret, O., G. B. Stefano, E. M. Smith, C. Dissous, and A. Capron. 1992. Immunosuppression in the definitive and intermediate hosts of the human parasite Schistosoma mansoni by release of immunoactive neuropeptides. *Proceedings of the National Academy of Sciences of the United States of America* 89:778-781.

160. Stavitsky, A. B. 2004. Regulation of granulomatous inflammation in experimental models of schistosomiasis. *Infection and Immunity* 72:1-12.

161. Weinstock, J. V., and D. L. Boros. 1981. Heterogeneity of the granulomatous response in the liver, colon, ileum, and ileal Peyer's patches to schistosome eggs in murine schistosomiasis mansoni. *Journal of Immunology* 127:1906-1909.

162. Haseeb, M. A., and J. P. Craig. 1997. Suppression of the immune response to diphtheria toxoid in murine schistosomiasis. *Vaccine* 15:45-50.

163. Muniz-Junqueira, M. I., J. Tavares-Neto, A. Prata, and C. E. Tosta. 1996. Antibody response to Salmonella typhi in human schistosomiasis mansoni. *Revista da Sociedade Brasileira de Medicina Tropical* 29:441-445.

164. Patriarca, P. A., P. F. Wright, and T. J. John. 1991. Factors affecting the immunogenicity of oral poliovirus vaccine in developing countries: review. *Reviews of Infectious Diseases* 13:926-939.

165. Sabin, E. A., M. I. Araujo, E. M. Carvalho, and E. J. Pearce. 1996. Impairment of tetanus toxoid-specific Th1-like immune responses in humans infected with Schistosoma mansoni. *The Journal of Infectious Diseases* 173:269-272.

166. Secor, W. E. 2006. Interactions between schistosomiasis and infection with HIV-1. *Parasite Immunology* 28:597-603.

167. Mountford, A. P., and F. Trottein. 2004. Schistosomes in the skin: a balance between immune priming and regulation. *Trends in Parasitology* 20:221-226.

168. MartinezPomares, L., N. Platt, A. J. McKnight, R. P. DaSilva, and S. Gordon. 1996. Macrophage membrane molecules: Markers of tissue differentiation and heterogeneity. *Immunobiology* 195:407-416.

169. Leenen, P. J. M., M. F. T. R. Debruijn, J. S. A. Voerman, P. A. Campbell, and W. Vanewijk. 1994. Markers of Mouse Macrophage Development Detected

by Monoclonal-Antibodies. *Journal of Immunological Methods* 174:5-19.

170. Fleming, T. J., M. L. Fleming, and T. R. Malek. 1993. Selective Expression of Ly-6g on Myeloid Lineage Cells in Mouse Bone-Marrow - Rb6-8c5 Mab to Granulocyte-Differentiation Antigen (Gr-1) Detects Members of the Ly-6 Family. *Journal of Immunology* 151:2399-2408.

171. Kobayashi, M., J. Nishihara, Y. Fujii, H. Maeda, M. Hosokawa, and N. Takeichi. 1994. Involvement of Oxygen Radicals in the Differentiation of Rat Myelomonocytic Leukemia-Cells in-Vitro and in-Vivo. *Leukemia Research* 18:199-203.

172. Yamashita, U., Y. Tanaka, and F. Shirakawa. 1993. Suppressive effect of interleukin-4 on the differentiation of M1 and HL60 myeloid leukemic cells. *Journal of Leukocyte Biology* 54:133-137.

173. Nakayama, N., K. Hatake, A. Miyajima, K. Arai, and T. Yokota. 1989. Colony-stimulating factors, cytokines and hematopoiesis. *Current Opinion in Immunology* 2:68-77.

174. Metcalf, D. 1989. Actions and interactions of G-CSF, LIF, and IL-6 on normal and leukemic murine cells. *Leukemia* 3:349-355.

175. Lui, O. L., N. K. Mak, and K. N. Leung. 2005. Conjugated linoleic acid induces monocytic differentiation of murine myeloid leukemia cells. *International Journal of Oncology* 27:1737-1743.

176. Mak, N. K., Y. L. Wong-Leung, S. C. Chan, J. Wen, K. N. Leung, and M. C. Fung. 1996. Isolation of anti-leukemia compounds from Citrus reticulata. *Life Sciences* 58:1269-1276.

177. Hu, S., Z. Wu, L. Yang, and M. C. Fung. 2009. Molecular cloning and expression of a functional anti-inflammatory protein, Sj16, of Schistosoma japonicum. *International Journal for Parasitology* 39(2):191-200.

}

8 List of publications

1. Hu, S., Wu, Z., Yang, L., Fung, M.C. 2009. Molecular cloning and expression of a functional anti-inflammatory protein, Sj16, of *Schistosoma japonicum*. *International Journal for Parasitology*, 39(2):191-200.
2. Hu, S., Law, P.K., Lv, Z., Wu, Z., Fung, M.C. 2008. Molecular characterization of a calcium-binding protein SjCa8 from *Schistosoma japonicum*. *Parasitology Research*, 103(5):1047-53.
3. Lv, Z.Y., Yang, L.L., Hu, S.M., Sun, X., He, H.J., He, S.J., Li, Z.Y., Zhou, Y.P., Fung, M.C., Yu, X.B., Zheng, H.Q., Cao, A.L., and Wu, Z.D. 2008. Expression profile, localization of an 8-kDa calcium-binding protein from *Schistosoma japonicum* (SjCa8), and vaccine potential of recombinant SjCa8 (rSjCa8) against infections in mice (*Parasitology Research*, in press: 10.1007/s00436-008-1249-0).
4. Hu, S., Law, P.K., Fung, M.C. 2008. Microarray analysis of cercarial stage-specific genes of *Schistosoma japonicum* and the characterization of the antigen Sj20H8 (Submitted and revised to the *Acta Tropica*).
5. Hu, S., Yang, L., Wu, Z., Mak, N.K., Leung, K.N., and Fung, M.C. 2008. Macrophage differentiation of the murine myeloid leukemia WEHI-3B JCS cell is induced by the *Schistosoma japonicum*-derived protein Sj16 (Submitted to the *European Journal of Immunology*).
6. Yang, L.L., Lv, Z.Y., Hu, S.M., Zhang, S.M., Zheng, H.Q., Li, M.T., Fung, M.C., and Wu, Z.D. 2008. Proteomics analysis of differentially expressed proteins from ultraviolet-attenuated cercariae of *Schistosoma japonicum* compared to normal cercariae (Submitted and revised to the *Parasitology Research*).
7. Hu, S., Fung, M.C., et al. Suppression of adaptive immunity to heterologous antigens by Sj16 through modulating the function of antigen presenting cells (manuscript in preparation).